2000

Development and evaluation of an externally air-cooled low-flow torch and the attenuation of space charge and matrix effects in inductively coupled plasma mass spectrometry

Narong Praphairaksit
Iowa State University

INFORMATION TO USERS

This manuscript has been reproduced from the microfilm master. UMI films the text directly from the original or copy submitted. Thus, some thesis and dissertation copies are in typewriter face, while others may be from any type of computer printer.

The quality of this reproduction is dependent upon the quality of the copy submitted. Broken or indistinct print, colored or poor quality illustrations and photographs, print bleedthrough, substandard margins, and improper alignment can adversely affect reproduction.

In the unlikely event that the author did not send UMI a complete manuscript and there are missing pages, these will be noted. Also, if unauthorized copyright material had to be removed, a note will indicate the deletion.

Oversize materials (e.g., maps, drawings, charts) are reproduced by sectioning the original, beginning at the upper left-hand corner and continuing from left to right in equal sections with small overlaps.

Photographs included in the original manuscript have been reproduced xerographically in this copy. Higher quality 6" x 9" black and white photographic prints are available for any photographs or illustrations appearing in this copy for an additional charge. Contact UMI directly to order.

Bell & Howell Information and Learning
300 North Zeeb Road, Ann Arbor, MI 48106-1346 USA

UMI®
800-521-0600

Development and evaluation of an externally air-cooled low-flow torch and the attenuation of space charge and matrix effects in inductively coupled plasma mass spectrometry

by

Narong Praphairaksit

A dissertation submitted to the graduate faculty

in partial fulfillment of the requirements for the degree of

DOCTOR OF PHILOSOPHY

Major: Analytical Chemistry

Major Professor: R. S. Houk

Iowa State University

Ames, Iowa

2000

Graduate College
Iowa State University

This is to certify that the Doctoral dissertation of

Narong Praphairaksit

has met the dissertation requirements of Iowa State University

Signature was redacted for privacy.

Major Professor

Signature was redacted for privacy.

For the Major Program

Signature was redacted for privacy.

For the Graduate college

TABLE OF CONTENTS

ABSTRACT

An externally air-cooled low-flow torch has been constructed and successfully demonstrated for applications in inductively coupled plasma mass spectrometry (ICP-MS). The torch is cooled by pressurized air flowing at ~ 70 L/min through a quartz air jacket onto the exterior of the outer tube. The outer gas flow rate and operating RF forward power are reduced considerably. Although plasmas can be sustained at the operating power as low as 400 W with a 2 L/min of outer gas flow, somewhat higher power and outer gas flows are advisable. A stable and analytical useful plasma can be obtained at 850 W with an outer gas flow rate of ~ 4 L/min. Under these conditions, the air-cooled plasma produces comparable sensitivities, doubly charged ion ratios, matrix effects and other analytical merits as those produced by a conventional torch while using significantly less argon and power requirements. Metal oxide ion ratios are slightly higher with the air-cooled plasma but can be mitigated by reducing the aerosol gas flow rate slightly with only minor sacrifice in analyte sensitivity.

A methodology to alleviate the space charge and matrix effects in ICP-MS has been developed. A supplemental electron source adapted from a conventional electron impact ionizer is added to the base of the skimmer. Electrons supplied from this source downstream of the skimmer with suitable amount and energy can neutralize the positive ions in the beam extracted from the plasma and diminish the space charge repulsion between them. As a result, the overall ion transmission efficiency and consequent analyte ion sensitivities are significantly improved while other important analytical aspects, such as metal oxide ion ratio, doubly charged ion ratio and background ions remain relatively unchanged with the

operation of this electron source. This technique not only improves the ion transmission efficiency but also minimizes the matrix effects drastically. The matrix-induced suppression of signal for even the most troublesome combination of light analyte and heavy matrix elements can be attenuated from 90-99 % to only 2-10 % for 2 mM matrix solutions with an ultrasonic nebulizer. The supplemental electron current can be adjusted to "titrate" out the matrix effects as desired.

CHAPTER 1. GENERAL INTRODUCTION

Since its introduction in 1980 [1], inductively coupled plasma mass spectrometry (ICP-MS) has revolutionized the practice of trace elemental and isotopic analysis with its exceptional analytical capabilities. These attractive features include a multielement analysis capability with high sensitivity and selectivity, superior detection power with detection limits in the part per trillion (ppt) range, a large linear dynamic range (6-8 orders of magnitude), broad elemental coverage, a relatively interference-free and simple mass spectrum, as well as the ability to perform a rapid and high precision semiquantitative analysis [2-6]. Through these virtues along with advancements in instrumentation, ICP-MS has established a prominent position for applications in various fields including geological chemistry, environmental chemistry, biological and clinical chemistry, semiconductor industry, nuclear chemistry, and forensic science [7-31].

Like any other analytical technique, problems and limitations associated with ICP-MS have been discovered over the course of its development. While most of these have been thoroughly studied and accounted for, there are still some challenging dilemmas to encounter and room for improvement in the world of ICP-MS research. One obvious obstacle of the technique, apart from its inevitable costly capital investment, is the high operating cost largely attributed to the high argon consumption (15-18 L/min). While most manufacturers strive to reduce the capital cost of their instruments, the running expense of the plasma has often been overlooked and not taken seriously. Another area of concern is the space charge effects in the ion extraction process. The space charge repulsion between ions in the extracted ion beam commonly results in a loss of analyte ions, a mass discrimination of

analyte responses, and matrix effects that deteriorate the analysis of matrix-rich samples to some extent. These two problems will be discussed and studied more extensively in this dissertation.

ICP-MS Instrumentation

The ICP is an electrical discharge of gas, typically argon, at atmospheric pressure sustained inside a torch by the energy supplied from a radio frequency (27.12 or 40.68 MHz) generator. The ICP torch, schematically illustrated in Figure 1, comprised of three concentric quartz tubes, through which corresponding argon flows (outer, auxiliary, and aerosol or nebulizer flow) are introduced. The open end of this torch is encircled by a series of water-cooled copper loops, known as the load coil, through which the energy of typically 1000-1500 W is coupled to the plasma. The plasma is initiated by a spark from a Tesla coil which produce "seeded" electrons to interact with the fluctuating magnetic field where electrical energy (RF power) is converted into kinetic energy of electrons. These energetic electrons repeatedly collide with and ionize argon from the outer gas flow (14-16 L/min) to form a stable plasma within a zone known as the induction region. Samples are introduced by the nebulizer gas flow (1-1.5 L/min) through the injector tube to the plasma. This flow punches a hole, commonly referred to as the central channel, and delivers samples through the center of the plasma where they are vaporized, dissociated, atomized and eventually ionized to form a beam of predominantly singly charged atomic ions. Although the temperature in this region is relatively cool, it is sufficient to produce a nearly complete ionization of most elements and a significant population of ions of others with higher ionization energy. The auxiliary gas flow, typically 1 L/min, is introduced to the inner annular space of the torch to

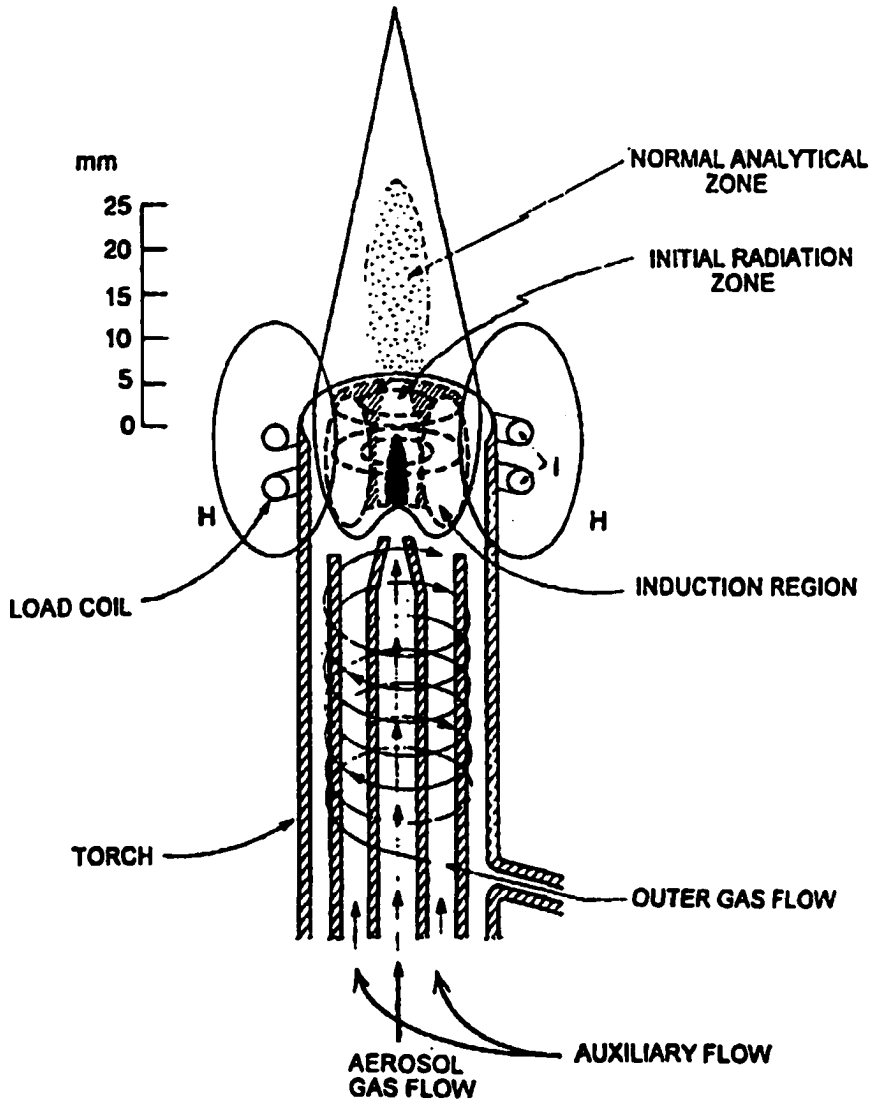

Figure 1. Schematic diagram of the ICP [3].

help stabilize the plasma and keep it from melting the injector tube.

Ions created in the atmospheric pressure plasma are then extracted into a mass analyzer. The operation of mass spectrometers stipulates that the pressure must be maintained under relatively high vacuum (less than 5×10^{-5} torr), therefore, a differentially pumped vacuum chamber is necessary. A schematic diagram of a typical ICP-MS system with a quadrupole mass analyzer is depicted in Figure 2.

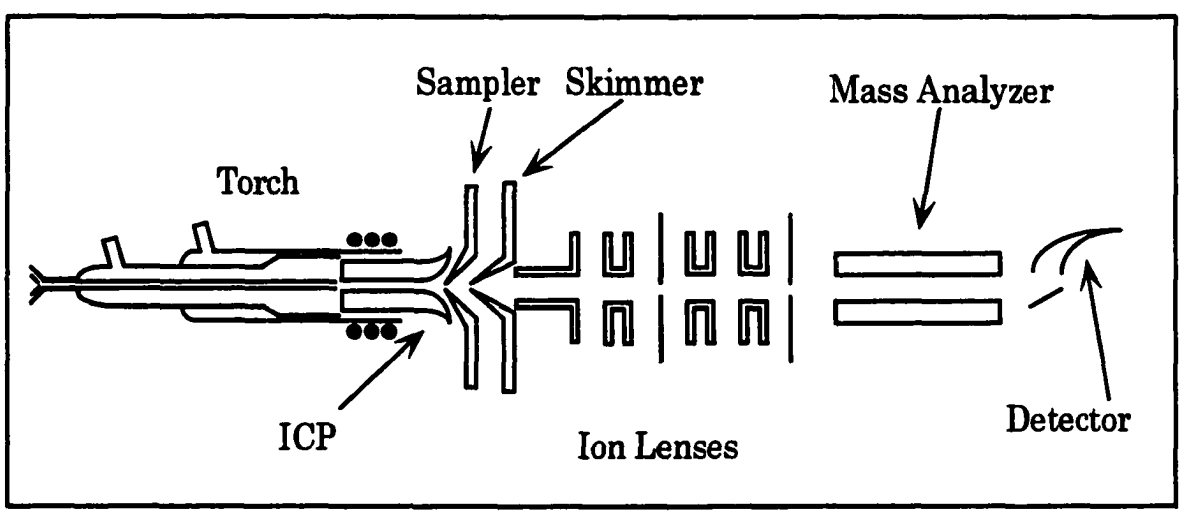

Figure 2. Schematic diagram of a typical ICP-MS system.

The mass spectrometer consists of three pumping stages. Ions are extracted through the sampler orifice into the first vacuum stage where the pressure is reduced to approximately 1 torr. The ion beam is then extracted further by the skimmer into a second vacuum stage where the pressure is roughly 10^{-4} torr. Analyte ions from the extracted beam are subsequently focused and transported through a series of ion lenses into the third vacuum stage where the pressure is typically maintained below 5×10^{-5} torr during the course of operation. Stationed inside this high vacuum stage is a mass analyzer where ions are resolved according to their mass to charge ratios. Though a variety of mass analyzers can be utilized, the quadrupole mass filter is the most commonly used device owing to its robustness, reliability, affordability and ease of operation. With the quadrupole, ions of only one desired m/z are transmitted at a time while the others experience unstable ion trajectories and are lost. Upon leaving the mass filter, the mass resolved ions are then measured by the detector and signals are further processed for data analysis.

ICP Torch and Gas Flow Requirements

An earlier version of the ICP torch required argon flow as much as 40 L/min and extremely high RF power (15 kW) for its operation. A major breakthrough in the ICP torch design came about when Wendt and Fassel [32] pioneered a three-tube torch that can be operated with a total flow of roughly 15-20 L/min and less than 2 kW of RF power. Although the argon consumption is still high, this Fassel torch has persisted to date and is widely used in most commercial ICP systems. It has been estimated that the average cost of argon consumption for a typical ICP system in the U.S., where relatively inexpensive argon is widely available, is approximately $18,000 per year based on regular usage (40 hours per

week) and as much as $50,000 for heavy usage [33]. This economic factor undoubtedly prompted concerns to many users about the affordability of the technique and triggered several studies of torch design during 1970s and 1980s.

The majority of argon consumption is the outer gas flow (14-16 L/min) which is introduced tangentially through the outer annular space to sustain the plasma and cool the torch. This flow produces a high-speed vorticular stream of gas to shield the plasma from the outer tube and prevent the torch from melting. The reduction of the outer gas flow has been the main focus in all torch design studies since the majority of this flow is simply wasted to create the protective shield for the torch. Moreover, an unnecessarily large fraction of RF power is wasted through heating this excessive flow [34]. A sufficient protective shield can be maintained at a substantially lower volume when the swirl velocity is increased. This can be achieved by either using a narrow directional nozzle to introduce the outer gas [35] or reducing the outer annular space of the torch [36]. Argon consumption can also be diminished by decreasing the overall physical dimension of the plasma, i.e. the torch. A series of reduced-size torches have been developed and evaluated for both ICP emission spectrometry and ICP-MS [37-40]. These torches are capable of sustaining a stable plasma with approximately 7-12 L/min of outer gas flow and 0.5-1.3 kW of RF power.

All of the modified torches discussed above have a limitation in that a certain level of the outer gas flow (7-10 L/min pending the operating power) must be retained in order to provide a sufficient protective shield to the torch. To break this barrier, different means of torch cooling were considered. Some types of jacket surrounding the outer tube is used as a pathway for cooling media to circulate the torch and cool the outer tube wall externally. Water has been used successfully to cool the torch [41-42] which reduce the outer gas flow

rate to as low as 1 L/min. Water is an extreme cooling medium, with a heat transfer coefficient of 10^4 W/m^2 K from water to silica [43], and is capable of keeping the torch wall cool even with such a low flow. Nonetheless, it is too effective as a substantial portion of the input power is uselessly drained away through heating this water. Furthermore, the formation of a bubble in the water jacket can easily lead to the melting or explosion of the torch. Taking this power efficiency and safety into consideration, air offers an excellent compromise as has been demonstrated by de Galan and coworkers [44-45]. Also put in to test is the use of a high-temperature resistant ceramic as an alternate material for ICP torch. Boron nitride was incorporated as a segment of the outer tube to radiatively release the heat from the plasma operated with 600 W RF power and only 1 L/min outer gas flow, but was discouraged by its performance and short lifetime [46].

These low-flow torches have satisfied the economical criteria in terms of argon consumption and, for most, power requirement. Unfortunately, analytical capabilities of these plasmas have always deteriorated in one way or another. Clearly, the acceptance of a low-flow torch will not be justified only by its economical achievement but more importantly by its analytical merits. The ultimate goal of this study is the demonstration of a low-flow torch for ICP-MS with no compromise in analytical performance.

Space Charge and Matrix Effects

When the plasma is extracted into a vacuum chamber through the sampler, a supersonic jet is formed. The extracted plasma, as a quasineutral mixture of neutral atoms and roughly equal numbers of ions and electrons, expands supersonically into a collision-free region known as the zone of silence. The centerline flow is further extracted through the

skimmer into the second vacuum stage. While the ion beam progresses through the skimmer, the quasineutral state breaks down as positive ions are drawn toward the ion lenses while the electrons are repelled. As a result, a space charge or a net charge imbalance develops in the beam. For a sufficiently intense beam, the electrostatic repulsion between ions easily overwhelms the applied electrostatic field from the ion lenses, resulting in a radial expansion or defocussing of the ions. This defocusing phenomenon is commonly referred to as the space charge effect.

Olivares and Houk [47] were the first to state that the space charge effect occurs in ICP-MS when they found that the ion current measured at the ion lens was much less than that estimated from the gas-dynamic theory. The mutual repulsion between ions limits the total number of ions that can be focused and collimated into a beam of a given size. The maximum ion current, or space charge-limited current, (I_{max} , μA) of an ion beam that can be transmitted through an ion lens is given by

$$I_{max} = 0.93\ (m/z)^{-1/2} (D/L)^2\ V^{3/2}$$

where m/z is the mass to charge ratio of the ion, D and L are the diameter and length of the ion lens, and V is the ion kinetic energy in eV. For a cylindrical lens with D/L of 0.5 and argon ions with kinetic energy of 3 eV, the calculated maximum current is 6 μA, similar to the actual value measured at the base of the skimmer [48]. However, the estimated ion current flowing through the skimmer is approximately 1.5 mA, several orders of magnitude higher, which clearly indicates that a severe space charge does occur behind the skimmer.

The space charge effect generally results in the defocusing and loss of ions. It has been estimated that, for a modern quadrupole ICP-MS, as many as 50,000-500,000 ions in the plasma are necessary in order to obtain a signal of one ion at the detector [49]. This low

ion transmission efficiency has been largely attributed to the space charge effects in the ion beam. Ion transmission under the space charge field is also a function of ion kinetic energy. Ions with higher masses, i.e. higher kinetic energies, tend to stay more focused and are transmitted more efficiently through the defocusing space charge field than lighter ions. These effects can be illustrated more clearly by theoretical modeling of ion trajectories [48, 50] of the ion beam as depicted in Figure 3. The ions are shown emerging from the skimmer at the left and travelling through three cylindrical ion lenses to the aperture plate at the far right. In the absence of space charge field (Figure 3a) where ion current is very small, the ions (Ar^+) are nicely collimated and efficiently transmitted through the aperture plate. On the contrary, under a space charge field of only 1.25 μA ion current (Figure 3b) the ion trajectories are scattered and a substantial fraction of Ar^+ are lost due to the defocusing effect. Meanwhile, heavy ions (Tl^+) with larger kinetic energy in Figure 3c clearly show more tolerance to the defocusing under the same space charge field.

Poor ion transmission efficiency is not the only problem. Other drawbacks ICP-MS suffers from the occurrence of the space charge effects include mass discrimination in the analyte responses, a bias toward higher mass in isotope ratio measurements, a shift of ion kinetic energy distribution particularly for the lower mass ions and most importantly, matrix effects. Matrix effects are characterized by changes in analyte signal in the presence of concomitant elements, which normally results in a signal suppression. The suppression is most severe for light analyte ions in the presence of higher mass matrix elements as a result of the defocusing nature of ions under the space charge field. Matrix effects are the most common yet challenging problems for many ICP-MS users as matrices are likely to be unavoidable ingredients in the analysis of real samples.

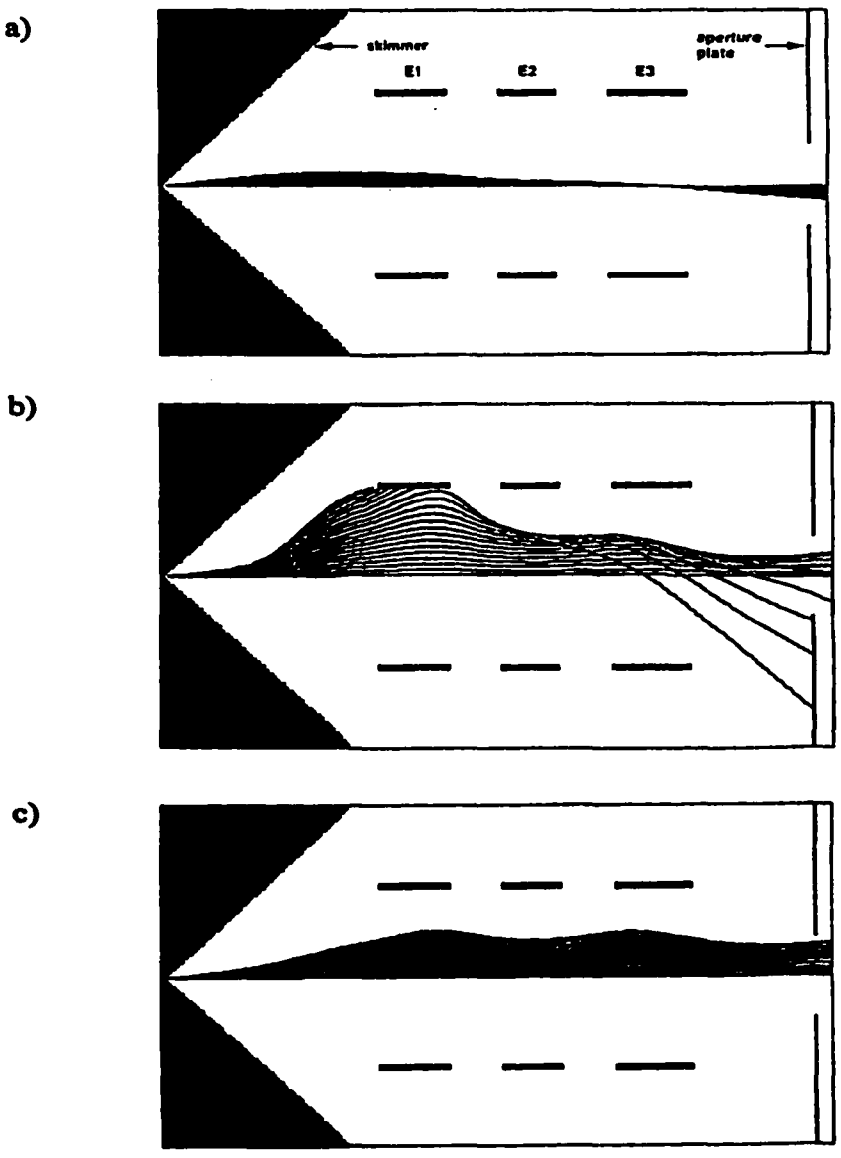

Figure 3. Theoretically calculated ion trajectories for a) Ar^+ in the absence of space charge field, b) Ar^+ for an ion current of 1.25 μA through the skimmer orifice, and c) Tl^+ under the same space charge field (1.25 μA). Potentials applied on the skimmer, lenses E1, E2, E3, and aperture plate were 0, -12, -130, -12, and –12 V, respectively. Only the upper half of the ion beam paths are shown for clarity [50].

Dissertation Objectives and Organization

This dissertation is presented in three separate chapters, each of which stands alone as a complete scientific manuscript with accompanying references, tables, and figures. The general conclusions summarizing significant outcomes of the studies along with suggestions for future research are presented in chapter 5.

Chapter 2 introduces a new air-cooled low-flow torch and evaluates its performances for ICP-MS analysis. The torch is cooled externally by cooling air blown against the exterior of the outer tube through an air jacket. As a result, the argon flow can be reduced significantly. A plasma stability curve was determined and plasma operating parameters were investigated. An analytically useful plasma can be operated at 850 W RF forward power with an outer gas flow rate of 4-4.5 L/min. This low-flow plasma produces comparable sensitivity, metal oxide ions, doubly charged ions, background ions, and matrix effects as a conventional system.

A new strategy to alleviate the space charge effects in the ion beam behind the skimmer is presented in chapter 3. A supplemental electron source similar to an electron impact ionizer is added to the base of the skimmer. Electrons emitted from this source, with appropriate current and energy, reduce the excess positive charge and the space charge repulsion between ions in the extracted ion beam when the quasineutral state breaks down. The overall ion transmission efficiency and consequent analyte sensitivities are improved drastically. Other analytical aspects possibly affected by the operation of this modified electron-enhanced skimmer in ICP-MS were also investigated.

Chapter 4 describes use of the supplemental electron source in the skimmer to attenuate matrix effects. Signal suppression by the matrix is improved considerably when the

electrons are supplied. Matrix effects can be attenuated to a greater extent by operating the source under electron-rich conditions. A charge titration technique is developed in that the operating conditions of the electron source are optimized with a matrix-rich sample to accommodate the presence of concomitant elements prior to the analysis. The matrix-induced suppressions of analyte signal are almost eliminated for practically all analyte and matrix elements by these measures.

References

1. Houk, R. S., Fassel, V. A., Flesh, G. D., Svec. H. J., Gray, A. L., and Taylor, C. E., *Anal. Chem.*, 1980, **52**, 2283.

2. Houk, R. S., *Anal. Chem.*, 1986, **58**, 97A.

3. Jarvis, K. E., Gray, A. L., and Houk, R. S., *Handbook of Inductively Coupled Plasma Mass Spectrometry*, Chapman and Hall, New York, 1992.

4. Hieftje, G. M., and Norman, L. A., *Int. J. Mass Spectrom. Ion Processes*, 1992, **118/119**, 519.

5. Houk, R. S., *Acc. Chem. Res.*, 1994, **27**, 333.

6. Montaser, A., *Inductively Coupled Plasma Mass Spectrometry*, Wiley-VCH, New York, 1998.

7. Hall, G. E. M., and Bonham-Carter, G. F., *J. Geochem. Explor.*, 1988, **30**, 255.

8. Jarvis, K. E., *Chem. Geol.*, 1988, **58**, 31.

9. Marabini, A. M., Passariello, B., and Barbaro, M., *Mater. Chem. Phys.*, 1992, **30**, 101.

10. Heumann, K. G., *Mass Spectrom. Reviews*, 1992, **11**, 41.

11. Jackson, L. L., Baedecker, P. A., Fries, T. L., and Lamothe, P. J., *Anal. Chem.*, 1995, **67**, 712.

12. Douglas, D. J., and French, J. B., *J. Anal. At. Spectrom.*, 1988, **3**, 743.

13. Arar, E. J., Long, S. E., Martin, T. D., and Gold, S., *Environ. Sci. Technol.*, 1992, **26**, 1944.

14. Poissant, L., Schmit, J. P., and Beron, P., *Atmospheric Environ.*, 1944, **28**, 339.

15. Mac Carthy, P., Klusman, R. W., Cowling, S. W., and Rice, J. A., *Anal. Chem.*, 1995, **67**, 525R.

16. Newman, R. A., Osborn, S., and Siddik, Z. H., *Clin. Chim. Acta*, 1989, **179**, 191.

17. Templeton, D. M., Paudyn, A., and Baines, A. D., *Biol. Trace Elem. Res.*, 1989, **22**, 17.

18. Vandecasteele, C., Vanhoe, H., and Dams, R., *J. Anal. At. Spectrom.*, 1993, **8**, 781.

19. Alcock, N. W., *Anal. Chem.*, 1995, **67**, 503R.

20. Nixon, D. E., and Moyer, T. P., *Spectrochim. Acta, Part B*, 1996, **51**, 13.

21. Fucsko, J., Tan, S. H., and Balazs, M. K., *J. Electrochem. Soc.*, 1993, **140**, 1105.

22. Fabry, L., Pahlke, S., Kotz, L., and Toelg, G., *Fresenius J. Anal. Chem.*, 1994, **349**, 260.

23. Tan, S. H., *Nucl. Inst. and Meth. in Phys. Res. B*, 1995, **99**, 458.

24. Laly, S., Nakagawa, K., Arimura, T., and Kimijima, T., *Spectrochim. Acta, Part B*, 1996, **51**, 1393.

25. Palmieri, M. D., Fritz, J. S., Thomson, J. J., and Houk, R. S., *Anal. Chim. Acta*, 1986, **184**, 187.

26. Blair, P. D., *Trends Anal. Chem.*, 1986, **5**, 220.

27. *Applications of Inductively Coupled Plasma Mass Spectrometry to Radionuclide Determinations*, eds. Morrow, R. W., and Crain, J. S., American Society of Testing and Materials, Philadelphia, 1995.

28. Hepiegne, P., Dall'ava, D., Clement, R., and Degros, J. P., *Talanta*, 1995, **42**, 803.

29. Marumo, Y., Inoue, T., and Seta, S., *Forensic Sci. Int.*, 1994, **69**, 89.

30. Heitkemper, D. T., Platek, S. F., and Wolnik, K. A., *J. Forensic Sci.*, 1995, **40**, 664.

31. Wells, R. J., Skopec, S. V., Ivatez, R., and Robertson, J., *Chem. Aust.*, 1995, **62**, 14.

32. Wendt, R. H., and Fassel, V. A., *Anal. Chem.*, 1965, **37**, 920.

33. Hieftje, G. M., *Spectrochim. Acta, Part B*, 1983, **38**, 1465.

34. Ripson, P. A. M., and de Galan, L., *Spectrochim. Acta, Part B*, 1983, **38**, 707.

35. Genna, J. L., Barnes, R. M., and Allemand, C. D., *Anal. Chem.*, 1977, **49**, 1450.

36. Allemand, C. D., and Barnes, R. M., *Appl. Spectrosc.*, 1977, **31**, 434.

37. Allemand, C. D., Barnes, R. M., and Wohlers, C. C., *Anal. Chem.*, 1979, **51**, 2392.

38. Weiss, A. D., Savage, R. N., and Hieftje, G. M., *Anal. Chim. Acta*, 1981, **124**, 245.

39. Ross, B. S., Chambers, D. M., Vickers, G. H., Yang, P., and Hieftje, G. M., *J. Anal. At. Spectrom.*, 1990, **5**, 351.

40. Ross, B. S., Yang, P., and Hieftje, G. M., *Appl. Spectrosc.*, 1991, **45**, 190.

41. Kornblum, G. R., van der Waa, W., and de Galan, L., *Anal. Chem.*, 1979, **51**, 2378.

42. Kawaguchi, H., Ito, T., Rubi, S., and Mizuike, A., *Anal. Chem.*, 1980, **52**, 2440.

43. Montaser, A., and Golightly, D. W., *Inductively Coupled Plasmas in Analytical Atomic Spectrometry*, VCH, New York, 1992.

44. Ripson, P. A. M., de Galan, L., and de Ruiter, J. W., *Spectrochim. Acta, Part B*, 1982, **37**, 733.

45. van der Plas, P. S. C., de Waaij, A. C., and de Galan, L., *Spectrochim. Acta, Part B*, 1985, **40**, 1457.

46. van der Plas, P. S. C., and de Galan, L., *Spectrochim. Acta, Part B*, 1984, **39**, 1161.

47. Olivares, J. A., and Houk, R. S., *Anal. Chem.*, 1985, **57**, 2674.

48. Gillson, G. R., Douglas, D. J., Fulford, J. E., Halligan, K. W., and Tanner, S. D., *Anal. Chem.*, 1988, **60**, 1472.

49. Niu, H., and Houk, R. S., *Spectrochim. Acta, Part B*, 1996, **51**, 779.

50. Tanner, S. D., *Spectrochim. Acta, Part B*, 1992, **47**, 809.

CHAPTER 2. AN EXTERNALLY AIR-COOLED LOW-FLOW TORCH FOR INDUCTIVELY COUPLED PLASMA MASS SPECTROMETRY

A paper submitted to Spectrochimica Acta Part B

Narong Praphairaksit, Daniel R. Wiederin, and R. S. Houk*

Abstract

A low-flow torch specifically designed for inductively coupled plasma mass spectrometry (ICP-MS) was developed and evaluated. The outside of the torch is cooled externally by pressurized air flowing at ~ 70 L/min through a fourth tube sealed onto the usual "outer" tube of a standard minitorch. This external air flow merely cools the outer tube of the torch and does not enter the plasma. Although plasmas can be sustained at operating power as low as 400 W with a 2 L/min outer Ar flow, somewhat higher power and flows are advisable. A stable and analytically useful plasma can be obtained at 850 W with an outer Ar flow rate of ~ 4 L/min. Under optimum operating conditions, the externally air-cooled plasma produces comparable sensitivities, M^{2+}/M^{+} signal ratios, matrix effects and other analytical figures of merit as those produced by a conventional torch while using much less argon. MO^{+}/M^{+} signal ratios are slightly higher with the externally cooled torch.

Introduction

Inductively coupled plasma mass spectrometry (ICP-MS) is a superior analytical tool for elemental and isotopic analysis. Nevertheless, the number of ICP-MS instruments currently in use remains limited. Apart from the capital investment, the high operating cost

*Corresponding author

represented mainly by argon consumption has made it somewhat unaffordable for smaller laboratories. This is a crucial problem in undeveloped countries, where there are few or no ICPs because Ar is either unavailable or too expensive.

These limitations have been recognized by a number of researchers who have modified ICP torches to reduce operating costs. Most ICP-MS instruments use a total argon flow of 15-18 L/min and incident power of 1.0 – 1.5 kW. In a conventional ICP, approximately 1 kW of the input power merely heats this large outer gas flow, while only less than 20% of the power is required to atomize and ionize the sample [1]. This argon flow creates a protective shield to prevent the torch from being overheated by the plasma. The outer gas also prevents entrainment of air, which produces strong molecular emission bands in the traditional use of the ICP as an emission source. Thus, analytical ICPs for atomic emission spectrometry (AES) are traditionally developed with high flows of outer gas [2-4].

These observations suggest that there is some room for developments in the torch design to reduce both the power and argon flow requirements. Several previous investigations demonstrate concepts for reduction of Ar consumption that are employed in the present work. Genna et al. [5] demonstrated that a swirl flow (angular velocity parallel to the circular torch walls from the tangential introduction of the outer gas flow) is a critical component to the stabilization of the discharge. With the use of a directional nozzle in the coolant port to increase such velocity, they operated the ICP with the outer gas flow 30-40% lower than that required in the conventional arrangement. Similarly, the swirl velocity can be increased when the annular separation between the outer and intermediate tubes (annular spacing) is reduced [6]. The smaller annular spacing essentially forces the outer gas to travel at a higher speed and directs it against the outer tube, thus cooling the torch more efficiently.

This strategy decreases both argon consumption and the input RF power, since less power is needed to heat the lower outer gas flow. The annular spacing, typically ~1 mm for a conventional torch, was optimum at 0.5 mm. A stable plasma could be sustained with 450 W of RF power and 6 L/min of outer gas flow for analysis by AES [7,8]. Under such conditions, however, the plasma was substantially weaker (excitation temperature = T_{exc} = 4036 K, electron density = $n_e = 1.7 \times 10^{14}$ cm^{-3}) than a conventional one (T_{exc} = 5575 K, n_e = 1.6×10^{15} cm^{-3}). These compromises make these plasmas less desirable for the measurement of elements with high ionization or excitation energy and more susceptible to problems with matrix interferences [9] and solvent loading.

Argon consumption can also be minimized by reducing the overall size of the plasma with a miniature torch. These "minitorches" (outer tube ID 13 or 9 mm) have been evaluated and compared with a conventional torch (18 mm ID) for ICP-AES [10-14]. The 0.5 mm annular spacing was also incorporated in the design of these minitorches to promote the cooling efficiency. A modified load coil with smaller ID was utilized to maintain coupling of RF power. With these configurations the outer gas flow rates were diminished to approximately 8-12 L/min for the 13 mm torch and 7-8 L/min for the 9 mm torch when operated at 0.5-1.0 kW of RF power. These smaller plasmas provide about the same detection limits but are relatively cooler and are somewhat more susceptible to changes in solvent load and matrix interference compared to the conventional system [13-14].

All of the modified torches mentioned earlier rely entirely on the cooling action of the Ar flow in the ICP to keep the torch from melting. Therefore, a certain minimum outer gas flow (at least 7 L/min for a plasma operated at less than 1 kW for ICP-AES) must be maintained in order to cool the outer tube. Consequently, further reduction of the argon flow

requires some means for additional cooling. The cooling provided by the internal argon flow toward the outer torch tube can be supplemented externally. Water is an obvious choice of cooling medium and has been used to externally cool the outer tube of the torch for ICP-AES [15-20]. A water jacket is built around the outer tube to circulate water and cool the tube wall effectively. As a result, the argon consumption is drastically reduced. A stable plasma reportedly could be sustained with the outer gas flow as low as 0.9-1 L/min at 0.7-1.1 kW RF power [16,18]. Unfortunately, the economical benefit of this water-cooled torch is compromised by its poor analytical performance. Detection limits and matrix interferences are significantly worse than those obtained with a conventional torch, presumably due to an inefficient coupling of RF power as the plasma and the load coil are separated further by a water jacket. Furthermore, occasional bubble formation inside the water jacket can easily result in local overheating and catastrophic destruction of torch. For these reasons, water-cooled torches have not seen widespread use.

External cooling by air or some other inexpensive gas is another, less risky possibility. Ripson and co-workers [21] constructed an unusual two-turn, flat-plated load coil containing 5 air inlet ports for ICP-AES. A stream of pressurized air (50 L/min) blows against the exterior of a standard torch through these inlets to cool the outer tube. The Ar outer gas flow can be reduced to as little as 0.75 L/min at low power (0.5 kW). Nevertheless, the plasma is visibly cooler and unstable under these conditions and the torch deforms rapidly when the power is increased. The air-cooled load coil was later modified into a standard helical coil surrounded by an air jacket containing 14 air inlets for more effective and homogeneous cooling [22]. With this refinement, the power can be raised up to 900 W at 1 L/min outer gas flow without melting the torch. Although the detection limits of

elements with high energy emission lines and matrix interference are substantially improved with higher operating power, the plasma obtained under this extremely low gas flow is spherical and unstable, and the plume formed when the plasma exits the torch is severely disturbed by air entrainment.

The majority of the low-flow torch research has been performed for ICP-AES; only a few studies have been reported for ICP-MS. It has been estimated that in a typical ICP-MS system the gas flow through the sampler is approximately 2 L/min [23]. This flow by itself exceeds the total gas flow of some low-flow torches [20-22]. Hence, the entire plasma is extracted along with the entrained air, which leads to more complicated mass spectra and serious interferences.

At very low flow and low RF power, the secondary discharge in ICP-MS is more severe as well [24,25]. Thus, the outer gas flow rate, and consequently the power, for low-flow torches have been kept higher in ICP-MS than in ICP-AES. A water-cooled torch was used with some success for ICP-MS with 2.1 L/min outer gas flow at 1.1 kW RF forward power [26]. Nonetheless, the spherical plasma obtained under these conditions appears to have less ionization efficiency and produces an intense secondary discharge, which results in high ion kinetic energies, more doubly charged ions and degradation of the sampler and skimmer. Minitorches (both 9 and 13 mm) have also been used with ICP-MS by Hieftje et al [27,28]. The 9 mm torch was operated at 7.5 L/min outer gas flow and 850 W while the optimum outer flow and RF power for the 13 mm torch were 8.3 L/min and 1.35 kW respectively. Sensitivities and detection limits of the elements with high ionization energy are worse in the 9 mm torch but improve substantially with the 13 mm torch when used at the higher RF powers. The levels of MO^+ and M^{2+} ions are either inferior or comparable to those

obtained with the conventional torch. One additional shortcoming of these two systems is that the analyte sensitivity is extremely sensitive to sampling position, aerosol gas flow rate, and power. Optimizing signal for different analyte ions often requires different sampling positions, so operating conditions must be adjusted for each element or groups of elements.

This previous work demonstrates valuable concepts for reducing argon consumption, but no single method has seen widespread analytical use. In general, certain sacrifices in analytical performance accompany the reductions in argon flow. *A torch that can be operated routinely with low to moderate argon flow with the same analytical performance as a conventional ICP is still needed.* In the present study a new externally air-cooled torch is introduced specifically for ICP-MS. A stable plasma with analytical capabilities similar to those of a conventional system can be sustained with 4 L/min of outer argon flow at 850 W RF forward power. This new torch exploits the fact that the signal in ICP-MS comes from inside the axial channel at the tip of the initial radiation zone [29]. The plasma need not stream out of the torch into the atmosphere. Thus, air entrainment is not a problem as long as the tip of the sampler cone can be inserted flush with or inside the end of the torch. The outer tube can be cooled largely by air passing along the outside, so the argon outer gas flow can be reduced to the minimum necessary to maintain the proper shape and analytical properties of the ICP.

Experimental

Torch design and cooling system

The new, externally air-cooled torch is illustrated in Figure 1. The actual ICP is created in a commercial minitorch (ARL, Precision Glassblowing), which serves as the

internal structure. The outside tube of this minitorch is referred to as the "outer tube" in keeping with the usual nomenclature.

An air jacket made of quartz tubing (18 mm ID, 20 mm OD) is sealed onto the outer tube from the end of the torch to just below the flared out portion of the intermediate tube. The minitorch together with the air jacket has the same OD as a conventional torch, so it fits well inside the usual load coil. The downstream end of the external air jacket is fused to the rim of the outer tube. The upstream part of the jacket, on the contrary, cannot be fused to the exterior of the outer tube without warping the inner surface of the tube. This perturbation upsets the vortex flow of the Ar outer gas. Fortunately, this part of the jacket can be simply glued onto the torch with a high-temperature resistant ceramic cement (Sauereisen ceramic cement, Scientific Instrument Services). The external tube need not be high precision and need not be fixed with high mechanical tolerance.

The external tube is equipped with a tangential air inlet port (5 mm ID) on the upstream part. Four circular holes (2.5 mm diameter, equally spaced) are drilled near the edge of the downstream end. Two of these holes are shown at the far left of the external cooling tube in Fig. 1. Air from the laboratory pressurized air system is applied tangentially into the air inlet at approximately 70 L/min to cool the torch during operation. This air flow exits sideways out of the four circular holes through the load coil to minimize interference or air entrainment to the plasma. The length of the outer tube that extends beyond the intermediate tube was reduced to 17 mm to allow a sampling position farther inside the plasma. This was necessary to obtain the optimum signal from the smaller plasma created with this torch at lower flow rates.

In the subsequent discussion, the performance of the externally air-cooled torch is compared to that of a conventional torch. The latter is a standard "Fassel" torch, 20 mm OD, operated under conditions given in Table 1.

ICP-MS Instrumentation

The home-made ICP-MS device used throughout this study has been described previously [30,31]. A slight change was made in the ion lens in that the conical electrode (next to the extraction lens) was replaced by a tapered cylindrical lens. Sample solutions were introduced at 1 mL/min uptake rate by a peristaltic pump (Minipuls 2, Gilson). Aerosols are generated by an ultrasonic nebulizer (U-5000, CETAC Technologies, Inc.) with a conventional desolvator (heating temp. 140 °C, condenser temp. 0 °C). The dried aerosol was then transported with a Tygon transfer tubing (6 mm ID x 1.2 m long) to the torch housed inside a home-made shielding box. The coupling box sat on a 3-dimensional positioning device for full control of sampling position.

A 27.12 MHz radio frequency generator with automatic impedance-matching network (Type HFP-2500D, Plasma-Therm Inc.) was used to couple energy through a standard 3-turn water-cooled copper load coil (24 mm ID) to the plasma. A reversed geometry load coil (i.e., high voltage on upstream end, downstream end grounded at coupling box with ground strap) was used. Note that some secondary discharge persists with this load coil arrangement [24,25,32].

All argon gas flows (outer, auxiliary and nebulizer flows) were precisely controlled by a multichannel mass flow controller (Model 8284, Matheson Gas Products) with individual mass flow transducers specifically calibrated for each argon flow. The quadrupole mass analyzer (QPS-638, Extranuclear Laboratories, Inc.) was operated with unit mass

resolution. A multichannel analyzer (Turbo-MCS, EG&G Ortec), operated synchronously with the quadrupole, was utilized to acquire data in either a scanning mode or a single ion monitoring mode.

Ignition and operating procedure

The plasma is ignited without external cooling air or aerosol gas flow using an outer Ar gas flow rate of roughly 10-12 L/min and forward power of 1.3-1.5 kW. The impedance-matching network easily matches the load under these conditions. Thus, the process begins with an ICP operated under conventional gas flow and power conditions.

Once the plasma is ignited, the external cooling air and nebulizer flow are applied and the Ar outer gas flow and RF power are diminished gradually to the desired levels. This conversion process from a conventional ICP to a very low flow one takes only ~ 5 minutes. Operating parameters, particularly nebulizer gas flow rate and ion lens potentials, are then adjusted in the usual way to maximize the La^+ signal from a 100 ppb La solution while maintaining reasonable levels of LaO^+ and La^{2+}. Typical operating conditions are listed in Table 1.

Samples

Aqueous solutions of the elements of interest were prepared by diluting ICP standard stock solutions (1000 ppm, SPEX CertiPrep) to the desired concentrations, usually 0.1-1 ppm, with aqueous 1% HNO_3. Ultra purity nitric acid (ULTREX II, J.T. Baker Inc.) was used in the sample preparation along with high purity deionized water (18 MΩ-cm) obtained from a water purification system (Milli-Q Plus, Millipore).

Results and Discussion

General observations

One major drawback suffered by the other air-cooled torches mentioned earlier [21,22] is air turbulence in the plasma. In previous designs, the cooling air is blown directly onto the exterior of the torch to keep it from overheating. At the end of the torch, part of this cooling air is inadvertently deflected into the plasma, causing severe air entrainment and an unstable, cool and less analytically useful plasma. This problem is minimized with our current air-cooled torch. The holes in the end of the air jacket (Fig. 1) divert the cooling air out sideways through the load coil behind the wall of the shielding box (Fig. 2b, 2c) with little or no disturbance to the plasma.

As shown in Figure 2, the plasma obtained with this torch maintains the same basic annular shape and characteristic tail plume as a conventional plasma. The tail plume becomes shorter as the outer Ar flow rate decreases, and the plume does not stream out of the end of the torch. This is not a problem as long as the sampling cone of the MS can be positioned close enough to the end of the torch to extract ions before air becomes entrained.

Observation of the usual plasma zones by yttrium emission indicates that the normal analytical zone (NAZ, Y^+ blue emission) is also further upstream than usual under these conditions (lower outer flow rates). This plume of analyte M^+ ions expands radially as it travels further downstream, so the normal sampling position (9 mm from the load coil) is too far away. With a conventional torch, this sensitivity can generally be recovered by increasing the nebulizer flow rate to "push" the tip of the initial radiation zone (IRZ) further downstream to the sampling orifice. This tactic causes problems with the smaller plasma, as the high nebulizer flow disturbs the ICP and destabilizes the signal. Therefore, the outer tube

is shortened to 17 mm (beyond the end of the intermediate tube) to allow a deeper sampling position (6 mm from the load coil). The M^+ signal can then be maximized without using overly high aerosol gas flow.

Plasma stability curve

After ignition and conversion to the externally-cooled mode, a stable plasma can be sustained over a wide range of forward power and outer Ar flow rate. To best describe the operating conditions under which a stable plasma can be operated, a "plasma stability curve" like that described by Rezaaiyaan et al. [7], was implemented. The outer gas flow and RF forward power are reduced decrementally until the plasma extinguishes or the torch begins to overheat (i.e., it glows orange). The minimum flow rates at each forward power determined under such conditions are plotted on a power vs. flow rate curve (Fig. 3). This stability curve essentially illustrates the minimum Ar outer gas flow rate required to operate a stable plasma without melting the torch at any given RF forward power. These minimum flow rates range from 3.1 L/min at 650 W to 5.0 L/min at 1000 W. At each power level plotted in Fig. 3, the minimum outer Ar gas flow required to keep the torch cool is substantially lower than that necessary if the external air flow is not used. For example, at 850 W (i.e., the power used for most of the subsequent analytical studies), the torch glows orange at 7 L/min outer gas flow, compared to 3.6 L/min with the external air flow. Operating the plasma at a higher forward power requires higher Ar flow, presumably to provide better cooling of the inner wall of the torch and dissipate the higher heat levels. To provide a safety margin, the outer gas flow is generally maintained 0.5-1.0 L/min above the minimum limit from the stability curve.

Note that the stability curve starts at a forward power of 650 W. The plasma can be sustained at a power as low as 400 W with less than 2 L/min of Ar outer gas flow, but it

becomes spherical and unstable and is obviously too cool. These problems are similar to those reported by the earlier versions of externally cooled torches at very low total Ar flow [15-22]. Apparently, production of an ICP with the proper toroidal shape with a clear channel through the center requires an outer gas flow in substantial excess of the aerosol gas flow. On the other hand, a stable and robust plasma can be operated at a power above 1000 W with substantially higher Ar flow to keep the torch from melting. This is not our main goal and has not been pursued further.

Effects of power and aerosol gas flow

With a new plasma, a search for analytically useful operating parameters is obviously necessary. Figure 4a displays the normalized Co^+ signal obtained at various operating powers. The aerosol gas flow rates are re-adjusted to produce the optimum signal under each condition. The usual "mountain" shaped plot of M^+ signal vs. aerosol gas flow rate is obtained at each power level (Fig. 5) [33,34].

In Fig. 4a, the best obtainable signal gradually improves as the power is increased between 650-850 W, with little additional improvement at higher power. The signal precision, represented by the relative standard deviation (RSD, n ~ 200), is shown in Fig. 4b. The RSD remains at 3-4% when the plasma is operated below 900 W but rises steeply above 950 W. This drastic rise can be attributed to the high aerosol gas flow rate required to optimize the signal at higher operating powers (Fig. 5), which consequently degrades the stability of the low-flow plasma. This observation is similar to those reported by Ross et al. [27] when a 9-mm torch was studied.

The rising trend of Co^+ signal (ionization energy = IE = 7.86 eV) at lower operating powers implies that the plasma may not be as hot and efficiently-ionized as a conventional

plasma under these conditions. The trend clearly suggests that the ionization efficiency of the plasma is raised as the operating power increases. Nevertheless, Fig. 4a shows that the signal is nearly maximum at 850 W; presumably, this is enough power for the ionization efficiency for Co to approach 100%. This deduction is supported by measurement of the signals for other elements. A solution containing 250 nM of Ga and As was utilized to determine the relative degree of ionization (As^+/Ga^+) in the plasma with the air-cooled torch at 850 W, compared to that from a conventional torch at 1300 W. The ratios were 0.474 for the air-cooled torch and 0.475 for the conventional plasma, which suggests that both plasmas have a similar ionization efficiency under these conditions.

Similar behavior was also observed for some other elements as illustrated in Fig. 6. Elements with lower ionization energy (Rb, Sr and Mn) exhibit the same trends as Co. The signal for As, which is not fully ionized in a conventional plasma due to its high IE (9.81 eV), continues to increase slightly after 850 W as the plasma becomes more robust. However, operating the plasma under these extreme conditions is not necessarily beneficial as the plasma and torch become somewhat unstable and the signal stability deteriorates from that at the best aerosol gas flow rate (Figure 4b). At higher power the plasma tends to produce more doubly charged ions as well.

The best signal to noise ratio (S/N) is obtained when the plasma is operated at a forward power between 850-900 W, so 850 W is chosen as the primary operating condition in subsequent experiments. The sensitivity for Co^+ obtained under this condition (2.65×10^6 counts.s^{-1}.ppm^{-1}) is similar to that produced by a conventional torch (2.38×10^6 counts.s^{-1}.ppm^{-1}) operated under its typical operating conditions (Table 1), while the precision is comparable as well.

Under optimum conditions for both low-flow and conventional ICP, the Co^+ sensitivities are almost the same under the two conditions, even though the aerosol gas flow rate is significantly lower for the low-flow torch. With the ultrasonic nebulizer used, the gas flow does not participate directly in droplet production. Even so, transport of droplets out of the spray chamber would be expected to be higher at higher gas flow rate, so better sensitivity at the optimum gas flow would be expected for the conventional torch. As shown in Fig. 2, under the combination of power, aerosol gas flow rate, and sampling position that maximizes analyte signal, the gap between the tip of the IRZ and the sampling orifice is 1 to 2 mm for either the conventional ICP or the new, low-flow version. A similar effect is commonly seen on most ICP-MS devices. It seems like the top of the sensitivity "mountain" generally corresponds to a sampling position just downstream from the tip of the IRZ for many combinations of torch design and operating conditions. This position serves as a good internal reference point for describing the performance of a variety of ICP-MS devices, like the "OH bullet" [35] and other reference concepts described for ICP-AES [29].

Effect of auxiliary gas flow rate

Many low-flow torches do not require auxiliary gas flow [6,10-11,14,17-22]. Although the ICP used in the present study remains operational without the auxiliary gas flow, this latter flow does affect precision and stability strongly (Fig. 7). The Co^+ signal increases slightly as the auxiliary gas flow rate is raised up to roughly 0.6-0.7 L/min and then reaches a plateau. On the other hand, the signal precision and consequent S/N improve greatly as the flow increases to 0.4-0.7 L/min. The signal stability then becomes worse again as the auxiliary flow is increased further. The best precision is achieved at 0.6 L/min, hence, this flow was subsequently incorporated in the primary operating conditions for all other

experiments. The 3% RSD achieved under these conditions is comparable to that obtainable with this device with a conventional ICP.

Multielement optimization

One weakness of some previous low-flow torches is greater element-to-element variability in optimum operating conditions than with a conventional ICP [27,28]. Figure 8 displays the influence of the nebulizer gas flow rate on the normalized signals of various elements across the full mass range in the periodic table. All analyte ions behave similarly and maximize at the same flow rate (~ 0.73 L/min). The only apparent difference is that the signals of La^+ and W^+ decline more extensively than those of the others as the flow is increased beyond the optimum value. These elements form strong oxide ions (dissociation energy, D_0 (LaO^+) = 8.89 eV, D_0 (WO^+) = 6.70 eV), which are especially abundant at high aerosol gas flow [34,36,37]. Thus, the plasma obtained with this air-cooled torch does not require individual optimization for different elements.

Under the optimum operating conditions, the sensitivities of various elements obtained from the air-cooled torch were measured and are compared to those produced by a conventional torch in Table 2. The optimum nebulizer gas flow rates used for the air-cooled torch and conventional torch were 0.73 and 1.01 L/min respectively. The sensitivities of all analyte ions for the air-cooled torch were comparable to within 20% of those generated by its conventional counterpart, which further corroborates the preceding discussion about the similarity of sensitivity if plasma conditions are adjusted so that ions are extracted from the same spot relative to the IRZ.

MO^+ and M^{2+} ions and secondary discharge

ICP-MS users are always concerned about the formation of oxide and doubly charged ions, especially with the low-flow torches. Excessive amounts of MO^+ and M^{2+} ions create potential interferences; M^{2+} ions also indicate the presence of a secondary discharge, which increases the ion kinetic energy and degrades the sampling cone, as shown in the study of a water-cooled torch [26]. In the current investigation, no such visual discharge was observed under the typical operating conditions. Lanthanum produces both MO^+ and M^{2+} significantly and is therefore selected as a representative element for studying such interference with our air-cooled torch.

The effect of the nebulizer gas flow rate on the La^+ signal and signal ratios for both LaO^+/La^+ and La^{2+}/La^+ are illustrated in Fig. 9. Generally the LaO^+/La^+ ratio from the air-cooled plasma is higher than that from the conventional plasma. Under the nebulizer gas flow rate that produces the maximum La^+ signal ("top of the mountain") [33,34], the signal ratio LaO^+/La^+ is 3.52% for the air-cooled plasma, compared to 0.97% for its conventional counterpart. Nonetheless, the LaO^+/La^+ ratio of the air-cooled plasma can be reduced drastically to 0.86% if the nebulizer gas flow rate is decreased slightly to 0.70 L/min. Only ~ 10% of the sensitivity for La^+ is sacrificed. Table 2 indicates that even with this loss, the sensitivity for various elements remains comparable to that obtained from the conventional plasma.

Under these conditions, Fig. 9 shows that the La^{2+}/La^+ ratio from the air-cooled plasma is only 1.07%, which is substantially lower than the ~ 4% ratio seen from the conventional plasma at its optimum aerosol gas flow rate. Altogether, operating the air-cooled plasma with an aerosol gas flow rate slightly lower than that which maximizes M^+

signal lowers the abundance of both MO^+ and M^{2+} with little sacrifice in M^+ sensitivity. The secondary discharge typically becomes worse at low power [24,25], but aerosol gas flow rate is reduced accordingly, and the sampler is inserted further into the plasma. Both these latter conditions mitigate the severity of the discharge, and the smaller La^{2+}/La^+ ratios from the air-cooled torch indicate that the secondary discharge is not a problem in this case.

Background ions

Many torches for AES that use extremely low Ar flow suffer from air entrainment, which cools the plasma, produces molecular emission or polyatomic ions, and degrades stability [8,9,15-22]. It is our experience that a scan of the background mass spectrum is a good tool to evaluate such effects. Figure 10a is a mass spectrum from the air-cooled plasma operated under its typical operating conditions (Table 1); that of a conventional plasma is displayed in Fig. 10b. In this experiment the detector gain is reduced and a small retarding voltage is applied to the quadrupole to minimize counting losses for the major background ions.

The low-flow plasma (Fig. 10a) produces a similar spectrum and background species as the conventional torch (Fig. 10b). The relative abundances of some species (OH^+, H_2O^+, O_2^+ and ArH^+) are moderately higher in the air-cooled plasma. The combination of solvent load and shorter residence time in the smaller externally cooled plasma might contribute to the less efficient dissociation of these species. Regardless, the background spectrum from the air-cooled plasma does not show signs of severe cooling or other disturbance from air entrainment. The outer Ar flow of 4.50-4.75 L/min used throughout these experiments provides adequate protective shielding, as long as the sampling orifice is flush with or inside

the end of the torch. If the plasma is retracted further from the end of the torch than the position shown in Fig. 2, air entrainment becomes an obvious problem.

Matrix effects

Matrix effects are generally described as a change of analyte signal under the influence of one or more concentrated concomitant elements. In ICP-MS, the matrix effect normally results in a suppression of signal [33,38-40], although some enhancements have been reported [41,42]. The current investigation is performed by monitoring the influence of Na matrix on signals for three analyte elements (Co^+, In^+ and Tl^+), which represent elements of low, moderate and high atomic weights. Naturally, such matrix effects are monitored for both the new air-cooled plasma and the conventional one. Both plasmas are operated under their own optimum operating conditions, as described above. Recall that a highly-efficient ultrasonic nebulizer is used, so the matrix effect should be more severe than that seen with a typical pneumatic nebulizer.

The signals obtained are normalized and plotted against Na concentration as shown in Figure 11a-11c. For the conventional plasma, the signal suppression for all three analyte ions follows the trends expected; Co^+ signal starts to decline in the presence of ~ 1 ppm Na and continues to fall considerably as the concentration is increased. Less than 0.02% of the original Co^+ signal remains in the 1000 ppm matrix solution. The suppression effects are less severe for In^+ and Tl^+, as more than 10 and 15% of the original signal are recovered in 1000 ppm matrix solutions. This observation agrees with other studies [31,43] in that heavier ions with greater kinetic energies are more tolerant to the matrix suppression.

For the air-cooled plasma, the matrix effect curve for Co^+ is very similar to that from the conventional ICP. Actually, the suppression effects for In^+ and Tl^+ in the air-cooled

plasma are slightly less severe than those from the conventional plasma. In general, both plasmas appear to possess comparable degrees of tolerance to matrix suppression.

Conclusions

An externally air-cooled torch has been developed with an air jacket added to a minitorch. This external air flow allows drastic reduction of the outer Ar flow, and a concomitant decrease in forward power, without other modifications to the load coil or the instrument. For ICP-MS, this low-flow plasma (total Ar flow ~ 6 L/min) produces the same basic analytical performance as a conventional ICP.

The plasma obtained under these conditions is slightly smaller than usual. Therefore, the sampling cone is thrust inside the end of the torch, so the ions are extracted before air can be entrained. The precision is sensitive to auxiliary gas flow; 0.5-0.6 L/min is necessary. An aerosol gas flow rate of 0.72-0.75 L/min provides maximum sensitivity for virtually all analyte elements, which indicates that the same conditions can be used for measurement of many elements. Although the metal oxide ion ratios are slightly higher than those obtained with a conventional plasma under this aerosol gas flow, a small reduction of the aerosol gas flow rate resolves this problem with little sacrifice in sensitivity. M^{2+}/M^{+} ion ratios are comparable to those produced by its conventional counterpart. The air-cooled plasma exhibits no signs of air disturbance or additional background ions. The secondary discharge and matrix effects are similar to those obtained with a conventional plasma.

In all, the externally air-cooled, low-flow torch is very attractive for reduction of operating costs in ICP-MS with no compromise in analytical performance. The same torch has been in use for 6 months or ~ 300-400 hours of ICP operation. This method of cooling

the torch has other potential uses in ICP spectrometry. In ICP-MS experiments with a metal shield between the load coil and torch, overheating and gradual degradation of the shield can be a problem. The external tube of this new torch should be cooler than the outer tube of a conventional one, which should mitigate this problem and extend the lifetime of the shield or facilitate its fabrication from inexpensive metals. The new torch is also viable for emission spectrometry if the plasma is viewed axially through a sampling orifice. This latter work will be reported in an upcoming paper [44].

Acknowledgements

Ames Laboratory is operated for the U. S. Department of Energy by Iowa State University under contract no. W-7405-Eng-82. This research was supported by the Office of Basic Energy Sciences. The ultrasonic nebulizer was provided by CETAC Technologies, Inc. ICP elemental standards were provided by SPEX CertiPrep. Trond Forre of the Chemistry Department Glassblowing Shop was of great assistance in sealing the external tubes.

References

1. P. A. M. Ripson, L. de Galan, *Spectrochim. Acta Part B* 38 (1983) 707.
2. R. H. Scott, V. A. Fassel, R. N. Kniseley, D. E. Nixon, *Anal. Chem.* 46 (1974) 75.
3. G. W. Dickinson, V. A. Fassel, *Anal. Chem.* 41 (1969) 1021.
4. S. Greenfield, D. T. Burns, *Anal. Chim. Acta* 113 (1980) 205.
5. J. L. Genna, R. M. Barnes, C. D. Allemand, *Anal. Chem.* 49 (1977) 1450.
6. C. D. Allemand, R. M. Barnes, *Appl. Spectrosc.* 31 (1977) 434.

7. R. Rezaaiyaan, G. M. Hieftje, H. Anderson, H. Kaiser, B. Meddings, *Appl. Spectrosc.* 36 (1982) 627.

8. R. Rezaaiyaan, G. M. Hieftje, *Anal. Chem.* 57 (1985) 412.

9. A. Montaser, G. R. Huse, R. A. Wax, S. Chan, D. W. Golightly, J. S. Kane, A. F. Dorrzapf Jr., *Anal. Chem.* 56 (1984) 283.

10. R. N. Savage, G. M. Hieftje, *Anal. Chem.* 51 (1979) 408.

11. C. D. Allemand, R. M. Barnes, C. C. Wohlers, *Anal. Chem.* 51 (1979) 2392.

12. R. N. Savage, G. M. Hieftje, *Anal. Chem.* 52 (1980) 1267.

13. R. N. Savage, G. M. Hieftje, *Anal. Chim. Acta.* 123 (1981) 319.

14. A. D. Weiss, R. N. Savage, G. M. Hieftje, *Anal. Chim. Acta.* 124 (1981) 245.

15. M. E. Britske, J. S. Sukach, L. N. Filimonov, *Zh. Prikl. Spectrosc.* 25 (1976) 5.

16. G. R. Kornblum, W. van der Waa, L. de Galan, *Anal. Chem.* 51 (1979) 2378.

17. H. Kawaguchi, T. Ito, S. Rubi, A. Mizuike, *Anal. Chem.* 52 (1980) 2440.

18. P. A. M. Ripson, L. de Galan, *Spectrochim. Acta Part B* 38 (1983) 707.

19. H. Kawaguchi, T. Tanaka, S. Muira, J. Xu, A. Mizuike, *Spectrochim. Acta Part B* 38 (1983) 1319.

20. P. A. M. Ripson, E. B. M. Jansen, L. de Galan, *Anal. Chem.* 56, (1984) 2329.

21. P. A. M. Ripson, L. de Galan, J. W. de Ruiter, *Spectrochim. Acta Part B* 37 (1982) 733.

22. P. S. C. van der Plas, A. C. de Waaij, L. de Galan, *Spectrochim. Acta Part B* 40 (1985) 1457.

23. D. J. Douglas, J. B. French, *J. Anal. At. Spectrom.* 6 (1991) 323.

24. A. L. Gray, R. S. Houk, J. G. Williams, *J. Anal. At. Spectrom.* 2 (1987) 13.

25. K. E. Jarvis, A. L. Gray, R. S. Houk, Handbook of Inductively Coupled Plasma Mass Spectrometry, Blackie, London, 1992, p. 21.

26. P. S. C. van der Plas, L. de Galan, *Anal. Chem.* 60 (1988) 372.

27. B. S. Ross, D. M. Chambers, G. H. Vickers, P. Yang, G. M. Hieftje, *J. Anal. At. Spectrom.* 5 (1990) 351.

28. B. S. Ross, P. Yang, G. M. Hieftje, *Appl. Spectrosc.* 45 (1991) 190.

29. S. R. Koirtyohann, J. S. Jones, D. A. Yates, *Anal. Chem.* 52 (1980) 1965.

30. K. Hu, P. S. Clemons, R. S. Houk, *J. Am. Soc. Mass Spectrom.* 4 (1993) 16.

31. K. Hu, R. S. Houk, *J. Am. Soc. Mass Spectrom.* 4 (1993) 28.

32. H. Niu, R. S. Houk, *Spectrochim. Acta Part B* 51 (1996) 779.

33. S. H. Tan, G. Horlick, *J. Anal. At. Spectrom.* 2 (1987) 745.

34. G. Horlick, A. Montaser, Analytical Characteristics of ICPMS, in A. Montaser, Ed. Inductively Coupled Plasma Mass Spectrometry, Wiley-VCH: New York, 1998, pp. 503-588.

35. P. J. Galley, G. M. Hieftje, *J. Anal. At. Spectrom.* 8 (1993) 715.

36. F. Vanhaeche, R. Dams, C. Vandecasteele, *J. Anal. At. Spectrom.* 8 (1993) 433.

37. H. P. Longerich, *J. Anal. At. Spectrom.* 4 (1989) 491.

38. J. A. Olivares, R. S. Houk, *Anal. Chem.* 58 (1986) 20.

39. J. S. Crain, R. S. Houk, F. G. Smith, *Spectrochim. Acta Part B* 44 (1989) 1355.

40. D. C. Gregoire, *Appl. Spectrosc.* 41 (1987) 893.

41. C. J. Pickford, P. M. Brown, *Spectrochim. Acta Part B* 41 (1986) 183.

42. A. R. Date, Y. Y. Cheung, M. E. Stuart, *Spectrochim. Acta Part B* 42 (1987) 3.

43. D. C. Gregoire, *Spectrochim. Acta Part B* 42 (1987) 895.

44. T. Hasan, N. Praphairaksit, R. S. Houk, in preparation.

Table 1. Typical operating conditions

Operating Parameter	Conventional Torch	Low-flow Torch
Plasma forward power (W)	1300	850
Reflected power (W)	< 5	< 5
Argon flow (L/min)		
Outer gas	15.00	4.50-4.75
Auxiliary gas	1.00	0.60
Nebulizer gas	1.02	0.73
Cooling air flow (L/min)	-	70
Solution uptake rate (mL/min)	1.00	1.00
Sampling position (mm from load coil)	9	6
Sampling orifice (mm)	1.40	1.40
Skimmer orifice (mm)	1.35	1.35

Table 2. Relative sensitivities of various elements obtained with the air-cooled torch and conventional torch under its optimum operating conditions.

Analyte ion	Sensitivity ($cts.s^{-1}.ppm^{-1}$)	
	Air-cooled torch	Conventional torch
$^{45}Sc^{+}$	$3.22x10^{6}$	$3.10x10^{6}$
$^{55}Mn^{+}$	$3.47x10^{6}$	$3.28x10^{6}$
$^{59}Co^{+}$	$2.65x10^{6}$	$2.38x10^{6}$
$^{75}As^{+}$	$4.97x10^{5}$	$5.17x10^{5}$
$^{88}Sr^{+}$	$2.81x10^{6}$	$2.47x10^{6}$
$^{115}In^{+}$	$3.25x10^{6}$	$3.51x10^{6}$
$^{139}La^{+}$	$3.54x10^{6}$	$3.36x10^{6}$
$^{184}W^{+}$	$2.04x10^{6}$	$2.23x10^{6}$
$^{208}Pb^{+}$	$3.96x10^{6}$	$4.52x10^{6}$

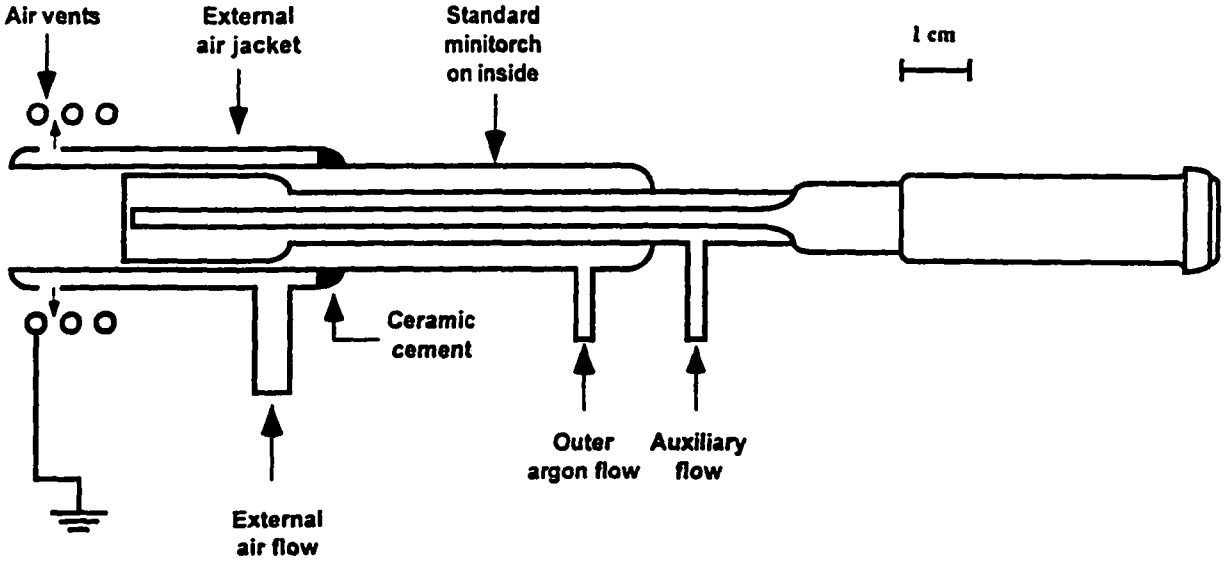

Figure 1. Schematic diagram of the new externally air-cooled torch.

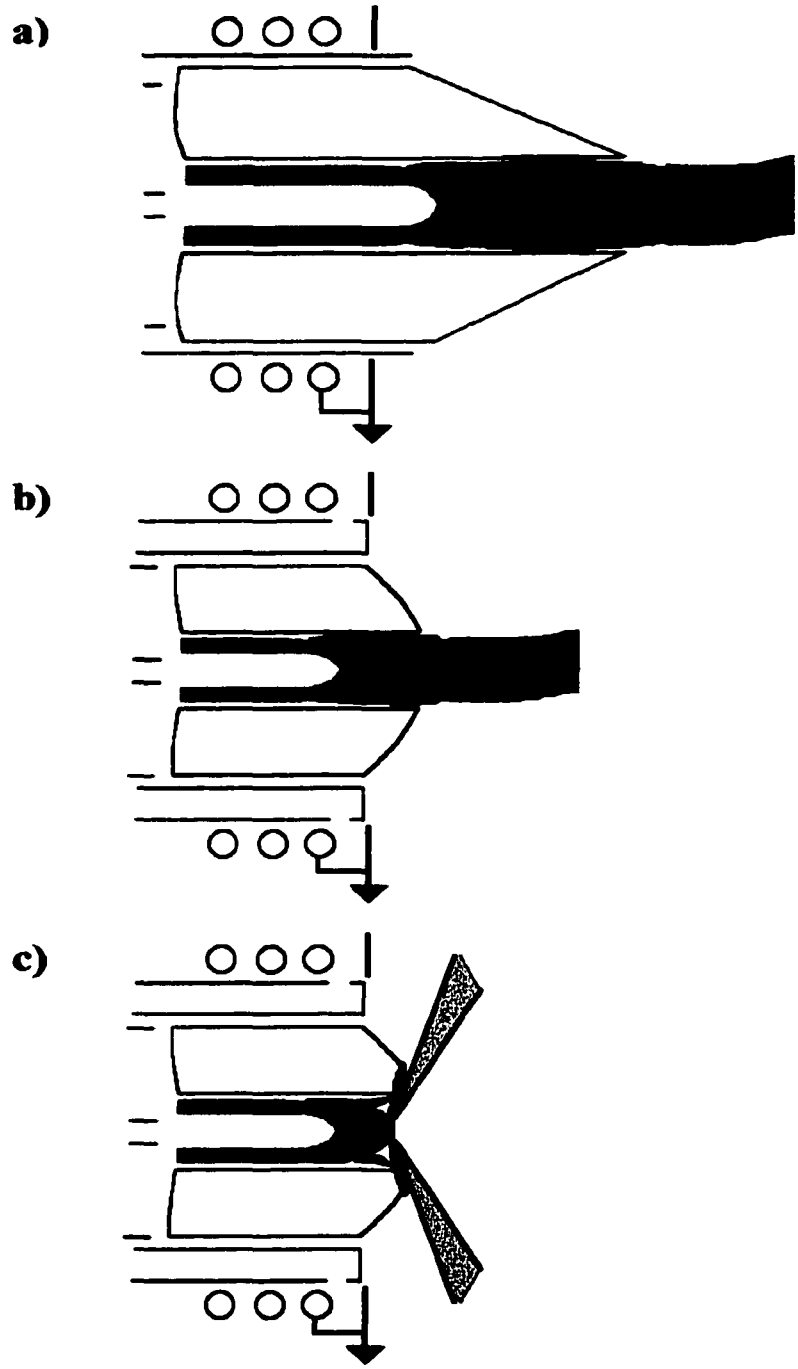

Figure 2. Drawing of a) conventional ICP, b) new externally air-cooled torch and ICP, 850 W, 0.75 L/min aerosol gas flow rate, and c) air-cooled ICP when sampled at the typical sampling position. A concentrated solution of yttrium is introduced to delineate the various zones of the plasma.

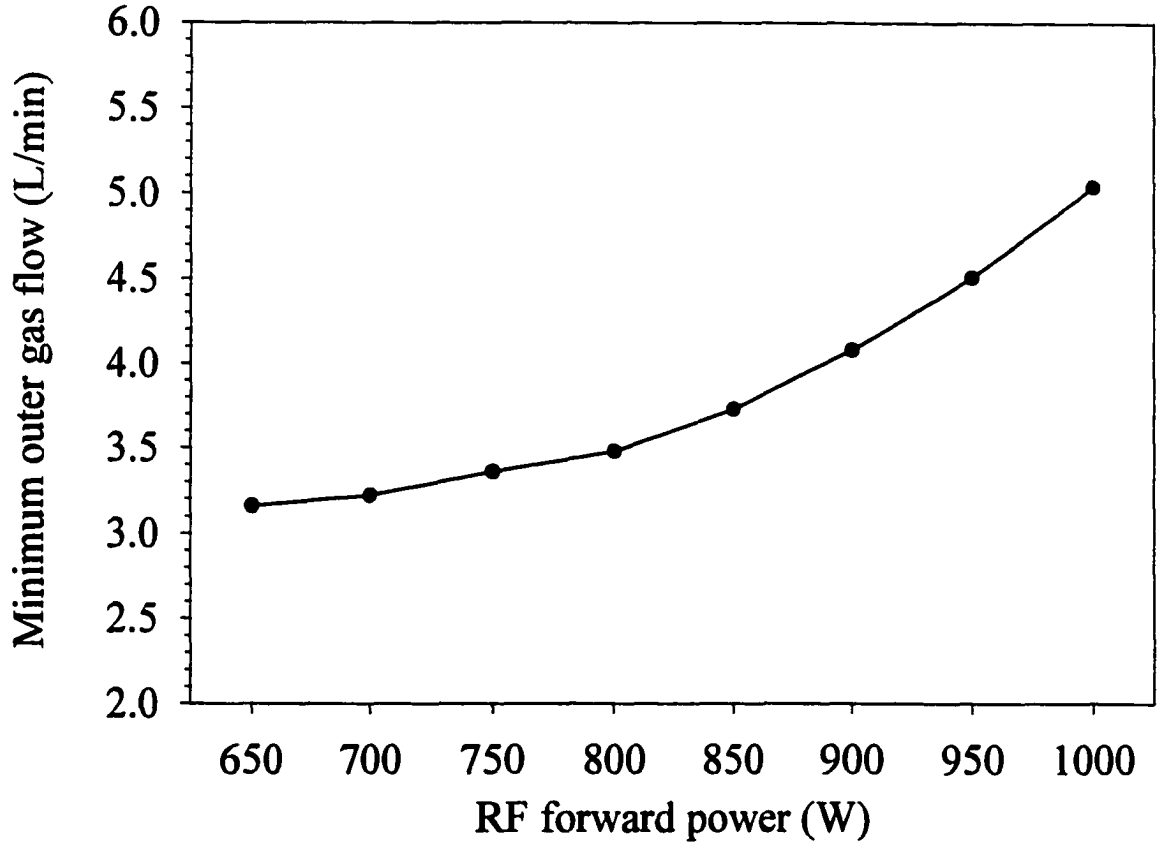

Figure 3. Plasma stability curve showing minimum outer gas flow required to safely operate the plasma at each forward power.

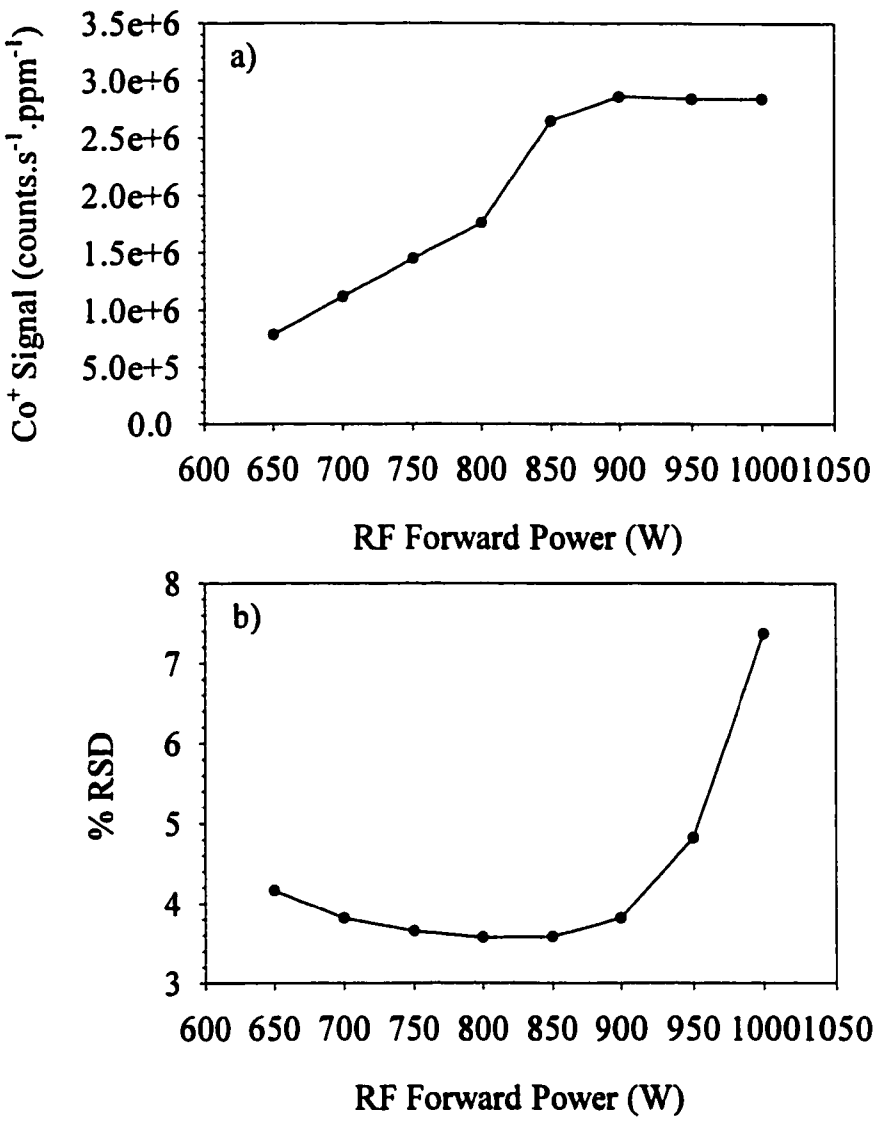

Figure 4. Effects of RF forward power on a) Co^+ signal and b) signal precision (%RSD, n = 200) for the plasma obtained with the air-cooled torch.

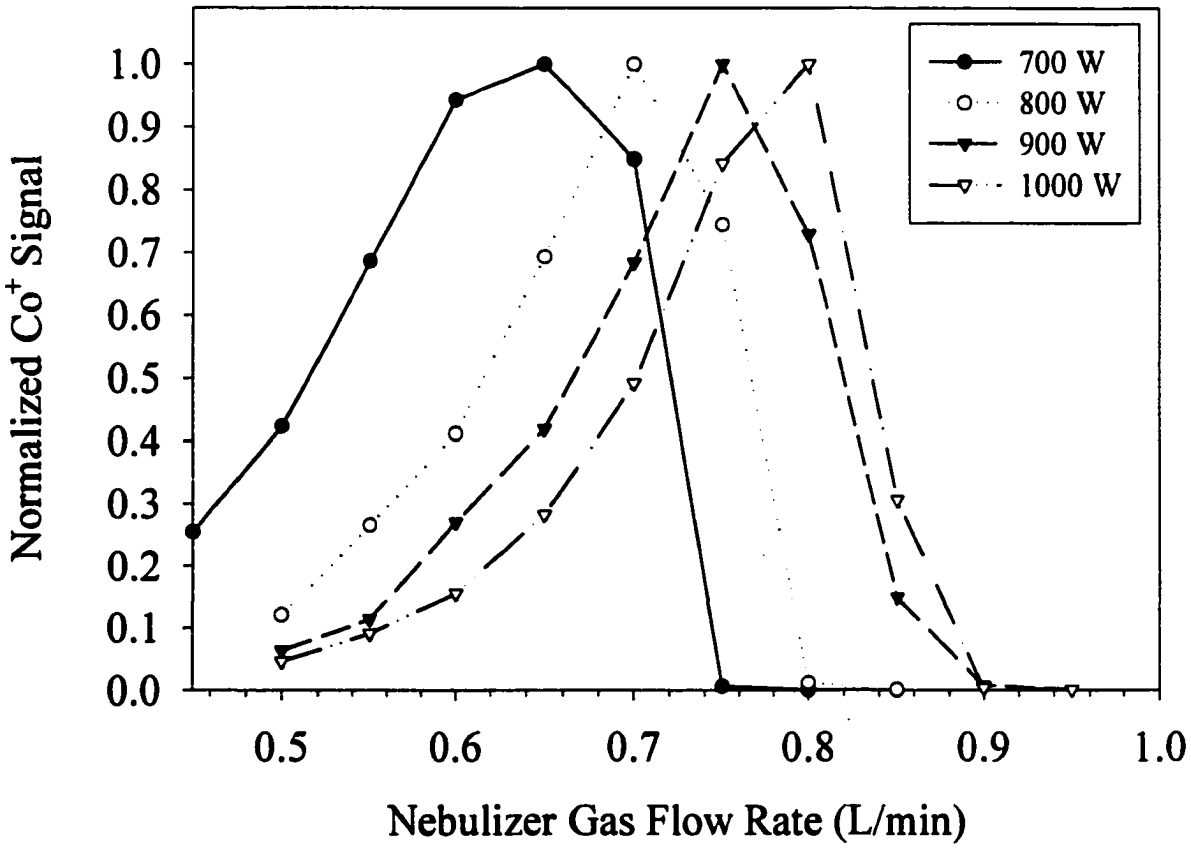

Figure 5. Plots of normalized Co^+ signal vs. nebulizer gas flow rate obtained with the air-cooled torch at various RF powers.

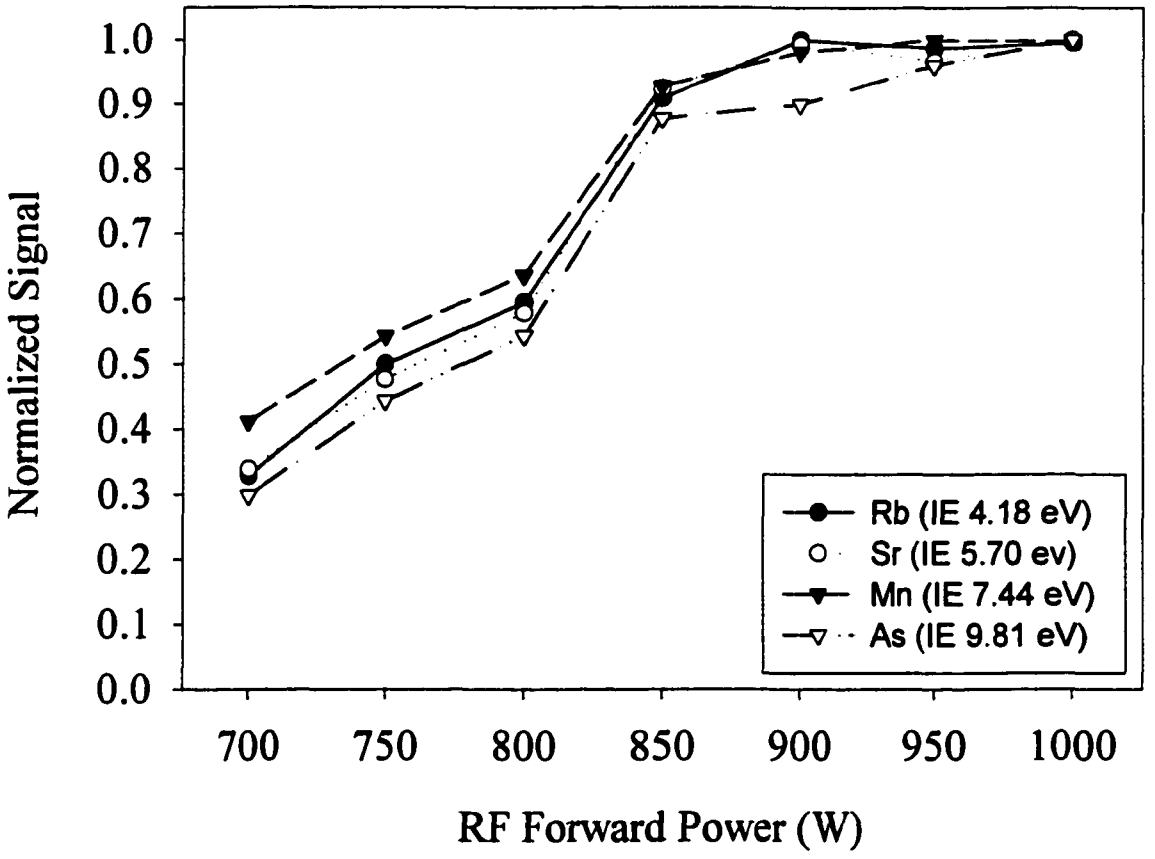

Figure 6. Effect of RF forward power of the air-cooled plasma on the signals of various analyte ions.

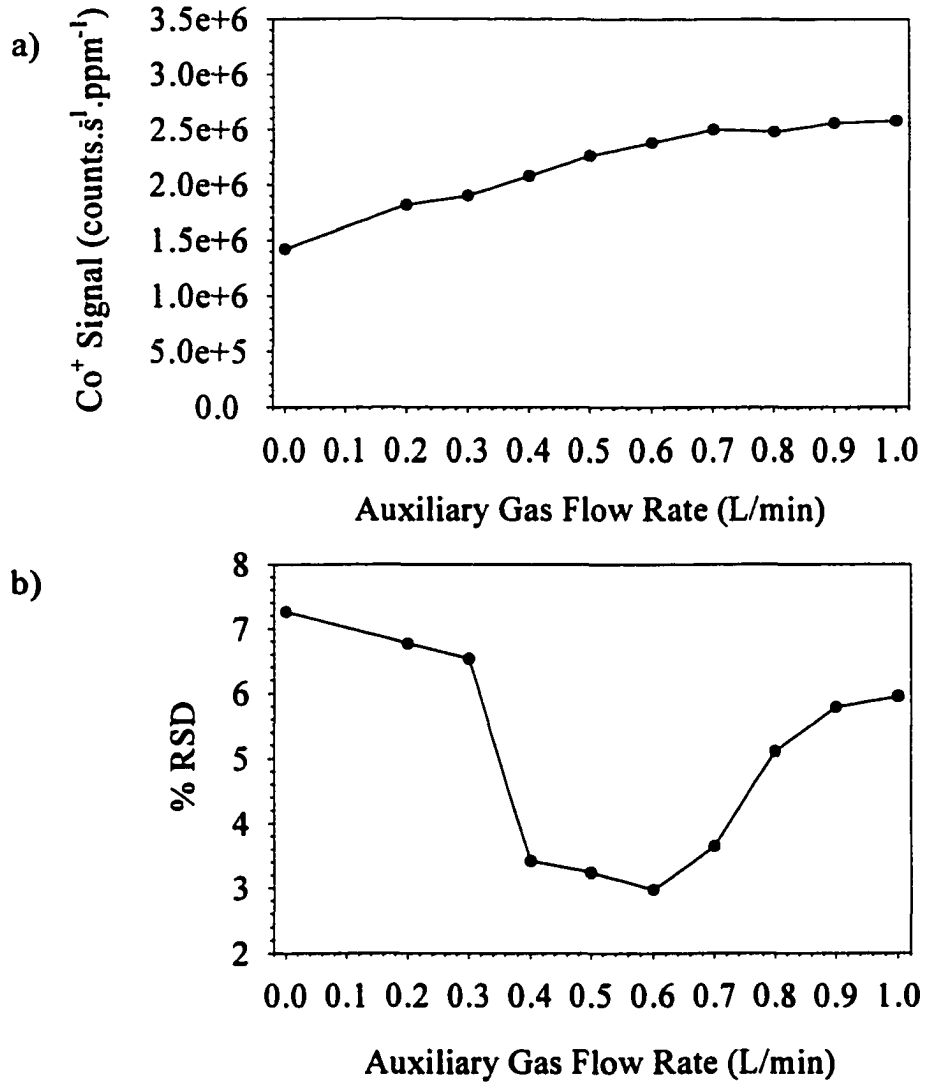

Figure 7. Influence of auxiliary gas flow rate on a) Co^+ signal and b) signal precision (%RSD, n = 200) from the air-cooled plasma operated at 850 W.

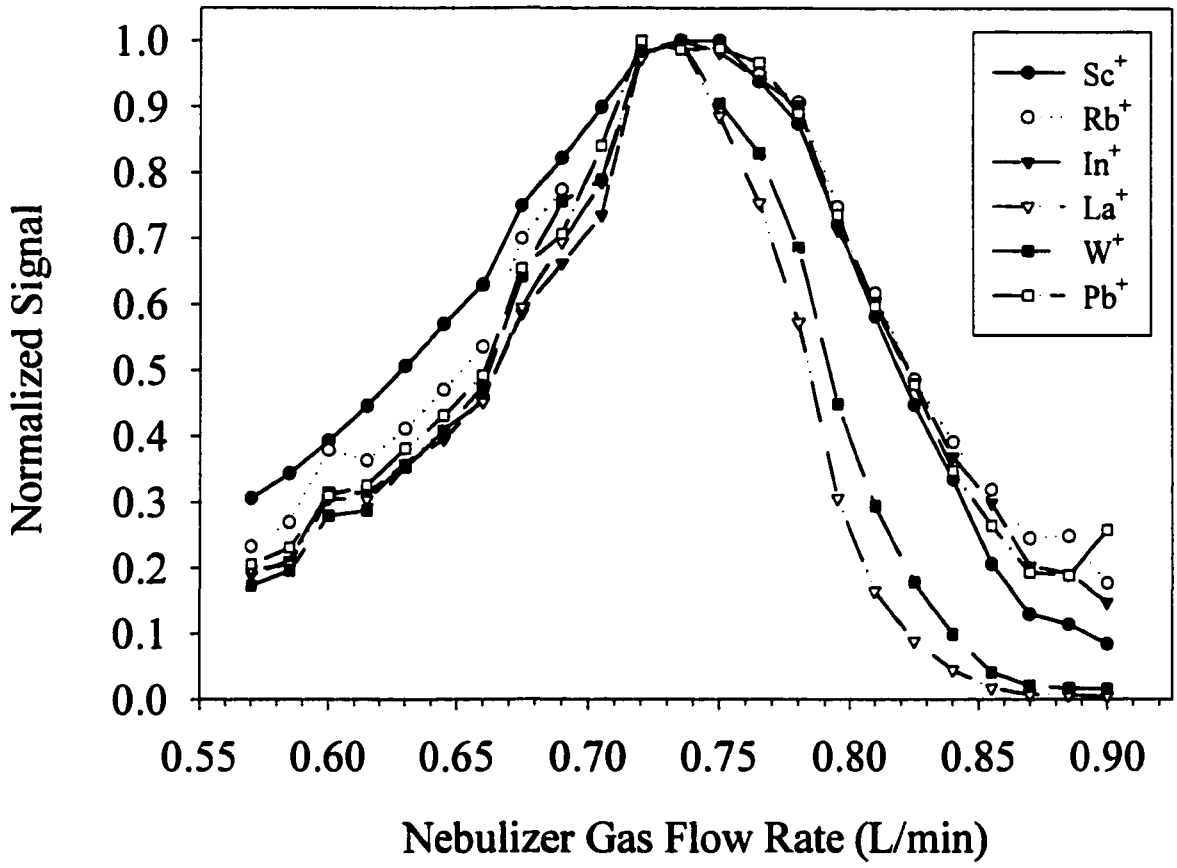

Figure 8. Dependence of various analyte ion signals on aerosol gas flow rate for the air-cooled plasma.

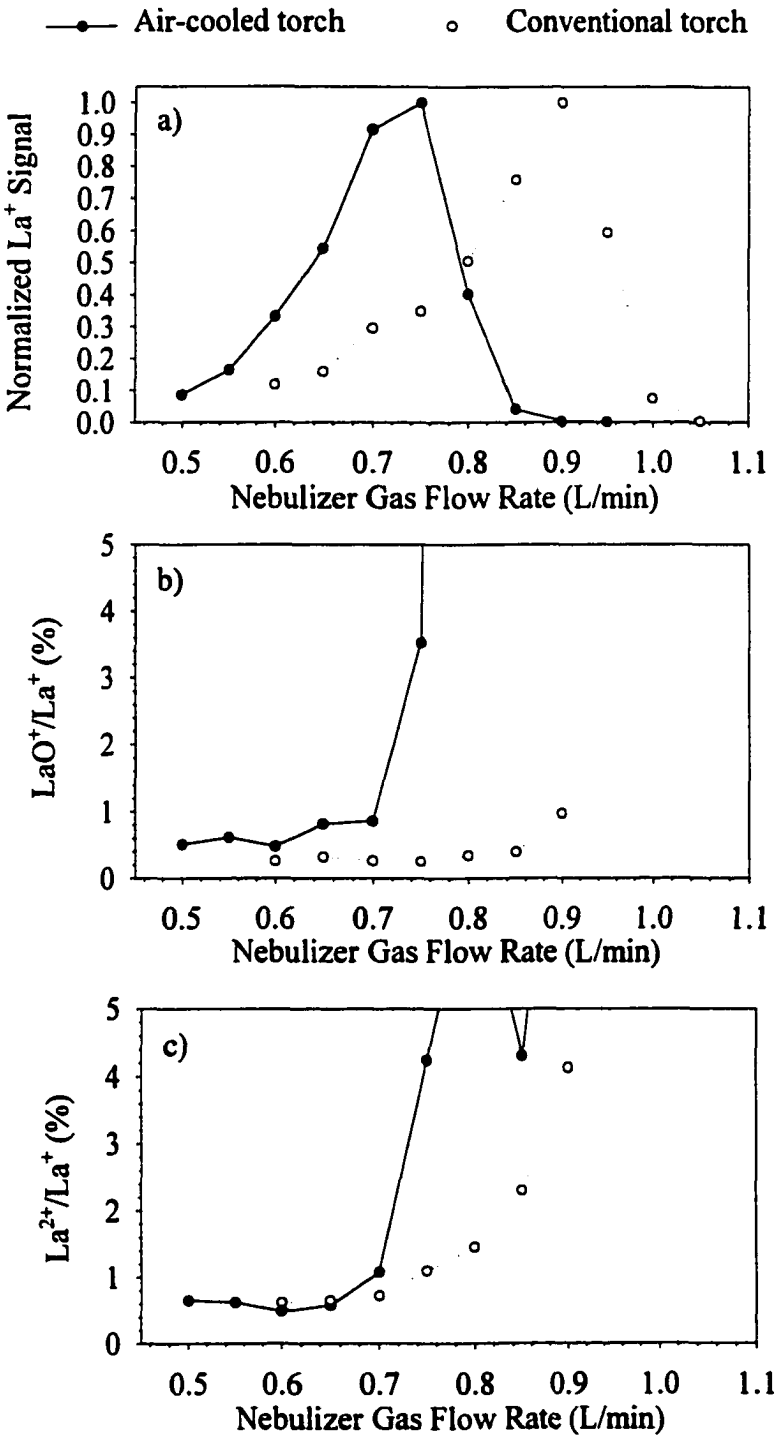

Figure 9. Effect of nebulizer gas flow rate on a) normalized La^+ signal, b) LaO^+/La^+ and c) La^{2+}/La^+ obtained with the air-cooled torch and a conventional torch.

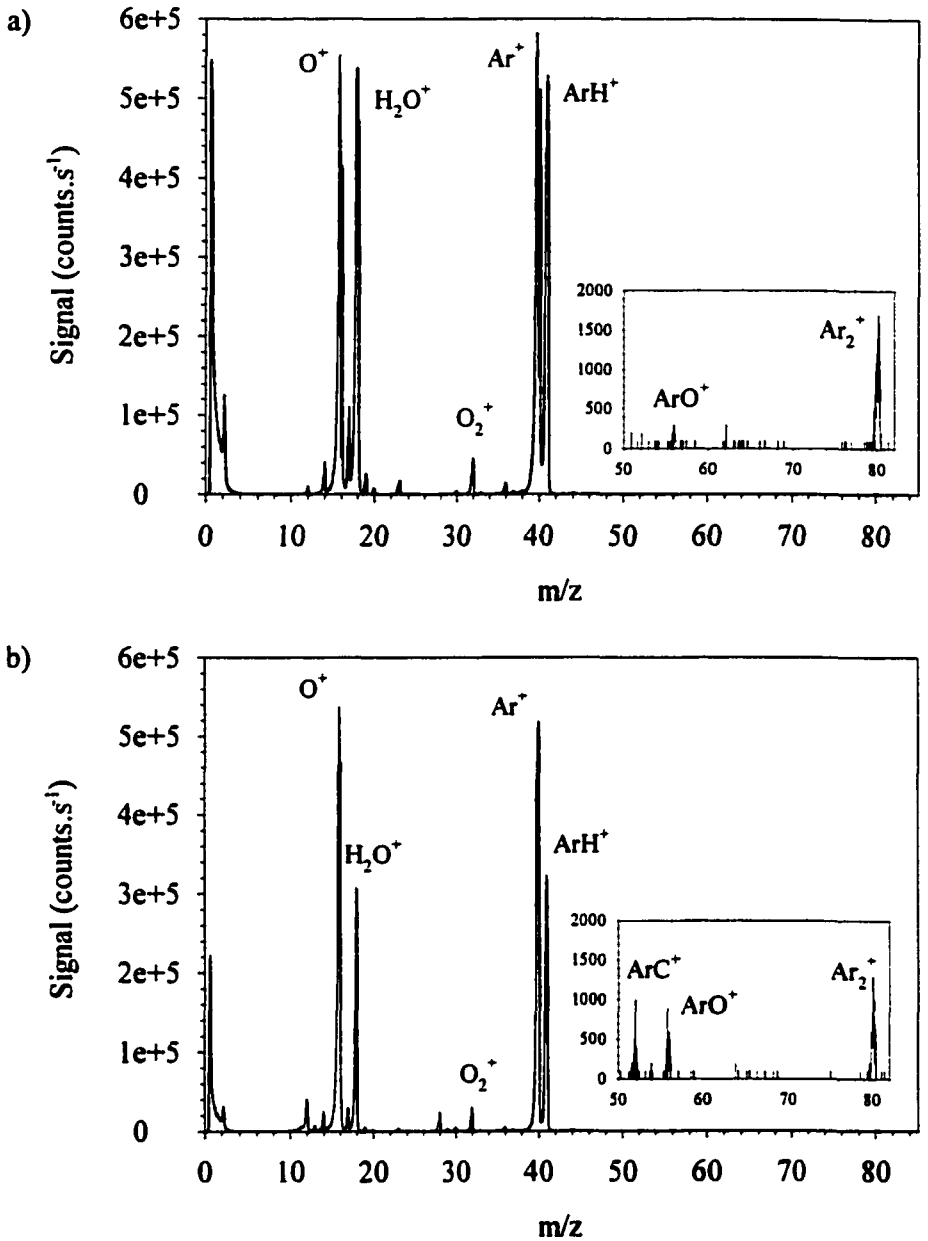

Figure 10. Background mass spectra obtained with a) the air-cooled plasma, and b) conventional plasma, both operated under their own optimum operating conditions. The sample is deionized water.

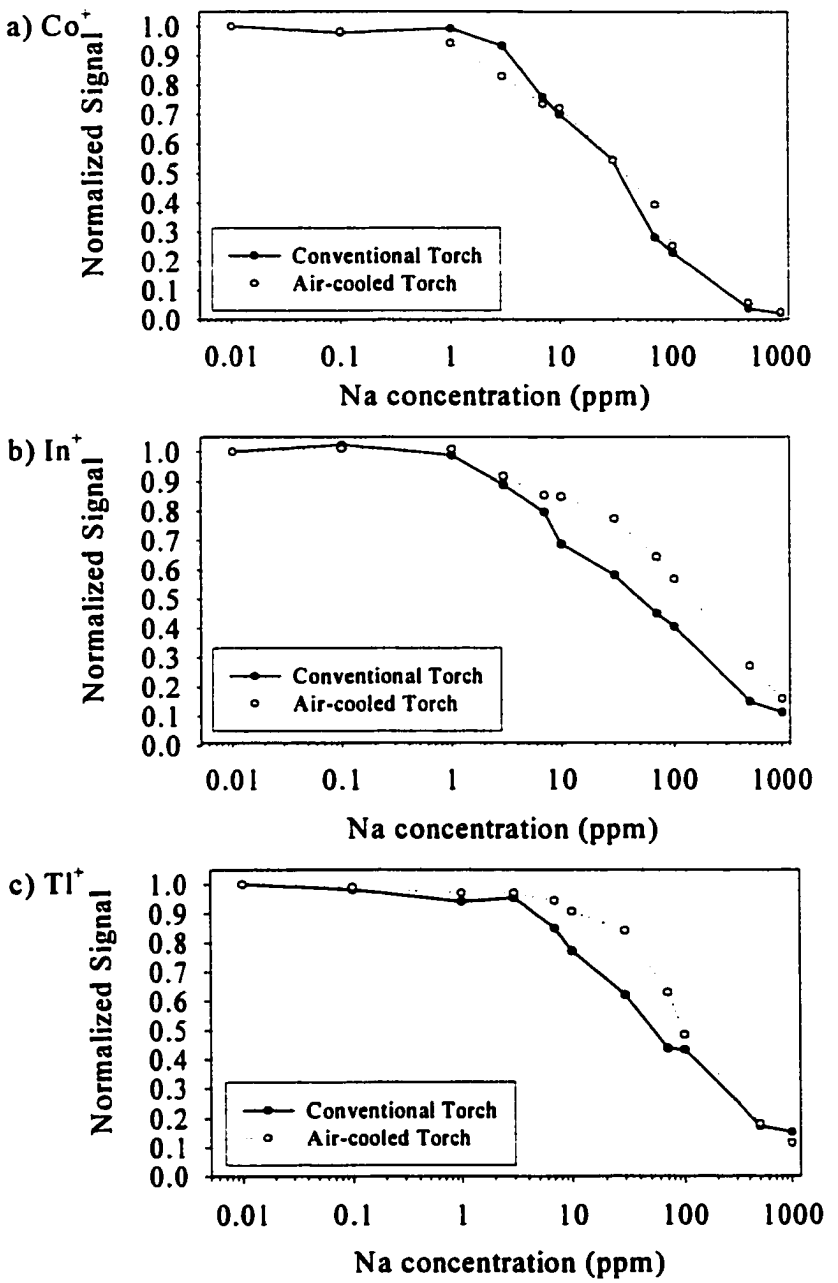

Figure 11. Influence of Na matrix at various concentrations on the signals of a) Co^+, b) In^+ and c) Tl^+ obtained from the air-cooled and conventional torches.

CHAPTER 3. REDUCTION OF SPACE CHARGE EFFECTS IN INDUCTIVELY COUPLED PLASMA MASS SPECTROMETRY USING A SUPPLEMENTAL ELECTRON SOURCE INSIDE THE SKIMMER: ION TRANSMISSION AND MASS SPECTRAL CHARACTERISTICS

A paper submitted to Analytical Chemistry

Narong Praphairaksit and R. S. Houk*

Abstract

An electron source adapted from a conventional electron impact ionizer has been added to the skimmer to suppress space charge effects in inductively coupled plasma mass spectrometry (ICP-MS). Electrons from this source can reduce the space charge repulsion between the positive ions in the ion beam. As a result, ion transmission efficiency and analyte ion sensitivities are significantly improved across the full mass range. MO^+/M^+ abundance ratios are not affected, M^{2+}/M^+ abundance ratios increase only slightly, and no new background ions are created by this electron injection technique.

Introduction

ICP-MS has become a powerful analytical technique for elemental and isotopic analysis. However, there are still some performance limitations that need to be studied and overcome. One of these is the low overall ion transmission efficiency in most instruments, which has been attributed largely to space charge effects.[1-3] Complications generated by space charge effects in ICP-MS also include mass discrimination in the analyte response (i.e. a bias against low-mass ions in favor of high-mass ions), and most importantly, matrix

*Corresponding author

effects which normally result in the suppression of analyte signals by concomitant element(s). These suppression effects are most severe for light analyte ions in the presence of heavy matrix elements.[4-7]

Space charge is a net charge imbalance caused by an excess of charged particles, which are positive ions in the beam extracted from the ICP. The mutual repulsion of these ions spreads the beam radially, resulting in a defocusing of the ion flow and an overall loss in the ion transmission efficiency and sensitivity. This sensitivity loss due to the defocusing effect is a function of the ion kinetic energy. Under continuum flow in the plasma extraction process, all ions travel at the speed (v) of the gas flow. Hence, the ion kinetic energy is proportional to the ion mass (K.E. = 1/2 mv^2). Ions of lower mass with lower kinetic energy are defocused more strongly and transmitted less efficiently than heavier ions with higher kinetic energies. The result is the disproportionate decrease in sensitivity or mass discrimination, which also contributes to the matrix effects.

The ICP is electrically neutral with comparable densities of positive ions and electrons. The gas-dynamic expansion of the plasma into the mass spectrometer through the sampling orifice is characterized as continuum flow where the plasma remains quasineutral, i.e. the positive ions are balanced by the equivalent number of electrons.[8] Therefore, no space charge field should develop between the sampler and skimmer. This theory of neutral flow in the interface has been supported by the work of several researchers.[9-12] The breakdown of charge neutrality of the plasma and the development of space charge effects is thought to begin somewhere inside the skimmer. As the ion beam passes through the skimmer orifice, the pressure and density drop in the high vacuum stage. The mobility of electrons increases as the beam density decreases. The electron mobility is much larger than

that of the positive ions. As a result, the electrons diffuse to form an electron sheath on the inner wall of the skimmer, leaving the positive ions behind in a flow that is no longer quasineutral.[3] The charge separation is also enhanced by the electrostatic field applied by the ion lens to draw positive ions from the skimmer and repel electrons.

In a conventional ICP-MS instrument, the ion current passing through the skimmer orifice is approximately 1.5 mA[1]. This is well above the few μA required for the development of a strong space charge field.[13] The space charge effects and the defocusing of the ion beam in this region was suggested by Gillson et al.[1], who found that the actual ion current measured at the base of the skimmer was only on the order of 6-20 μA. These observations were later supported by the electron density measurements of Niu and Houk,[9] the time-resolved measurements of the effect of matrix on the ion pulses by Allen et al.[14] and Stewart and Olesik,[15] and the theoretical modeling of Tanner.[1-2] The latter studies show a strong defocusing of the ion beam caused by space charge effects even at an ion current of only a few μA and that light ions with lower kinetic energies are less effectively transmitted than the heavier ions.

Thus, space charge is a serious problem in ICP-MS and techniques to eliminate, or at least, minimize space charge effects are desirable. Immediate acceleration of the ions to reduce the ion density and the space charge was proposed by Turner.[16] An acceleration cone with a bias potential of -2000 volts was placed behind the skimmer to accelerate ions through the ion lens system. This process is not ideally practical for a quadrupole mass analyzer, as the space charge effects could return when ions are decelerated before entering the analyzer. Although Turner reported some improvements in the mass bias and matrix effects, present

instruments that employ this ion acceleration concept still suffer from mass bias and matrix effects.[17]

Tanner et al.[11-12] took a different approach to cope with the space charge effects by utilizing a three-aperture interface. The interface consists of a conventional sampler and skimmer with a third 0.2 mm diameter aperture on a blunt tipped conical support offset 1.5 mm from the ion beam axis. This third aperture reduces the ion current (by reducing the ion flux) in order to minimize the space charge field. The current measured behind the third aperture is approximately 10 nA, much lower than the μA level needed to trigger the space charge repulsion. Although the ion flux is lower by a factor of approximately 150 compared to that in a conventional instrument, this ion loss is offset by the improvement of ion transmission efficiency, so the overall sensitivity is comparable to that obtained from a standard interface. The mass discrimination and matrix effects were also improved as a result of the absence of the space charge effects along with a more uniform ion kinetic energies, a character of a transitional flow through the third aperture.

Another strategy to deal with space charge effects is to modify the ion optics to retain the charge neutrality in the ion beam, minimize the extent of charge separation, and thus prevent space charge effects until the ions travel well downstream. Ross and Hieftje[18] employed this strategy by removing the ion lens between the skimmer and the differential pumping orifice while Hu et al.[19-20] used a slightly positive bias potential on the extraction lens. Recently, Denoyer et al.[21] introduced a simplified ion lens system with only a grounded photon stop, a single cylinder lens biased with a small positive potential and a grounded differential pumping aperture. The photon stop is mounted close to the skimmer so that the ion beam expands freely around it without a substantial charge separation. The cylinder lens

then serves as a kinetic energy analyzer. The optimum voltage on this lens is found to be directly proportional to the ion kinetic energy or mass of the ion and thus can be adjusted to improve the sensitivity for each analyte ion. The voltage on the cylinder lens can also be used to discriminate against unwanted ions (e.g. matrix ions) and reduce matrix effects. Unfortunately, this technique is effective only when the matrix ions have substantially different kinetic energy than the analyte, i.e., when the masses of the matrix ions differ from that of analyte ions.

In the present work, we introduce a new approach to balance the charge of the extracted ion beam behind the skimmer orifice. Previous experiments showed that the matrix effects occur mainly between the skimmer and the first extraction lens.[14] An electron impact source is added to a side port on the skimmer to add extra electrons to this region. This electron source supplies an adjustable amount of moderate energy electrons to neutralize the ion beam in the general region where the charge separation begins. This paper shows that this electron injection technique reduces the space charge effects and improves the overall ion transmission efficiency. The companion paper describes substantial reductions in matrix effects by this method.

Experimental

Instrumentation

All the experiments were performed on a home-made ICP-MS system described elsewhere.[19-20] Modifications to the skimmer and the ion lens are illustrated in Figure 1. A new skimmer with two side ports at the base was custom built from stainless steel. The

skimmer has a 1.05 mm diameter orifice and the overall height of 4.45 cm which is longer than the original skimmer. The sampler-skimmer separation is 9.5 mm.

One side port is equipped with a coiled tungsten filament (0.15 mm thick, 1.3 mm coil OD, 1 cm long, R = 0.8 Ω) welded to two electrical feedthroughs on a removable flange. This filament is commercially available as a spare part in an electron impact ionizer for an organic GC-MS (Spectrel Ionizer Model 275-R2, Extranuclear Laboratories, Inc.). A rectangular stainless steel plate on another feedthrough welded to the negative input of the filament was positioned just below the filament to repel the electrons out of the port. The two connections to the filament pass through the interface chamber to an electron impact ionizer controller (Model 275-E2, Extranuclear Laboratories, Inc.), which controls the electron emission current and electron energy.

Although the extent of electron emission is normally controlled by measurement of the emission current (the current of electrons emitted from the filament onto a counter electrode), this parameter was difficult to measure with our system. The extracted plasma strikes the skimmer and contributes a high, noisy background current on the skimmer. Therefore, the current supplied to the filament (filament current) was used as an indication of the electron emission instead. A digital multimeter (Model 3457A, Hewlett Packard) was employed for this purpose.

The other side port contains a circular stainless steel plate welded on a feedthrough. This plate (collector) is either grounded or biased to a slight positive potential to draw electrons from the source across the ion beam. The former condition was found to perform better in most cases.

The ion lens stack contains 7 electrodes, one perforated cylinder, one tapered cylinder and five circular stainless steel plates with holes aligned in such a manner that bend the ions off axis to eliminate the photons and neutral species from the plasma and back on axis before entering the differential pumping orifice. The cylindrical extraction lens was cut approximately 10 mm shorter than the original one to accommodate the skimmer and avoid blocking the electron beam path. The ion lens voltages and other typical operating parameters are listed in Table 1.

The extraction lens is held at + 4 volts, which typically provides the best sensitivity for this device. Some of the electrons from the filament may move out of the base of the grounded skimmer toward the ion lens. Since some of the space charge effect may occur inside the lens,[14] generating the electrons in a region where the voltages are such that they can move along with the ion beam helps minimize the space charge problem.

Operating procedures

Samples were introduced at an uptake rate of 1 mL/min via a peristaltic pump (Minipuls 2, Gilson). An ultrasonic nebulizer (U-6000AT$^+$, CETAC Technologies, Inc.) was used. Only the regular desolvator was utilized with a heating temperature of 140 °C and a condenser temperure of 2 °C. The resulting aerosol was carried through Tygon transfer tubing (6 mm ID, 1.2 m long) to a standard Fassel torch (Model # 350-05, Precision Glassblowing) inside a home-made shielding box. The argon gas flows were precisely controlled by a mass flow controller system (Model 8284, Matheson). The nebulizer gas flow rate, the ionizer filament current ($I_{filament}$) and the electron energy (E_e) were optimized from day to day to produce the highest sensitivity for Co^+ and La^+ while maintaining the signal ratio LaO^+/La^+ less than 0.5%. Data were collected using a multichannel analyzer

(Turbo-MCS, EG&G Ortec) in either a scanning mode or a single ion monitoring mode. The quadrupole mass analyzer (QPS-638, Extranuclear Laboratories, Inc.) was adjusted to provide a required mass window with unit mass resolution.

Samples and sample preparation

Solutions of the elements of interest were prepared by diluting 1000 ppm ICP elemental standards from SPEX CertiPrep (Metuchen, New Jersey) with aqueous 1% HNO_3. The nitric acid used was Optima ultrapure grade from Fisher Scientific. High purity deionized water (18 MΩ-cm resistivity) was obtained from a water purification system (Milli-Q Plus, Millipore).

Results and Discussion

General observations

A viewport is present on the second stage vacuum chamber so the emission of the tungsten filament can be seen. A solution of Co and La at 1 ppm is used to tune the instrument (nebulizer gas flow, ion lens potentials, etc.) to the optimum operating conditions before the filament current is turned on. This is referred to as operation in "normal mode" where the new electron source skimmer with no current should behave just like a conventional skimmer. Likewise, the performance when the filament is turned on is referred to as "supplemental electron mode". The measurement and control of the $I_{filament}$ used throughout these experiments seems to be very accurate and does not suffer from the background current or RF interferences from the extracted plasma at all. The tungsten filament can sustain the current as much as 3.0 A for a long period of time, even though the

pressure in this region is fairly high. We have used only one filament for all of our experiments and it remains in perfectly good shape.

Measurement of electron emission current

Although it is difficult to measure the actual electron current when the plasma is on, some estimate of this parameter is necessary to provide insight into the role of the emitted electrons. Presently, the electron current can be measured accurately only when the plasma is off and the sampler is plugged. For this experiment, the skimmer is insulated from the grounded vacuum flange with a ceramic spacer and Nylon screws. The emission current is then measured from the skimmer wall, which assumes the role of the counter electrode. Figure 2 is a calibration plot of emission current vs. filament current at E_e = 30 eV. There is no significant emission current for $I_{filament}$ up to roughly 1.50 A. The emission current increases rapidly as the filament current is turned up from 1.60 A to 2.20 A and the increase rate is slightly lower after that. The measured electron emission current is in the same range as the estimated ion current flowing through a skimmer (1-2 mA).[1, 9] Although these measured values for electron current may not be quite the same while the plasma is sampled, the trend should be similar, and this plot should still be useful to estimate the emission current at different $I_{filament}$ values.

Effects of filament current and electron energy

Obviously, the electron current, the filament current, and the electron energy are crucial factors in the performance of the electron source. Five medium mass range elements (Co, As, Y, Sb and La) varying widely in ionization energies were chosen to investigate these effects. All other operating parameters, particularly the nebulizer gas flow rate, were adjusted to yield the maximum M^+ signal and kept constant throughout the measurements.

First, the electron energy was fixed at 30 eV to study the effect of filament current. A plot of normalized signals for these analyte ions vs. filament current is shown in Figure 3. The signals apparently are not affected up to $I_{filament}$ = 1.5 A; at low current the filament emits only a few electrons as suggested by the emission current calibration plot (Figure 2). As $I_{filament}$ is turned higher, the analyte signals increase rapidly and maximize at approximately 1.90 A. The sensitivity improvements range from 70% for As^+ up to 120% for Co^+. The signals fall off slightly as current is increased further.

The electron energy is determined by the potential difference between the voltage on the repelling plate and filament vs. the grounded skimmer and the collector. The filament current was fixed at 1.90 A (electron current ~ 0.8 mA, Figure 2) to examine the effect of electron energy on analyte signals (Figure 4). Below 15 eV, the additional electrons from the filament do not improve the signals even though the filament is operated at the optimum current. Presumably, such low-energy electrons are not driven out of the port into the ion beam path. Above 20 eV, the signals increase significantly and eventually reach a plateau when the electron energy is greater than 30 eV for all analyte ions except As^+ whose signal falls off only slightly. Arsenic is the toughest element to ionize (IE = 9.81 eV) among the five elements studied and is chosen to investigate whether the electron beam at high energy can improve its ionization efficiency. This is found not to be the case even if the electron energy is as high as 90 eV, the maximum energy that can be provided by the ionizer controller.

Background ions and background mass spectra

Initially, there was a concern that the electron source used in our experiments would create additional background ions from the residual gas, particularly the diffusion pump oil

vapor. This electron source is similar to the electron impact ionizer employed for the ionization of gaseous samples in a GC-MS system. Deionized water is nebulized to acquire a background mass spectrum. The detector voltage was turned down slightly and a small retarding potential was applied to the quadrupole bias to keep the major background ions (Ar^+, ArH^+, O^+, etc.) on scale without counting loss.

Figures 5 and 6 are spectra of background ions produced under the optimum operating conditions in the normal mode and supplemental electron mode respectively. In Figure 5, the background spectrum is dominated by Ar^+ along with the typical distribution of other common background ions. A background spectrum with the filament operating at 1.90 A and 30 eV electron energy (Figure 6) is almost identical to that obtained without the added electrons. No new background ions of any kind were seen. The only difference is that the signals from virtually all ions increase significantly when the electrons are supplied. On the other hand, the background count rates remain the same under both conditions (approximately 16 counts.s^{-1} for the normal mode and 18 counts.s^{-1} for the supplemental electron mode) which means only the signals generated by ions from the plasma are enhanced.

An extensive scan of the background spectrum over the high mass region reveals neither additional background ions nor W^+ or other ions containing tungsten from the filament. Such ions would not be expected anyway, since the voltage on the extraction lens is kept more positive than that on the skimmer.

It should be noted that the signal from $^{40}Ar_2^+$ in the spectrum under the supplemental electron mode is almost 20 fold larger than that obtained from the normal mode. This cannot be explained based on the enhanced ion transmission efficiency alone when compared to the

enhancement factor for $^{75}As^+$. Apparently, Ar_2^+ is produced more extensively with the supplemental electron source but the mechanism is not known at this time.

Metal oxide and doubly charged ions

Lanthanum was chosen for this study because LaO^+ is one of the most refractory oxides (dissociation energy = 8.89 eV). This element can produce a significant amount of La^{2+} (2^{nd} ionization energy of La = 11.06 eV) as well. Figure 7a shows the relationship between normalized La^+, LaO^+ and La^{2+} signals vs. nebulizer gas flow rate under the normal mode with no supplemental electrons. The best La^+ sensitivity is obtained at a flow rate of approximately 0.98 L/min. The M^+ signals for other elements also peak at this flow rate.

For the other ions, LaO^+ and La^{2+}, the tops of the "mountains" are located at substantially higher flows, by 0.22 and 0.10 L/min respectively. Under the best analytical flow rate (maximum La^+ signal), these two interfering ions are kept relatively low as can be seen in Figure 7b where both LaO^+/La^+ and La^{2+}/La^+ signal ratios are approximately 0.2-0.3%.

Similar plots obtained with the electron source at 1.91 A filament current and 35 eV electron energy are depicted in Figures 8a and 8b. The "mountain" patterns for LaO^+ and La^{2+} are nearly identical to the ones shown earlier, whereas the peak for La^+ shifts to a slightly higher flow rate, roughly 1.02 L/min. At this optimum flow rate, the sensitivity for La^+ is approximately 3 times higher than that obtained with the best condition under the normal mode. Although the tops of the mountains are brought a little closer, the peaks of LaO^+ and La^{2+} are still well separated from that of La^+. Because of the steep slopes of the plots for LaO^+ and La^{2+}, the levels of these two interference ions are still small under the best operating condition. The LaO^+/La^+ and La^{2+}/La^+ signal ratios at this flow rate remain only

0.3 and 0.5% respectively. The slight increase of La^{2+}/La^{+} signal ratio can be attributed to more efficient recovery of doubly charged ions in the reduced space charge field induced by the supplemental electrons.

Sensitivity enhancement

A variety of elements listed in Table 2 ranging from a low mass ($^{7}Li^{+}$) to a high mass ($^{208}Pb^{+}$) are selected to evaluate the magnitude of signal improvement. The sensitivity was measured from the peak signal and converted into the ion count rate per unit concentration. The measurement was performed under a single set of operating conditions for all elements. This multielement condition is optimized simply by maximizing Co^{+} signal. A slightly higher nebulizer flow rate is required to meet the multielement condition with the operation of the electron source as seen from the previous experiment. The electron source was operated at the best current and electron energy of 1.90 A and 37 eV respectively.

The sensitivity for each analyte ion under both modes along with its sensitivity enhancement factor are also listed in Table 2. Admittedly, the overall sensitivity is relatively low compared to that obtained from most commercial ICP-MS instruments, which is a characteristic of this home-made instrument. Nonetheless, the sensitivity is less important to this study than the sensitivity enhancement factor. As expected, the sensitivity of all analyte ions is improved by at least a factor of 2-3 under a single operating condition. The enhancement factors are slightly higher for the lower mass ions, as much as 5.68 for Li^{+}. This sensitivity enhancement when used with appropriate blanks also ensures an improvement in detection limits for those ions that are not obscured by interfering ions from the plasma, e.g. higher mass elements. This could prove to be a very useful benefit in some

applications that deal with trace elemental analysis of very low concentration samples, for example, radioactive materials or chromatographic samples.

Space charge vs. supplemental ionization

The sensitivity improvements shown in Table 2 could be caused either by enhanced ion transmission as a result of the reduced space charge effects or simply by additional ionization of neutral atoms by electron impact. The following observations lead us to believe that this sensitivity enhancement is truly the result of a reduced space charge field.

First of all, the extraction lens is more positive than the skimmer by + 4 volts. Thus, positive ions produced by electron impact inside the skimmer should not enter the extraction lens. Ions made inside the extraction lens by electrons from the filament would be transmitted into the rest of the ion lens, however. Second, the sensitivity enhancement factor for As^+ is similar to those of other elements that are supposedly 100% ionized in the plasma.[8] If the additional metal ions were created mainly by electron impact on neutrals extracted from the plasma, more As^+ signal and little or no enhancement for other easily ionized elements would have been seen. Changing the electron kinetic energy above 10 eV does not substantially affect the signal ratios As^+/Co^+ or La^{2+}/La^+ (Figure 9), which corroborates this point.

Third, the enhancement factors of the lower mass ions are substantially higher than those of heavier ions. This observation is expected from space charge considerations, which indicate that lower mass ions of lower kinetic energy are defocused and lost more extensively under the space charge field. Thus, the transmission for these ions should improve proportionately more than that for the heavier ions when the space charge is reduced. Fourth, the nebulizer gas flow rate that maximizes M^+ signal under the electron-enhanced mode is

similar to that obtained under the normal mode (Figures 7 and 8). If additional ions were produced mainly by electron impact, the optimum flow would shift to a substantially higher flow rate that favors the production of neutral atoms in the plasma. Except for Ar_2^+, supplemental electrons do not change the relative abundance of background ions. Fifth, the electron source used in this study is similar to an electron impact ionizer utilized in a GC-MS system. The ionization efficiency of even a "closed" or "tight" ionizer is seldom better than ~ 0.1%.[22] One should not expect much additional ionization from the electron source in the relatively large volume of the skimmer. Finally, the electron current (~ 0.8 mA) that maximizes M^+ signal is close to the ion current expected through the skimmer (~ 1.5 mA).

Overall, the results clearly indicate that the ion transmission efficiency and the analytical sensitivity of all analyte ions can be improved significantly with the addition of electrons to the ion beam behind the skimmer orifice. The supplemental electrons presumably balance the excess positive charge in the ion beam as the quasineutral state breaks down and reduce the space charge repulsion among ions as they are transmitted further downstream. A similar result is seen when ions are trapped (with electrons) in an electron impact ion source prior to analysis by time-of-flight[23] or multiple pass quadrupole[24] mass spectrometers.

Conclusions

The supplemental electron source inside the skimmer proves to be a very useful technique. When operated properly, these electrons can counteract space charge problems in the ion beam downstream of the skimmer. As a result, the overall ion transmission efficiency is significantly improved. For maximum improvements in ion transmission, the source is

best operated at a filament current of 1.90-1.95 A with electron energy of 30-40 eV, of which the corresponding electron current is approximately 1 mA, comparable to the typical ion current through the skimmer. Analyte ion sensitivities can be improved by at least a factor of 2-3 across the whole mass range under a single operating condition. The LaO^+/La^+ and La^{2+}/La^+ signal ratios and the levels of most background ions remain comparable to those obtained without the added electrons. The new technique apparently does not create any new background ions and only improves the analyte ion signals while maintaining the same low background count rate similar to that obtained from a typical skimmer. These observations can also be used as supportive evidence that the space charge effects occur mainly between the skimmer and the extraction lens, because this is where the extra electrons are aimed.

Other space charge-related problems such as matrix effects are also reduced using this electron source, as described in the companion paper.[25] Recent experiments show that the same concept can be adapted for ICP-MS devices with a negative voltage on the extraction lens, so this method is of potential value for all types of ICP-MS device. Furthermore, this electron source may be useful for reducing multiply charged ions and space charge effects in electrospray mass spectrometry as well.[26-27]

Acknowledgements

Ames Laboratory is operated for the U.S. Department of Energy by Iowa State University under Contract no. W-7405-Eng-82. This research was supported by the Office of Basic Energy Sciences. The ultrasonic nebulizer was provided by Transgenomic CETAC Technologies, Inc. ICP elemental standards were provided by SPEX CertiPrep.

References

1. Gillson, G. R.; Douglas, D. J.; Fulford, J. E.; Halligan, K. W.; Tanner S. D. *Anal. Chem.* **1988**, 60, 1472-1474.

2. Tanner, S. D. *Spectrochim. Acta, Part B* **1992**, 47, 809-823.

3. Douglas, D. J.; Tanner, S.D. Fundamental Considerations in ICPMS, in Montaser, A., Ed. Inductively Coupled Plasma Mass Spectrometry, Wiley-VCH: New York, 1998, pp. 656-666.

4. Olivares J. A.; Houk, R. S. *Anal. Chem.* **1985**, 57, 2674-2679.

5. Tan, S. H.; Horlick G. *J. Anal. At. Spectrom.* **1987**, 2, 745-751.

6. Gregoire, D. C. *Appl. Spectrosc.* **1987**, 41, 897-903.

7. Evans, E. H.; Giglio, J. J. *J. Anal. At. Sprectrom.* **1993**, 8, 1-18.

8. Douglas, D. J.; French, J. B. *J. Anal. At. Spectrom.* **1988**, 3, 743-747.

9. Niu, H.; Houk, R. S. *Spectrochim. Acta, Part B* **1994**, 49, 1283-1303.

10. Niu, H.; Houk, R. S. *Spectrochim. Acta, Part B* **1995**, 50, 1247-1261.

11. Tanner, S. D.; Cousins, L. M.; Douglas, D. J. *Appl. Spectrosc.* **1994**, 48, 1367-1372.

12. Tanner, S. D.; Douglas, D. J.; French, J. B. *Appl. Spectrosc.* **1994**, 48, 1373-1378.

13. Douglas, D. J. Fundamental Aspects of Inductive Coupled Plasma-Mass Spectrometry, in Montaser, A.; Golightly, D. W., Eds., Inductively Coupled Plasmas in Analytical Atomic Spectrometry, VCH: New York, 1992, pp. 638-641.

14. Allen, L. A.; Leach, J. J.; Houk, R. S. *Anal. Chem.* **1997**, 69, 2384-2391.

15. Stewart, I. I.; Olesik, J. W. *J. Am. Soc. Mass Spectrom.* **1999**, 10, 159-174.

16. Turner, P. J. Some Observations on Mass Bias Effects Occurring in ICP-MS Systems, in Holland, G.; Eaton, A. N., Eds. Applications of Plasma Source Mass Spectrometry, Royal Society of Chemistry, Cambridge, 1991, pp.71-78.

17. Bradshaw, N.; Hall, E. F. H.; Sanderson, N. E. *J. Anal. At. Spectrom.* **1989**, 4, 801-803.

18. Ross, B. S.; Hieftje, G. M. *Spectrochim. Acta, Part B,* **1991**, 46, 1263-1273.

19. Hu, K.; Clemons, P. S.; Houk, R. S. *J. Am. Soc. Mass Spectrom.* **1993**, 4, 16-27.

20. Hu, K.; Houk, R. S. *J. Am. Soc. Mass Spectrom.* **1993**, 4, 28-37.

21. Denoyer, E. R.; Jacques, M. D.; Debrah, E.; Tanner, S. D. *At. Spectrosc.* **1995**, 16, 1-6.

22. Koontz, S. L.; Denton, M. B. *Int. J. Mass Spectrom. Ion Phys.* **1981**, 37, 227-239.

23. Grix, R.; Gruner, U.; Li, G.; Stroh, H.; Wollnik, H. *Int. J. Mass Spectrom. Ion Proc.* **1989**, 93, 323-330.

24. Amad, M. H.; Houk, R. S. *J. Am. Soc. Mass Spectrom.* **2000**, 11, accepted.

25. Praphairaksit, N.; Houk, R. S. *Anal. Chem.* To be submitted together.

26. Scalf, M.; Westphall, M. S.; Smith, L. M. ASMS Conference on Mass Spectrometry and Allied Topics, Dallas, TX, June 1999, Paper No. 908.

27. Busman, M.; Vogel, C. R.; Sunner, J. *J. Am. Soc. Mass Spectrom.* **1991**, 2, 1-10.

Table 1. Typical operating conditions

Plasma conditions	
Forward power	1.3 kW
Reflected power	< 5 W
Outer gas flow	15.0 L/min
Auxiliary gas flow	1.0 L/min
Nebulizer gas flow	0.9 – 1.1 L/min
Solution uptake rate	1.0 mL/min
Sampling position	8 mm from load coil
Sampling orifice	1.40 mm
Skimmer orifice	1.05 mm
Ionizer filament current	1.9 – 2.0 A
Electron energy	30 – 40 eV
Ion lens potentials	
Extraction lens	+ 4 V
Lens # 2	- 150 V
Lens # 3	- 225 V
Lens # 4	+ 46 V
Lens # 5	- 500 V
Lens # 6	+ 8 V
Lens # 7	+ 3 V
Differential pumping plate	- 105 V

Table 2. Relative sensitivity and enhancement factor for various elements measured with the normal and supplemental electron operation modes.

Analyte ion	Sensitivity ($cts.s^{-1}.ppm^{-1}$)		Enhancement
	Normal mode	Supplemental electron mode	factor
$^{7}Li^{+}$	119	676	5.68
$^{27}Al^{+}$	$3.38x10^{4}$	$1.21x10^{5}$	3.58
$^{45}Sc^{+}$	$1.28x10^{5}$	$4.03x10^{5}$	3.16
$^{59}Co^{+}$	$1.27x10^{5}$	$3.83x10^{5}$	3.02
$^{64}Zn^{+}$	$2.26x10^{4}$	$4.59x10^{4}$	2.03
$^{75}As^{+}$	$1.26x10^{4}$	$2.77x10^{4}$	2.20
$^{89}Y^{+}$	$3.03x10^{5}$	$6.21x10^{5}$	2.05
$^{103}Rh^{+}$	$6.37x10^{4}$	$1.44x10^{5}$	2.26
$^{139}La^{+}$	$6.11x10^{4}$	$1.49x10^{5}$	2.43
$^{175}Lu^{+}$	$2.07x10^{5}$	$6.19x10^{5}$	2.99
$^{208}Pb^{+}$	$1.90x10^{5}$	$5.52x10^{5}$	2.90

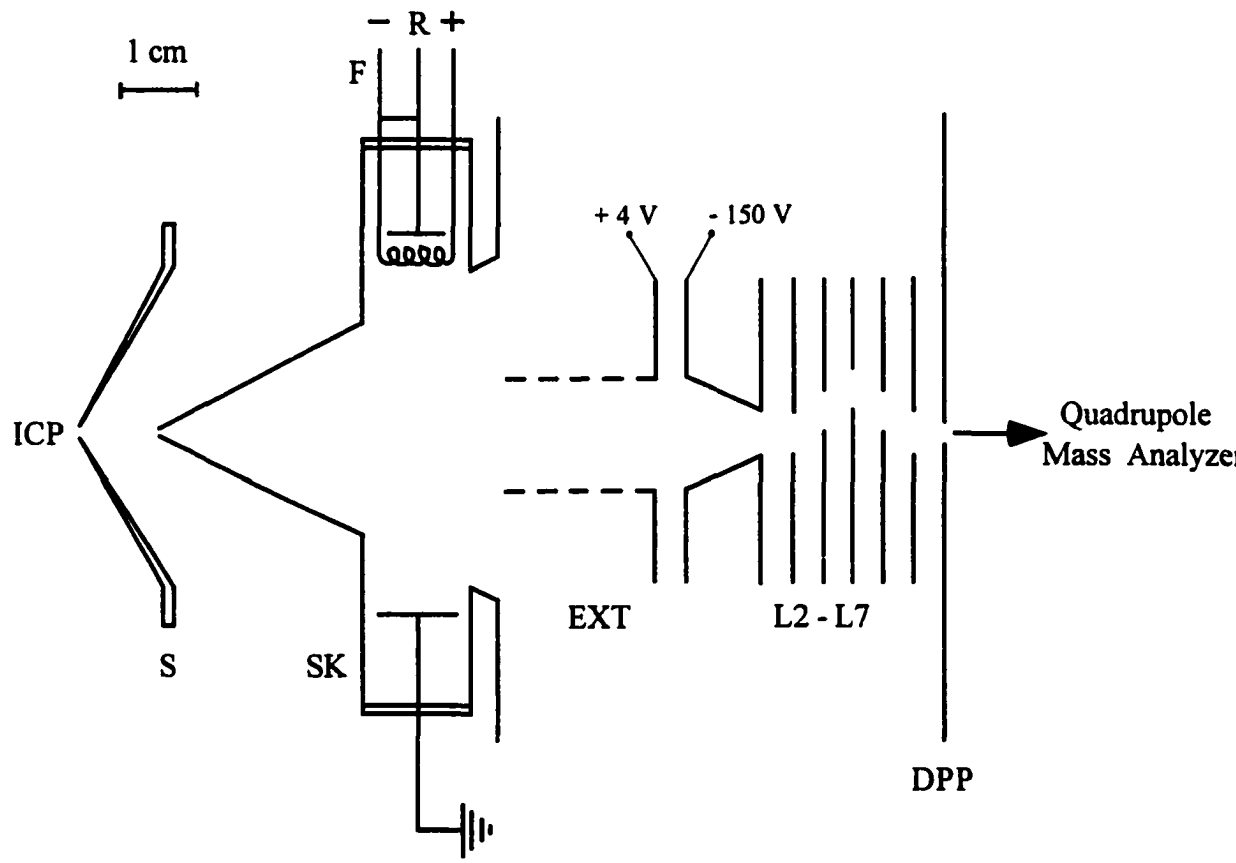

Figure 1. Schematic diagram of the modified electron source skimmer and the ion lens system. S: sampler; SK: electron source skimmer; F: Tungsten filament; R: electron repeller; EXT: extraction lens; L2-L7: lens # 2 - lens # 7; DPP: differential pumping plate.

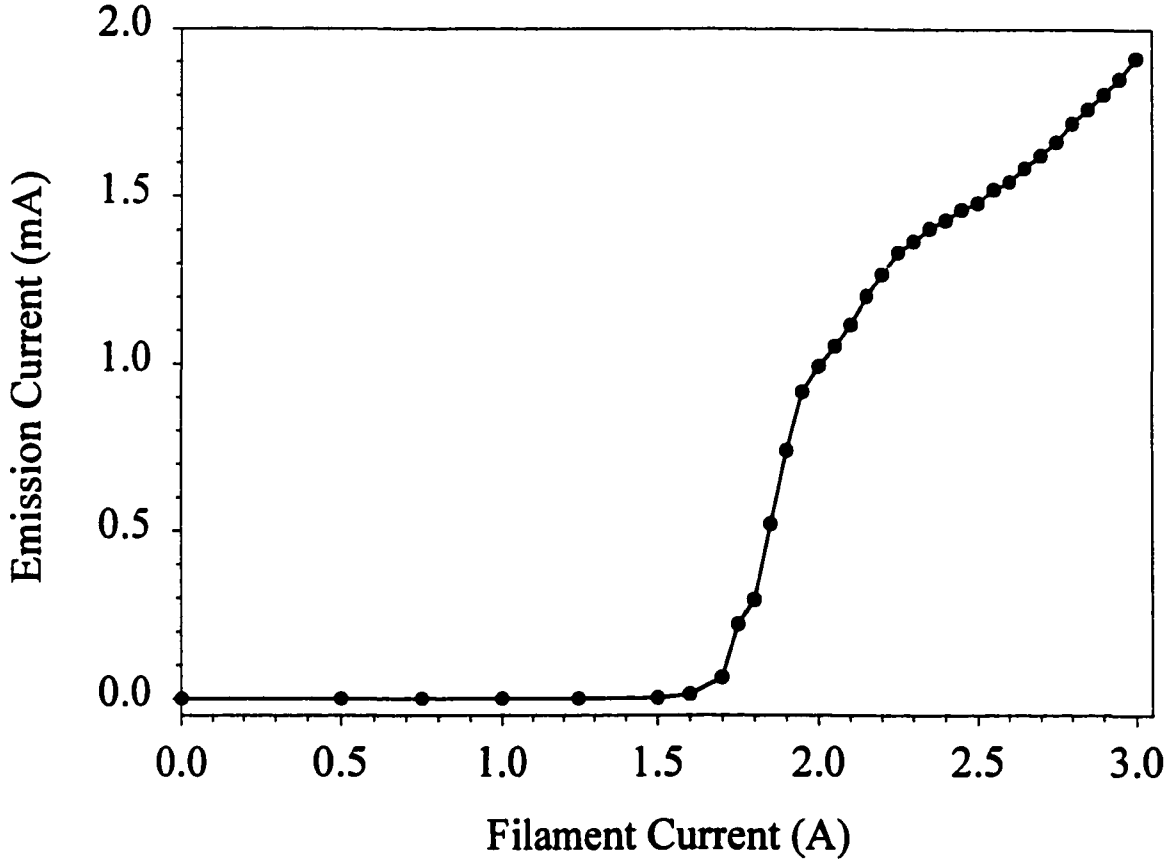

Figure 2. Calibration plot of emission current vs. filament current, electron energy = 30 eV.

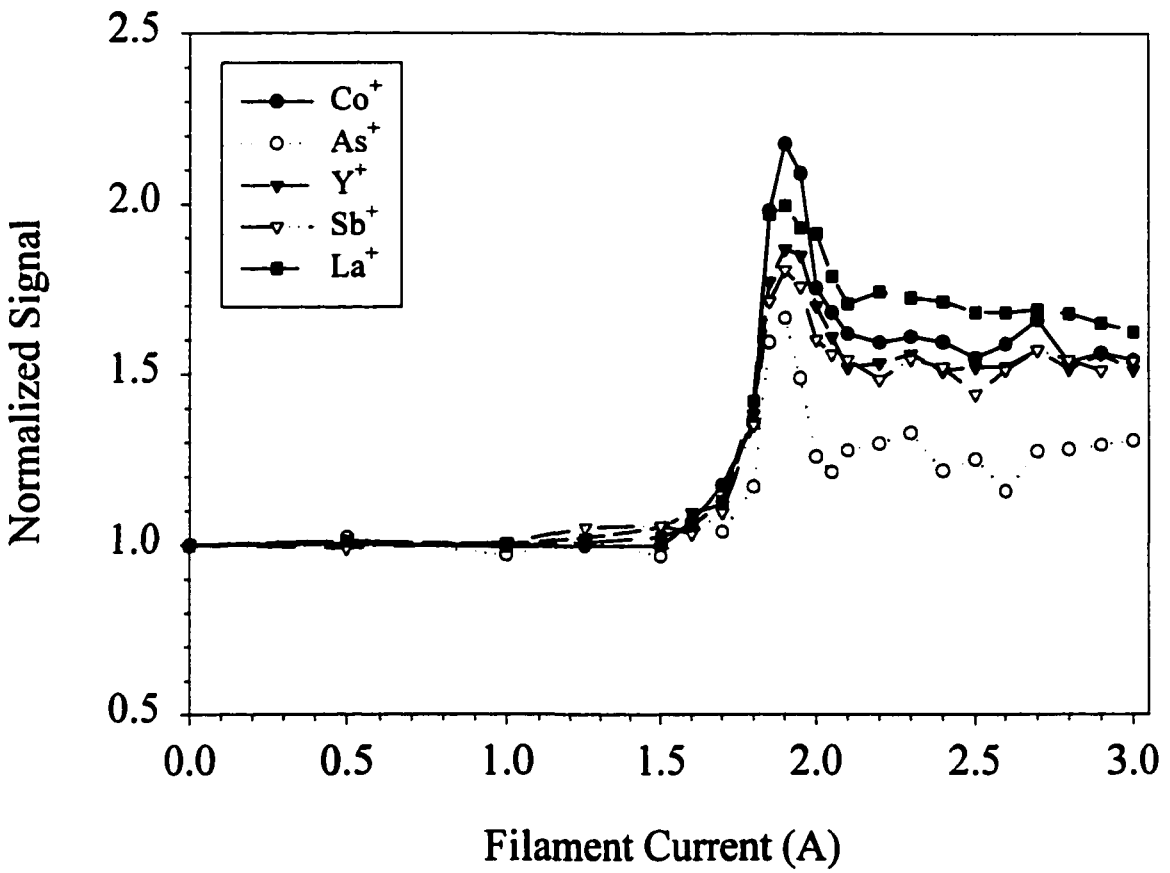

Figure 3. Plots of normalized signals for various analyte ions vs. filament current. $E_e = 30$ eV.

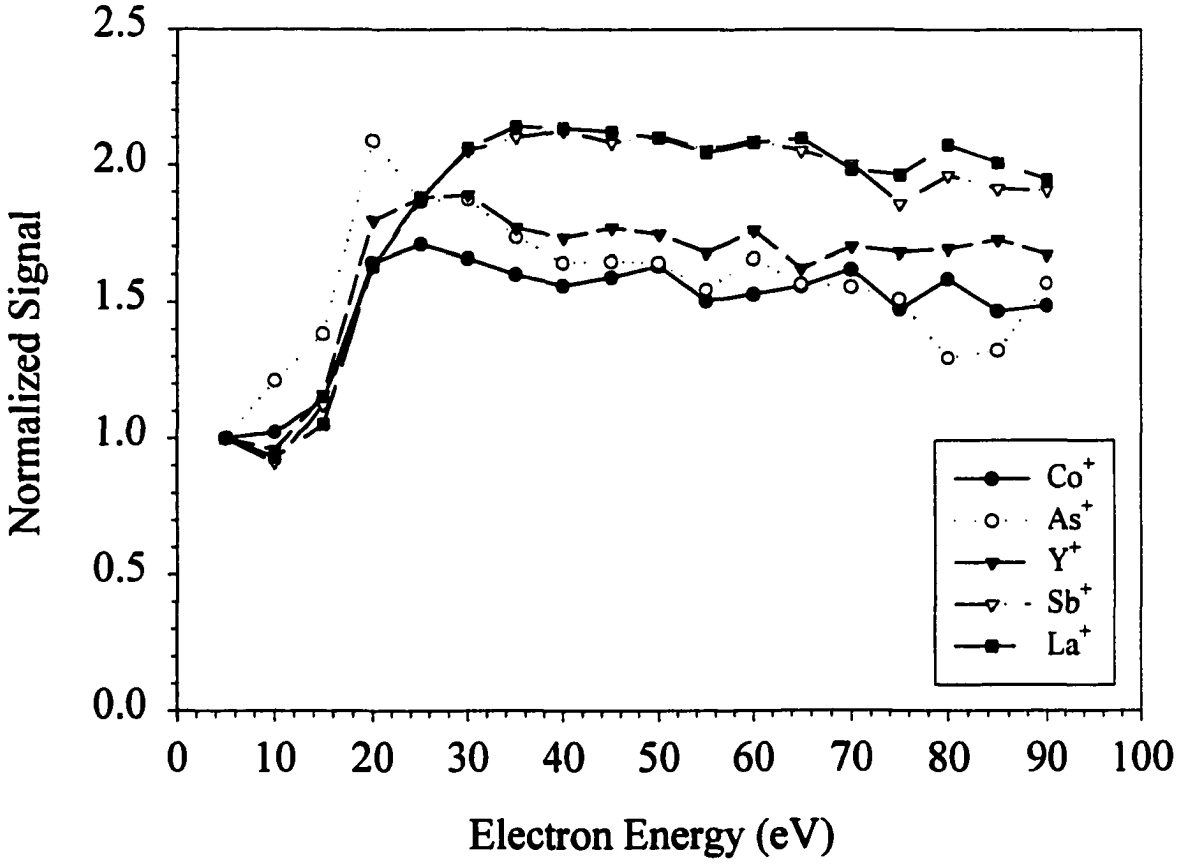

Figure 4. Dependence of various analyte ion signals on the electron energy. $I_{filement}$ = 1.90 A.

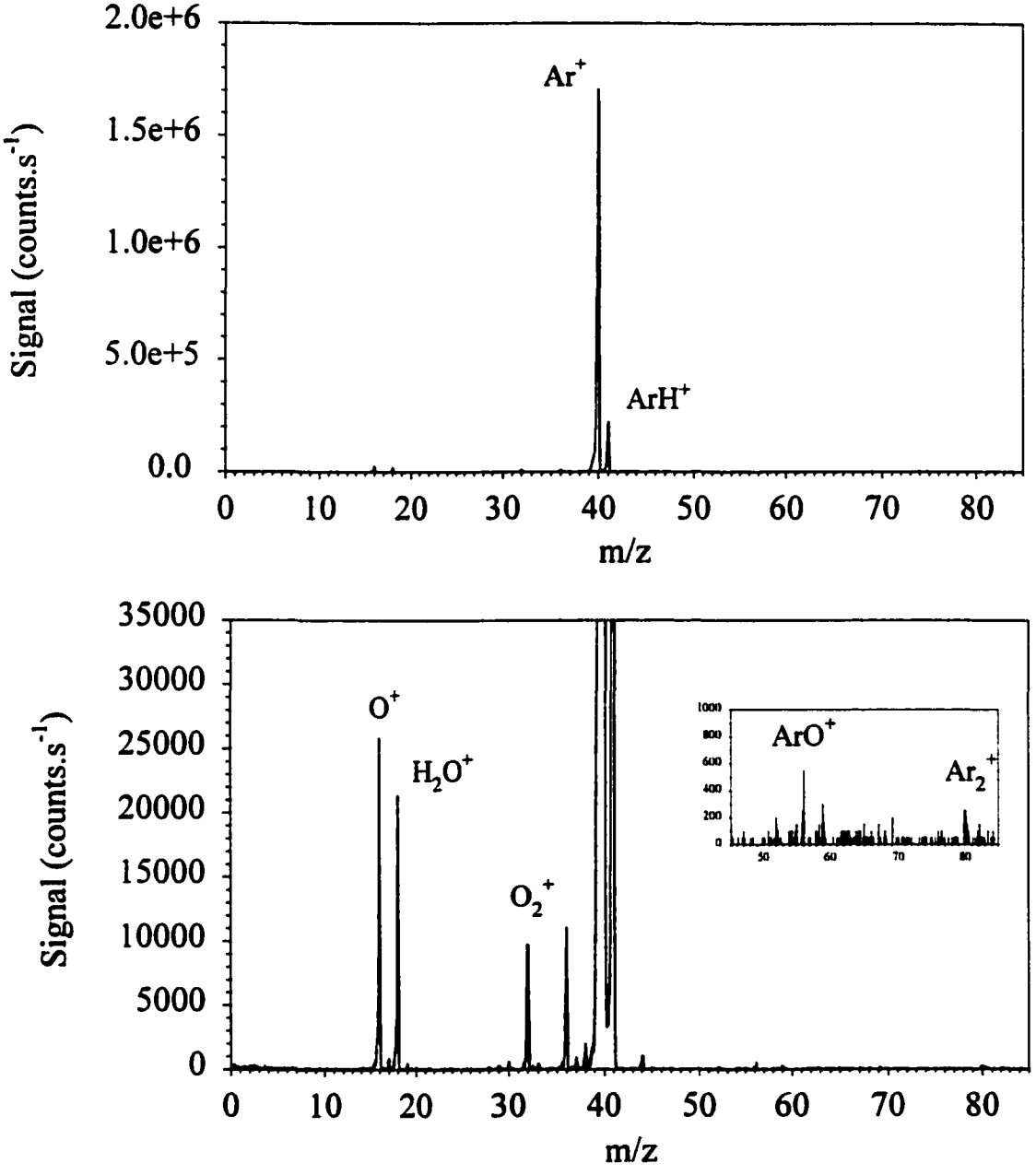

Figure 5. Background spectrum obtained from deionized water under the normal operation.

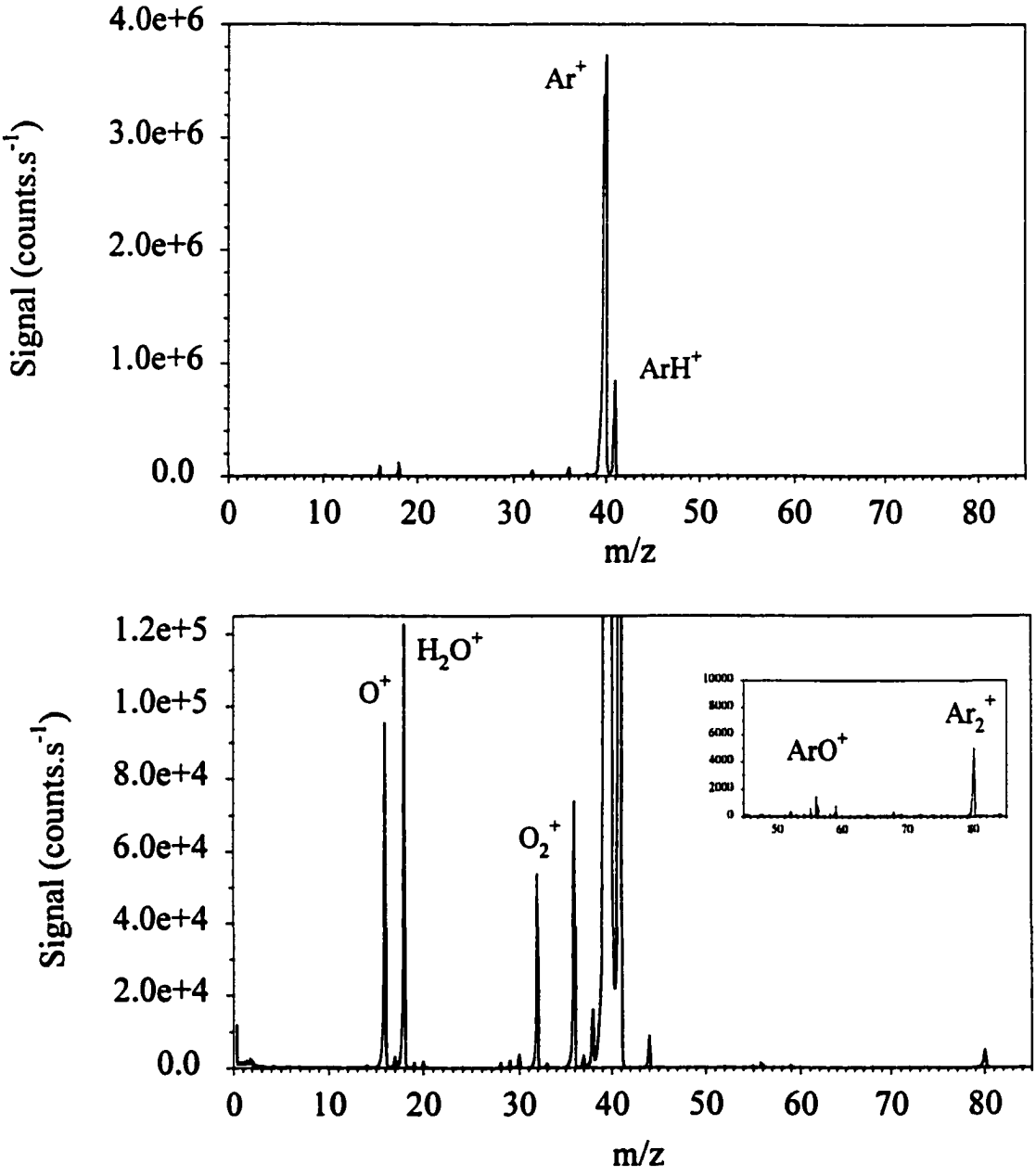

Figure 6. Background spectrum obtained from deionized water under the operation of electron source at $I_{filament}$ = 1.90 A, E_e = 30 eV.

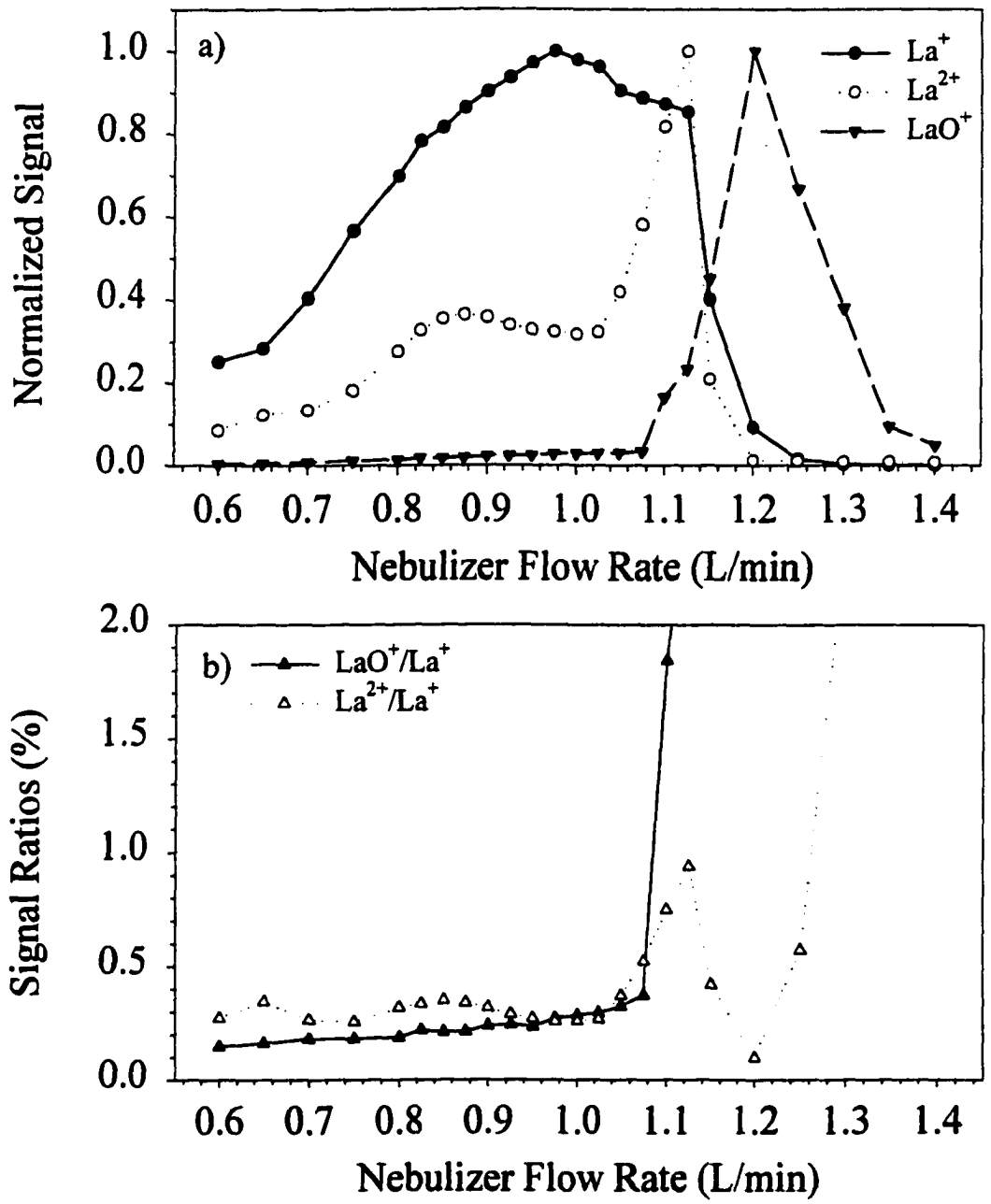

Figure 7. Effect of nebulizer flow rate on a) normalized La^+, LaO^+ and La^{2+} signals, and b) LaO^+/La^+ and La^{2+}/La^+ ratios under the normal mode operation.

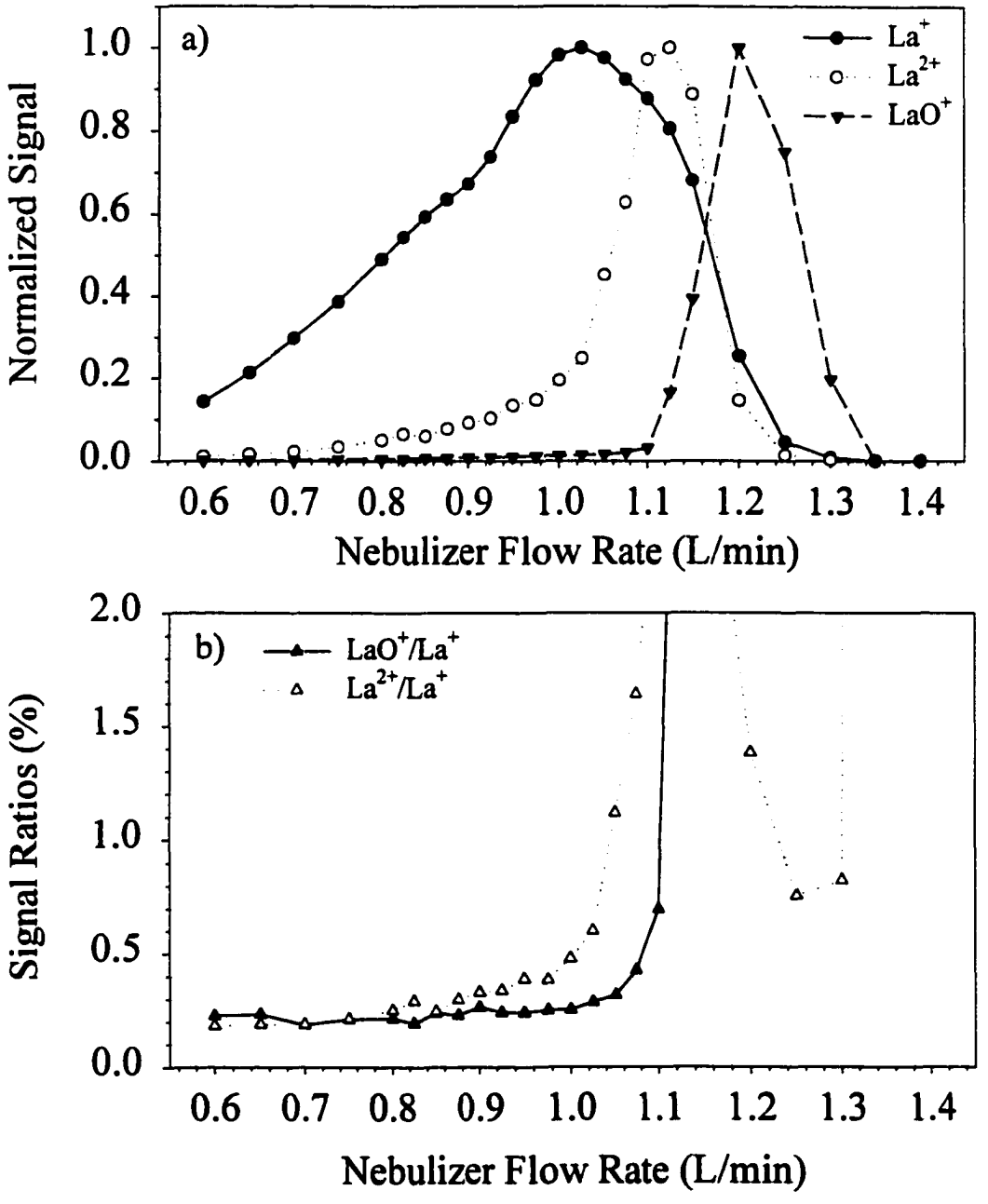

Figure 8. Effect of nebulizer flow rate on a) normalized La^+, LaO^+ and La^{2+} signals, and b) LaO^+/La^+ and La^{2+}/La^+ ratios under the supplemental electron mode with $I_{filament} = 1.91$ A, $E_e = 35$ eV.

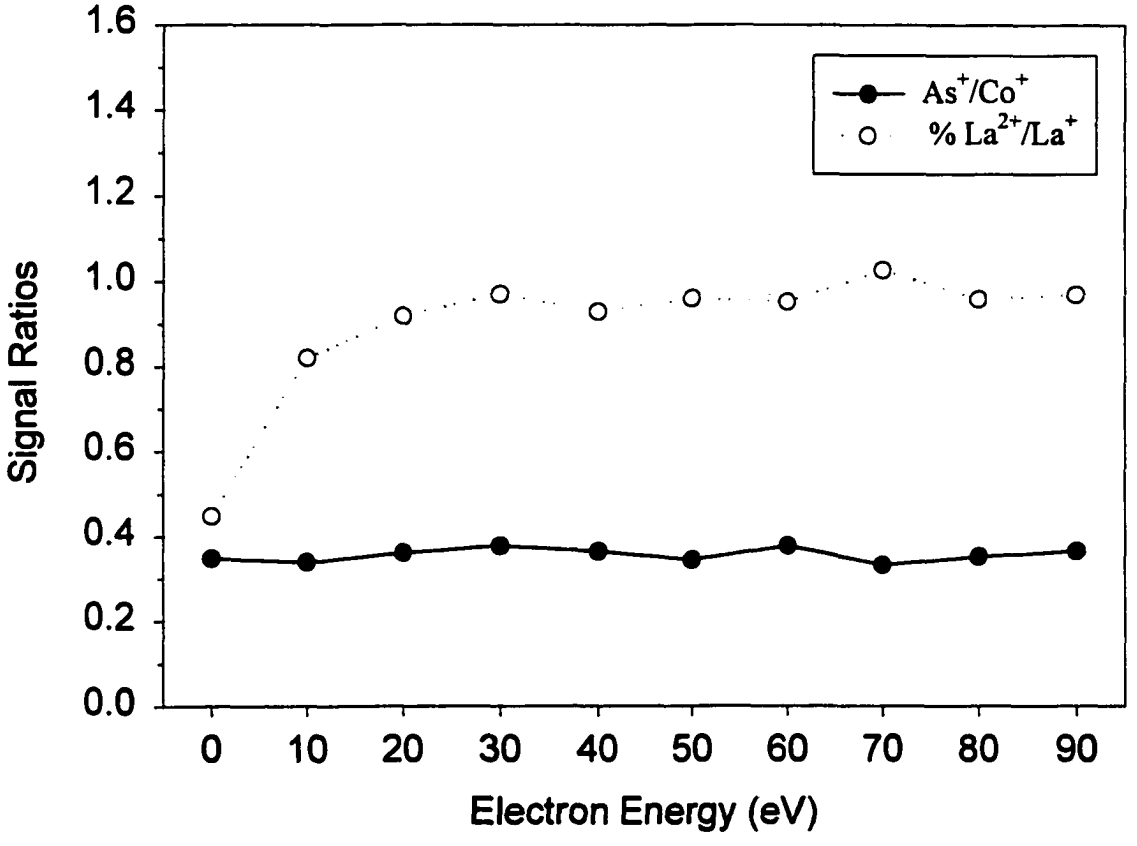

Figure 9. Effect of electron energy on As^+/Co^+ and $\%La^{2+}/La^+$ signal ratios, $I_{filament}$ = 1.90 A.

CHAPTER 4. ATTENUATION OF MATRIX EFFECTS IN INDUCTIVELY COUPLED PLASMA MASS SPECTROMETRY WITH A SUPPLEMENTAL ELECTRON SOURCE INSIDE THE SKIMMER

A paper submitted to Analytical Chemistry

Narong Praphairaksit and R. S. Houk*

Abstract

Electrons are added from a heated filament at the base of the skimmer to reduce the space charge repulsion in the ion beam. This technique improves the analyte sensitivity moderately and also minimizes the matrix effects caused by other elements in the sample significantly. The suppression of signal for even the most troublesome combination of light analyte and heavy matrix elements can be attenuated from 90 - 99% to only 2 - 10% for 2 mM matrix solutions with an ultrasonic nebulizer. The supplemental electron current can be adjusted to "titrate" out the matrix effects as desired.

Introduction

Despite its overwhelming success for elemental and isotopic analysis, inductively coupled plasma mass spectrometry (ICP-MS) is still somewhat vulnerable to some problematic interferences. Interferences encountered by ICP-MS can be classified into two categories, spectroscopic and non-spectroscopic interferences. Spectroscopic interferences are generally spectral overlaps caused by the atomic or polyatomic (e.g. oxide, hydroxide, argide, etc.) ions produced by the background ions or the matrix elements. The nature of

*Corresponding author

most of these interferences has been studied and a variety of techniques, e.g. solvent removal[1-6], cool plasma[7-10], collision cells[11-13], high resolution mass spectrometer[14-16], etc., have been developed to successfully counter the problems.

Non-spectroscopic interferences, commonly known as matrix effects, are characterized by changes in analyte signal influenced by the presence of matrix elements. This normally results in a suppression of analyte ion signals as the concentration of matrix increases[17-25], although signal enhancements sometimes have been observed as well.[20, 25-26] The magnitude of the matrix effect is strongly dependent on the atomic mass of analyte and matrix ions and somewhat dependent on their degrees of ionization. Typically, the matrix effect is most severe when the analyte ions are light with high ionization energy in the presence of heavy matrix elements with low ionization energy. Furthermore, the extent of the matrix effect is dependent on the absolute concentration of the matrix element rather than on the relative concentration of analyte to matrix elements.[22]

Matrix samples can influence analyte sensitivity in many aspects from the sample introduction to the ion transport inside the mass spectrometry. A change in the viscosity and density of the sample due to the matrix can alter the nebulization efficiency, droplet size distribution and solvent load to the plasma and eventually the temperature and ionization efficiency of the plasma.[27] Deposition of matrix salt on the sampler and skimmer can clog the orifices and significantly reduce the analyte sensitivity as well as affect the long term stability of signal. However, the most troublesome influence from matrix elements has been attributed mainly to space charge effects in the ion beam. A positively charged ion beam focused toward the ion lens creates a space charge field, which results in coulombic repulsion

between ions. Ions are defocused under a space charge field with the transmission loss being greatest for light ions with low kinetic energy.

A variety of techniques have been utilized to overcome the matrix effects. Internal standardization has been the most widely used and effective means to compensate for the matrix effects.[28-29] However, the selection of proper internal standard elements, ones that behave similarly to analyte elements in the plasma (e.g. close in mass and ionization energy) and do not interfere with the analytes, can be challenging. Adding the internal standard also risks contamination of the sample. Several polyatomic ions, e.g. $^{12}C^+$, $^{14}N_2^+$, $^{16}O_2^+$, $^{40}Ar^{16}O^+$, $^{40}Ar_2^+$, MO^+ etc., have been proposed as alternate internal standards to minimize the number of added elements.[20,30] Despite some success with this approach, caution should be taken as the formation mechanism and the nature of these polyatomic ions are different from those of analyte ions, and a possible mass discrimination could influence the validity of the correction as well.

Another strategy to counter the matrix effects is to reduce the matrix ion density in the ion beam. This can be accomplished by simply diluting the sample or adjusting the operating and instrumental parameters such as changing the nebulizer gas flow rate, increasing sampling position, increasing the solvent load, readjusting the ion lens potentials, etc.[22, 31-34] Although these techniques mitigate the matrix effects to some extent, they usually come with the expense of analyte sensitivity or additional polyatomic interferences and sometimes can be quite a time consuming process. Furthermore, dilution of samples is also limited by the purity of blank.

Matrix effects can be eliminated with chemical or physical separation methods. Precipitation and solvent extraction have been used successfully to remove the matrix from

samples prior to analysis by ICP-MS.[35-37] However, chromatography has been the most popular means for this task owing to its on-line nature. Chromatography using either ion-exchange or chelating resins for matrix removal has proved to be a very successful technique in eliminating the matrix for the analysis of real samples.[38-41] Matrix separation can also be achieved by controlled potential electrodeposition[42] and selective volatilization using electrothermal vaporization (ETV).[43] Unfortunately, all these sample pre-treatment processes can be lengthy and can cause some drawbacks such as serious sample contamination and unnecessary dilution.

Recently, several instruments have been described that reduce the matrix effects substantially. Tanner and co-workers[44] developed a three-aperture interface intended to minimize space charge effects. A small third aperture positioned off axis from the ion beam path reduced the total ion density and lowered the space charge field. As a result, matrix effects from space charge repulsion were improved appreciably. Denoyer et al.[45] employed a new ion optical system which allows the ion beam from the skimmer to expand freely around a photon stop into a single cylindrical ion lens. This ion lens also serves as a kinetic energy analyzer and the lens potential can be adjusted to discriminate against the matrix ions. This latter scheme only works well when the masses (i.e. the kinetic energies) of analyte and matrix ions differ significantly.

In the accompanying paper[46], we introduced a new method for reducing the space charge effect. An electron source similar to that in an electron impact ionizer was added to a side port of the skimmer. This source supplies electrons to balance the excess charge of positive ions in the ion beam behind the skimmer. This is the region where the matrix ions influence losses of analyte ions most substantially.[47] Consequently, space charge repulsion is

reduced and ion transmission efficiency as well as analyte sensitivity are improved significantly. The current investigation will focus mainly on the use of this electron-enhanced interface to attenuate the matrix effect, which is a serious space charge-related problem in ICP-MS.

Experimental

The home-made ICP-MS device used throughout this study as well as the configuration and the operation of the electron-enhanced skimmer have been described in the companion paper.[46] In brief, a tungsten filament was used as a source of thermionically emitted electrons in a side port located on the skimmer base. The emission of electrons is regulated by the current supplied to the filament ($I_{filament}$) from an electron impact ionizer controller (Model 275-E2, Extranuclear Laboratories, Inc.). Electron energy is determined by the bias potential on the repeller (relative to the grounded skimmer), which is positioned just under the filament. The optimum operating conditions that reduce the space charge and improve the ion transmission and analyte sensitivity were found to be a filament current of 1.90-1.95 A and electron energy of 30-40 eV.

All analyte and matrix element solutions were prepared from either 1000 or 10000 ppm ICP elemental standards from SPEX CertiPrep (Metuchen, New Jersey). The standards were diluted to the desired concentration with aqueous 1% HNO_3 prepared from an ultrapure grade concentrated nitric acid (Optima, Fisher Scientific) and high purity deionized water (18 MΩ-cm) obtained from a water purification system (Milli-Q Plus, Millipore). Matrix-matched blank solutions (containing concomitant elements only) were also prepared in the same manner.

All samples were introduced with a peristaltic pump (Minipuls 2, Gilson) at 1 mL/min to an ultrasonic nebulizer (U-6000AT$^+$, CETAC Technologies, Inc.). The desolvator was operated at 140 °C heating and 2 °C cooling temperatures and was used without the membrane desolvator. Solutions were introduced using the following procedure. For each matrix effect study, a solution containing only analyte element(s) was introduced first followed by a 1% HNO_3 blank solution. The signal was allowed to return to baseline to ensure the absence of memory effects. The next solution containing analyte and matrix elements was then nebulized, followed by a blank solution to check for memory. Matrix-matched blank solutions were also analyzed in between each matrix sample to determine if there was analyte signal from reagent impurity and background corrections were made when necessary.

The instrument was optimized on a daily basis with some key parameters particularly nebulizer gas flow rate, filament current and electron energy adjusted to maximize the analyte ion signal. Other common operating parameters, such as ion lens voltages, are described in the companion paper.[46] A multichannel analyzer (Turbo-MCS, EG&G Ortec) was used to collect data. The data acquisition was performed in either a scanning mode when a multielement sample was analyzed or a single ion mode when only one analyte element was monitored. All the values reported are the average of at least 5-10 measurements for each sample.

Results and Discussion

Effect of easily ionized element

Matrix ions with low ionization energy (< 8 eV), which are fully ionized in plasma, cause more severe matrix interferences than those with higher ionization energy.[17, 48] Therefore, Na (IE = 5.14 eV, 100% ionized) was chosen as the first matrix element for study. In addition, Na is a common element often present at a relatively high concentration in many important samples. A solution of 1 ppm Co in different concentrations of Na (0.01-1000 ppm) was analyzed in both normal mode and electron-enhanced mode. The matrix-induced suppression of Co^+ signal as a function of Na concentration is illustrated in Figure 1. In normal mode, i.e. electron source off, Co^+ signal starts to suffer from the presence of Na matrix at a concentration of 10 ppm with almost 20% signal loss and continues to drop until only approximately 1 % of original signal is left at 1000 ppm Na. The signal suppression observed here is more severe than usual mainly because of the high transport efficiency (20% or more) of the ultrasonic nebulizer used in our instrument, which presents an additional challenge to our system.

A substantial improvement in the recovery of the signal is clearly observed with the operation of supplemental electron source ($I_{filament}$ = 1.95 A and E_e = 35 eV). The matrix-induced suppression of Co^+ signal shifts to a higher Na concentration by approximately one order of magnitude and there is more than 30% of original Co^+ signal left at 1000 ppm Na. Moreover, a complementary sensitivity enhancement of almost a factor of two over that obtained in the normal mode is observed, as expected.[46]

Titration with electrons to minimize matrix effect

The matrix suppression can be reduced even further simply by adjusting the filament current to maximize analyte signal in the presence of matrix elements. This tactic is conceptually similar to a titration technique; in this case the excess positive charge in the extracted ion beam is titrated with electrons from the filament. Analyte solutions with the highest matrix concentration (1000 ppm) were used to optimize the operating conditions of the electron source. The filament current and electron energy were adjusted to maximize Co^+ signal under this hostile environment ($I_{filament}$ = 2.07 A and E_e = 27 eV), and these optimum conditions were then applied for the analysis of all solutions.

Figure 2a shows plots of Co^+ signals vs. Na concentration under all three operating conditions. Clearly, operating the electron source under the electron-rich environment (high current, $I_{filament}$ = 2.07 A) further attenuates the matrix-induced suppression significantly. All the signal can be recovered with Na concentration up to 100 ppm, and there is approximately 80% of the Co^+ signal remaining at 1000 ppm Na. This improvement is accomplished with a minor sacrifice in the analyte sensitivity as previously seen when the electron source is operated with high filament current[46], nonetheless, the signal is still approximately 50-60% better than that obtained without the electron source.

Similar investigations were performed on two other analyte elements with higher masses (In and Pb, Figure 2b and 2c). When operated in the normal mode, typical matrix suppressions are seen for both elements. The matrix effect is less severe for Pb than for In or Co, as expected.[31,33] The suppression of In^+ signal is reduced appreciably as the electron source is operated at 1.95 A and even further when operated under the electron-rich condition ($I_{filament}$ = 2.07 A). Lead is one of the heaviest elements and the matrix effect is generally less

severe due to its high kinetic energy. Operating the electron source under the regular supplemental electron mode does not greatly improve the signal recovery, however, the suppression is reduced drastically under the charge-titrated condition ($I_{filament}$ = 2.12 A). The response is almost a straight line over the full matrix concentration range with nearly 95% of signal recovery in 1000 ppm Na solution.

Effect of atomic weight of matrix elements

The effects of the supplemental electron technique on the matrix effect induced by different elements were evaluated by monitoring Co^+ signal in various concomitant elements (Na, Ti, Ga, Rh, Ba, Tb, Ta, and Bi) present at 2 mM (46 ppm for Na, 418 ppm for Bi). Plots of normalized Co^+ signal vs. atomic mass of matrix element under all three operating modes (normal, electron-enhanced, and electron-rich) are depicted in Figure 3. Without the supplemental electrons, the magnitude of the matrix suppression is directly proportional to the atomic weight of the concomitant element. Only 8% of the Co^+ signal remains when Bi is present at 418 ppm (2 mM). With the electron current value that maximizes sensitivity ($I_{filament}$ = 1.90 A), the matrix suppression is still present but substantially less severe. The analyte sensitivity is greatly increased as usual.

The charge titration technique was then performed with the most challenging matrix (Bi), and the resulting electron current was then applied for the analysis of all solutions. The signal recovery is greatly improved under this electron-rich condition ($I_{filament}$ = 2.09 A). A full recovery of Co^+ signal is observed from solutions containing low to medium atomic mass matrix elements (Na, Ti, Ga, Rh, and Ba). The signal then falls off only slightly afterward with nearly 90% of the signal remaining in the Bi matrix solution.

Effect of atomic weight of analyte elements

Barium was selected to evaluate the matrix effects on analyte ions of different masses because it is relatively heavy and is a common matrix. A solution containing various analyte elements across the whole mass range in the periodic table (Mg, Co, Y, In, Pr, Lu, and Pb) was prepared in both clean solutions (1% HNO_3) and 200 ppm Ba. Analyte responses were measured under both normal and electron-rich operating modes for both solutions. The signal ratios are then taken and plotted as a function of analyte ion mass as shown in Figure 4. As expected, without the additional electrons (normal mode, I = 0), analyte ions of all masses are suppressed by the Ba matrix. The magnitude of the suppression is most severe at low mass and declines smoothly as the analyte mass increases.

A significant improvement is observed when the skimmer is operated under the electron-rich condition ($I_{filament}$ = 2.08 A). The matrix suppression is far less dependent on the ion mass. The signal ratios obtained are nearly identical with close to 100% of signal recovery for the medium to high mass ions and 90% for the relatively low mass ions.

Suggested mechanism for signal enhancement and reduction of matrix interferences

Altogether, the supplemental electron source and charge titration method counter the matrix suppression quite effectively. These results confirm those in the companion paper[46] and the previous work[47] that the space charge effects occur mainly between the skimmer and the extraction lens. The additional electrons applied to the ion beam behind the skimmer orifice are believed to reduce the space charge repulsion and mitigate the matrix effects. These excess electrons presumably counteract the excess charge and shield the analyte ions from the greater space charge repulsion induced by matrix ions.

This phenomenon is qualitatively depicted in Figure 5. Analyte ions, matrix ions, background ions (not shown), and electrons, entrained in the flow of neutral atoms from the plasma are extracted through the sampler and a typical skimmer in Figure 5a. As the beam advances beyond the skimmer orifice, the highly mobile electrons diffuse away and the charge separation takes place. The space charge repulsion then develops in the ion beam. With much of the ion beam being matrix ions, light analyte ions are defocused and lost more extensively creating a typical matrix-induced signal suppression.

On the other hand, electrons added to the ion beam via the supplemental electron source (Figure 5b) shield the positive ions and reduce the space charge repulsion between them as the quasineutral state breaks down. These electrons presumably accompany the ions into the ion optical system, as suggested by the positive potential on the extraction lens, thus keeping analyte ions from being defocused. Typically, the ion beam density decreases proportionally to $1/z^2$ as ions travel to the axial position z behind the skimmer. Therefore, the density eventually drops to a point where the total ion current is low and the space charge is no longer severe. This probably occurs in the extraction lens where ions are then drawn into a highly negative second lens while a representative population of ions still remains intact. As a result, the defocusing of light analyte ions is much less severe and the matrix-induced suppression as well as the overall sensitivity are greatly improved. Although the sensitivity improvement under this electron-rich mode (50-80% depending on the element) is lower than the best achievable (200-300%), it is still significantly better than that of the normal mode and the sensitivity loss is easily outweighed by the minimal matrix effects.

While the charge titration technique performs best when the electron current is titrated for each matrix solution, the optimum filament currents for all matrices tested fall in a

close range (2.07-2.12 A). In addition, Figure 3 suggests that a fixed current under electron-rich conditions can suppress the matrix effects for all matrix elements. In practice, a fixed high electron current (e.g. 2.1 A filament current) can be used to accommodate all matrix samples for convenience, although the electron current can be fine-tuned for a particular matrix, if desired.

Conclusions

This article and its companion[46] describe the advantages of adding electrons behind the skimmer in ICP-MS. Presumably, the supplemental electrons assist in shielding and balancing the excess positive charge, thus reducing the space charge repulsion between ions. Analyte sensitivity as well as other space charge-related problems, particularly matrix effects, are improved substantially. One distinct benefit of this electron source is that the number and kinetic energy of the emitted electrons can be controlled fully. Matrix effects can be improved even further by operating the electron source at moderately higher current than that which provides the greatest sensitivity enhancement. The matrix-induced suppression of analyte signal can be greatly minimized for virtually all analyte and matrix elements for matrix concentrations up to at least 1000 ppm. This technique could prove to be an ideal solution for the trace analysis of difficult matrices without a compromise in sensitivity. Selection of internal standards to correct for the remaining matrix effects[49] should be simplified by reduction of the severity of the problem in the first place.

Acknowledgements

Ames Laboratory is operated for the U. S. Department of Energy by Iowa State University under contract no. W-7405-Eng-82. This research was supported by the Office of Basic Energy Sciences. The ultrasonic nebulizer was provided by Transgenomic CETAC Technologies, Inc. ICP elemental standards were provided by SPEX CertiPrep.

References

1. Houk, R. S.; Fassel, V. A.; Flesch, G. D.; Svec, H. J.; Gray, A. L.; Taylor, C. E. *Anal. Chem.* **1980**, 52, 2283-2289.

2. Tsukahara, R.; Kubota, M. *Spectrochim. Acta, Part B* **1990**, 45, 581-589.

3. McLaren, J. W.; Lam, J. W.; Gustavsson, J. W. *Spectrochim. Acta, Part B* **1990**, 45, 1091-1094.

4. Alves, L. C.; Wiederin, D. R.; Houk, R. S. *Anal. Chem.* **1992**, 64, 1164-1169.

5. Alves, L. C.; Allen, L. A.; Houk, R. S. *Anal. Chem.* **1993**, 65, 2468-2471.

6. Alves, L. C.; Minnich, M. G.; Wiederin, D. R.; Houk, R. S. *J. Anal. At. Spectrom.* **1994**, 9, 399-403.

7. Jiang, S. J.; Houk, R. S.; Stevens, M. A. *Anal. Chem.* **1988**, 60, 1217-1221.

8. Nonose, N. S.; Matsuda, N.; Fudagawa, N.; Kubota, M. *Spectrochim. Acta, Part B* **1994**, 49, 955-974.

9. Sakata, K.; Kawabata, K. *Spectrochim. Acta, Part B* **1994**, 1027-1038.

10. Tanner, S. D. *J. Anal. At. Spectrom.* **1995**, 10, 905-921.

11. Rowan, J. T.; Houk, R. S. *Appl. Spectrosc.* **1989**, 43, 976-980.

12. Douglas, D. J. *Can J. Spectrosc.* **1989**, 34, 38-49.

13. Turner, P.; Merren, T.; Speakman, J.; Haines, C. Interfaces Studies in the ICP-MS Spectrometer, in Holland, G.; Tanner, S. D., Eds. Plasma Source Mass Spectrometry : Developments and Applications, Royal Society of Chemistry, Cambridge, 1997,

pp. 28-34.

14. Bradshaw, N.; Hall, E. F. H.; Sanderson, N. E. *J. Anal. At. Spectrom.* **1989**, 4, 801-803.

15. Morita, M.; Ito, H.; Uehiro, T.; Otsuka, K. *Anal. Sci. (Japan)* **1989**, 5, 609-610.

16. Feldmann, I.; Tittes, W.; Jakubowski, N.; Stuewer, D.; Giessmann, U. *J. Anal. At. Spectrom.* **1994**, 9, 1007-1014.

17. Olivares, J. A.; Houk, R. S. *Anal. Chem.* **1986**, 58, 20-25.

18. Gillson, G. R.; Douglas, D. J.; Fullford, J. E.; Halligan, K. W.; Tanner, S. D. *Anal. Chem.* **1988**, 60, 1472-1474.

19. Gray, A. L.; Date, A. R. *Analyst* **1983**, 108, 1033-1050.

20. Beauchemin, D.; McLaren, J. W.; Berman, S. S. *Spectrochim. Acta, Part B* **1987**, 42, 467-490.

21. Gregoire, D. C. *Appl. Spectrosc.* **1987**, 41, 893-903.

22. Tan, S.; Horlick, G. *J. Anal. At. Spectrom.* **1987**, 2, 745-763.

23. Longerich, H. P.; Fryer, B. J.; Strong, D. R. *Spectrochim. Acta, Part B* **1987**, 42, 101-109.

24. Crain, J. S.; Houk, R. S.; Smith, F. G. *Spectrochim. Acta, Part B* **1989**, 44, 1355-1364.

25. Pickford, C. J.; Brown, P. M. *Spectrochim. Acta, Part B* **1986**, 41, 183-187.

26. Date, A. R.; Cheung, Y. Y.; Stuart, M. E. *Spectrochim. Acta, Part B* **1987**, 42, 3-20.

27. Blades, M. W.; Caughlin, B. L., *Spectrochim. Acta, Part B* **1985**, 40, 579-591.

28. Vandecasteele, C.; Nagels, M.; Vanhoe, H.; Dams, R. *Anal. Chim. Acta* **1988**, 211, 91-98.

29. Vandecasteele, Vanhoe, H.; Dams, R. *J. Anal. At. Spectrom.* **1993**, 8, 781-786.

30. Chen, X.; Houk, R. S. *J. Anal. At. Spectrom.* **1995**, 10, 837-841.

31. Gregoire, D. C. *Spectrochim. Acta, Part B* **1987**, 42, 895-907.

32. Ross, B. S.; Hieftje, G. M. *J. Am. Soc. Mass Spectrom.* **1992**, 3, 128-138.

33. Hu, K.; Houk, R. S. *J. Anal. At. Spectrom.* **1993**, 4, 28-47.

34. Sheppard, B. S.; Shen, W. L., Caruso, J. A. *J. Am. Soc. Mass Spectrom.* **1991**, 2, 355-361.

35. Hall, G. M.; Pelchat, J. C.; Loop, J. J. *J. Anal. At. Spectrom.* **1990**, 5, 339-349.

36. Ting, B. T.; Mooers, C. S., Janghorbani, M. *Analyst* **1989**, 114, 667-674.

37. Shabani, M. B.; Akagi, T.; Shimizu, H.; Masuda, A. *Anal. Chem.* **1990**, 62, 2709-2714.

38. Jiang, S. J.; Palmieri, M. D., Fritz, J. S., Houk, R. S. *Anal. Chim. Acta* **1987**, 200, 559-571.

39. Beauchemin, D.; Berman, S. S. *Anal. Chem.* **1989**, 61, 1857-1862.

40. Ketterer, M. *Anal. Chem.* **1990**, 62, 2522-2526.

41. Mukai, H.; Ambe, Y.; Morita, M. *J. Anal. At. Spectrom.* **1990**, 5, 75-80.

42. Park, C. J.; Park, S. R.; Yang, S. R.; Han, M. S.; Lee, K. W. *J. Anal. At. Spectrom.* **1992**, 7, 641-645.

43. Seubert, A.; Meinke, R. *Fresenius J. Anal. Chem.* **1994**, 348, 510-519.

44. Tanner, S. D.; Cousins, L. M.; Douglas, D. J. *Appl. Spectrosc.* **1994**, 48, 1367-1372.

45. Denoyer, E. R.; Jacques, M. D.; Debrah, E.; Tanner, S. D. *At. Spectrosc.* **1995**, 16, 1-6.

46. Praphairaksit, N.; Houk, R. S. *Anal. Chem.*, To be submitted together.

47. Allen, L. A.; Leach, J. J.; Houk, R. S. *Anal. Chem.* **1997**, 69, 2384-2391.

48. Kim, Y.; Kawaguchi, H.; Tanaka, T.; Mizuike, A. *Spectrochim. Acta* **1990**, 45, 333-339.

49. Sartoros, C.; Salin, E. D. *Spectrochim. Acta Part B* **1999**, 54, 1557-1571.

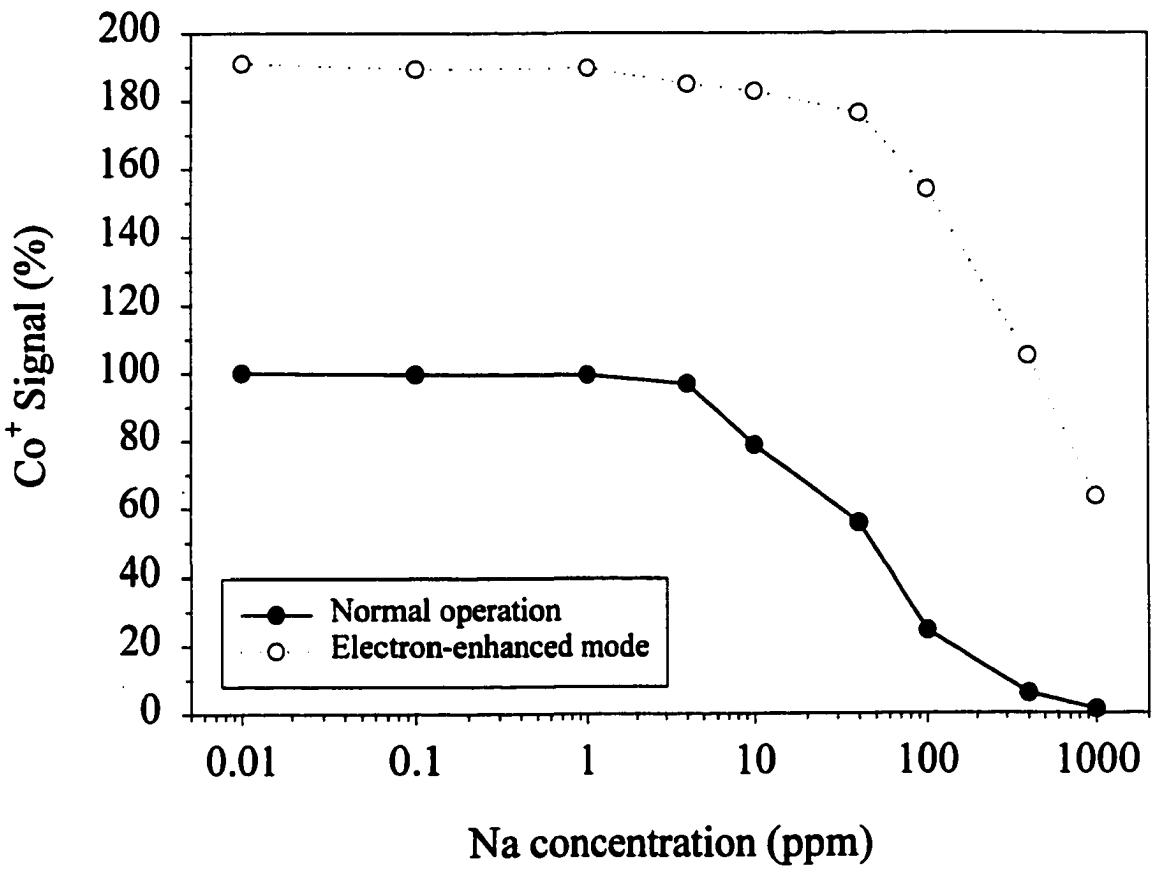

Figure 1. Plots of normalized Co^+ signal vs. Na matrix concentration under normal operation and electron-enhanced mode.

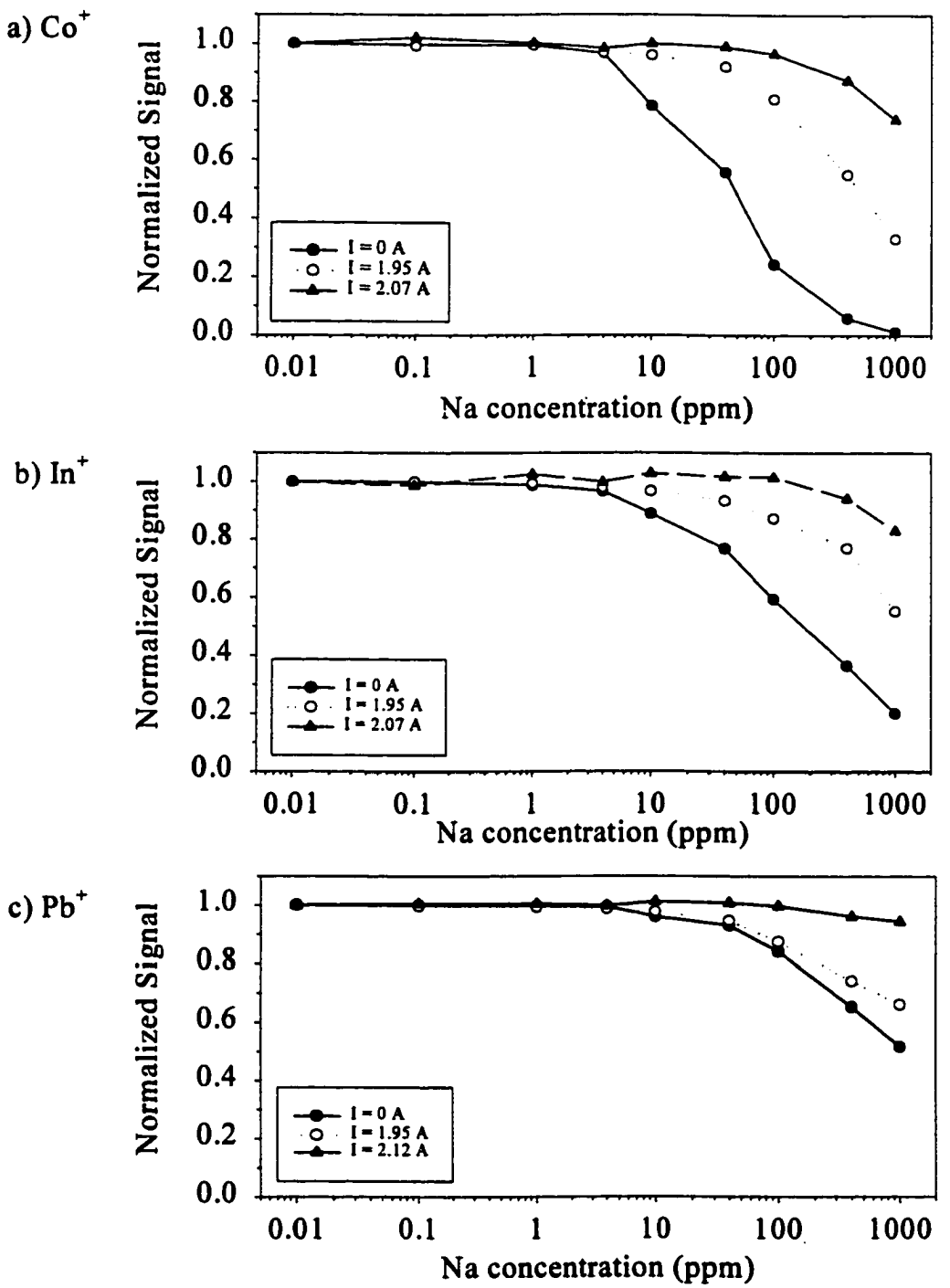

Figure 2. Signal suppressions for a) Co^+, b) In^+ and c) Pb^+ in the presence of Na matrix at various concentrations for different values of filament current.

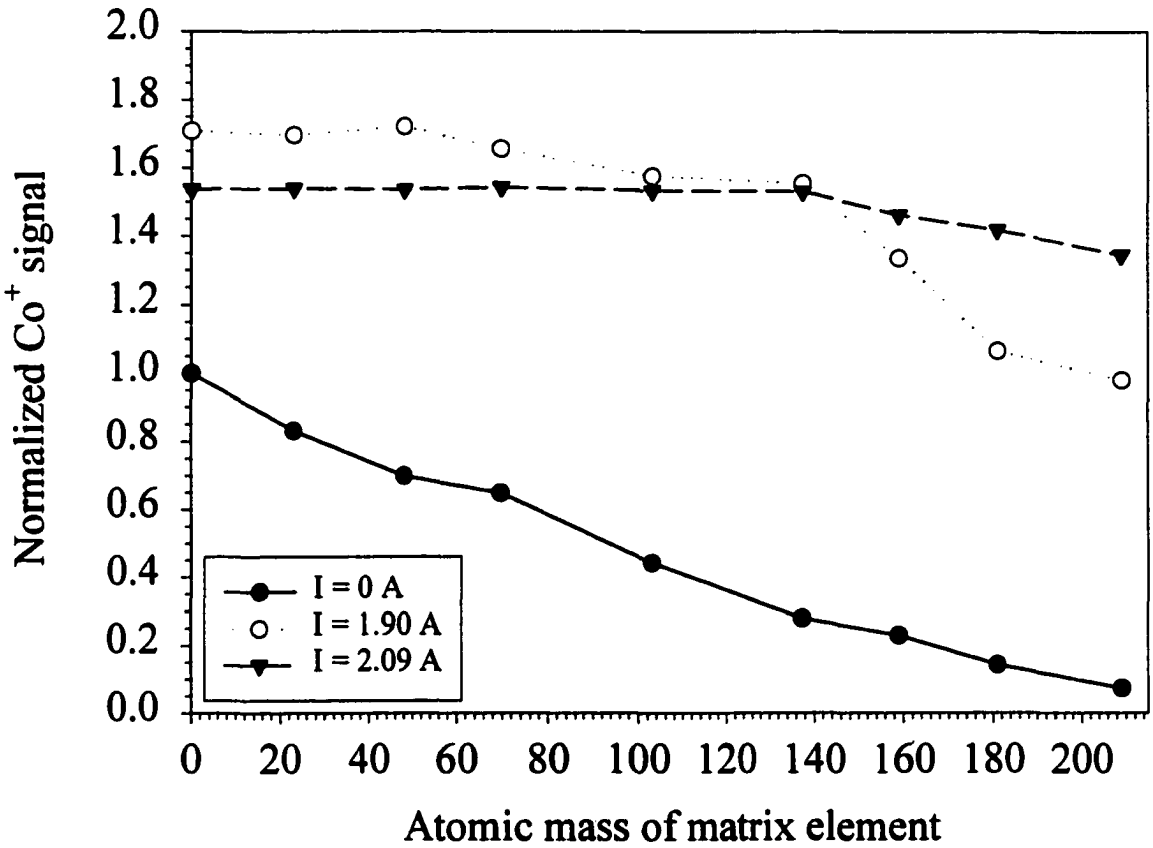

Figure 3. Dependence of Co^+ signal on the atomic mass of concomitant element (0 = clean solution), matrix concentration = 2 mM.

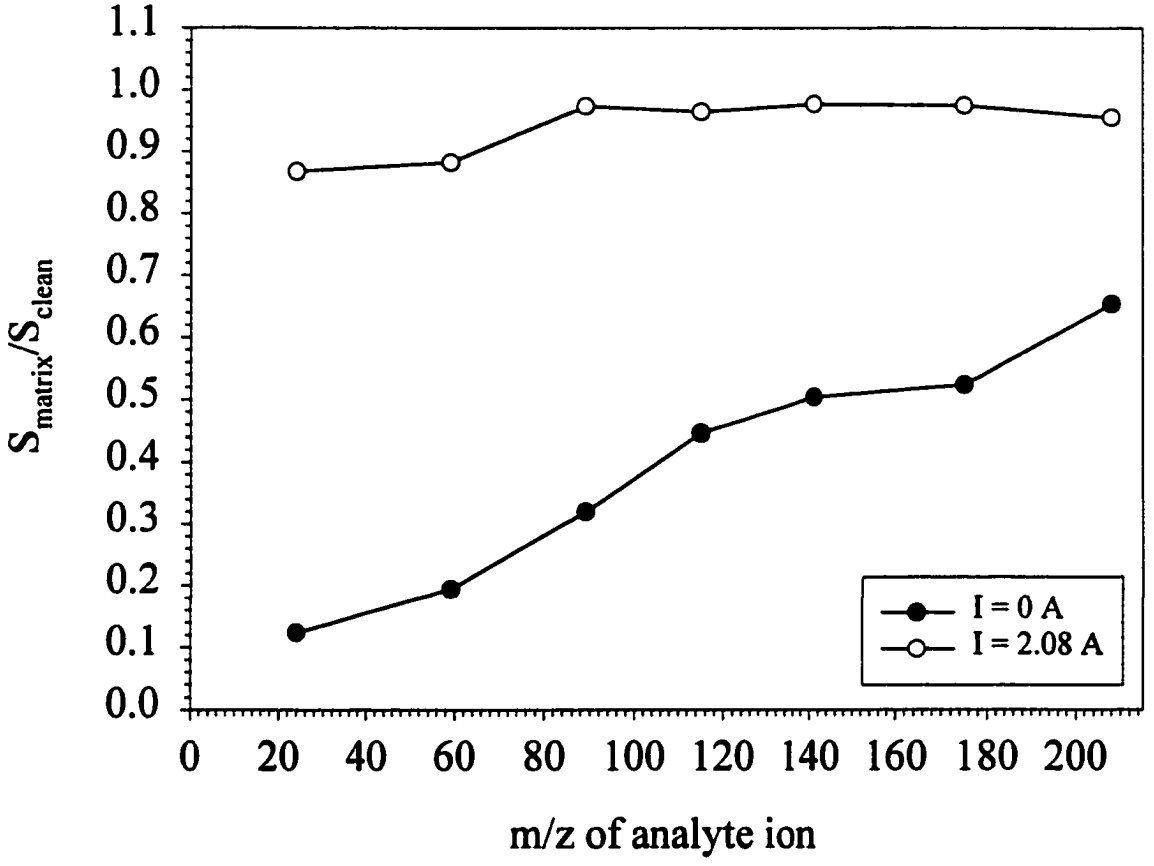

Figure 4. Ratios of analyte signal in Ba matrix (S_{matrix}) over signal in clean solution (S_{clean}) as a function of atomic mass of analyte ion.

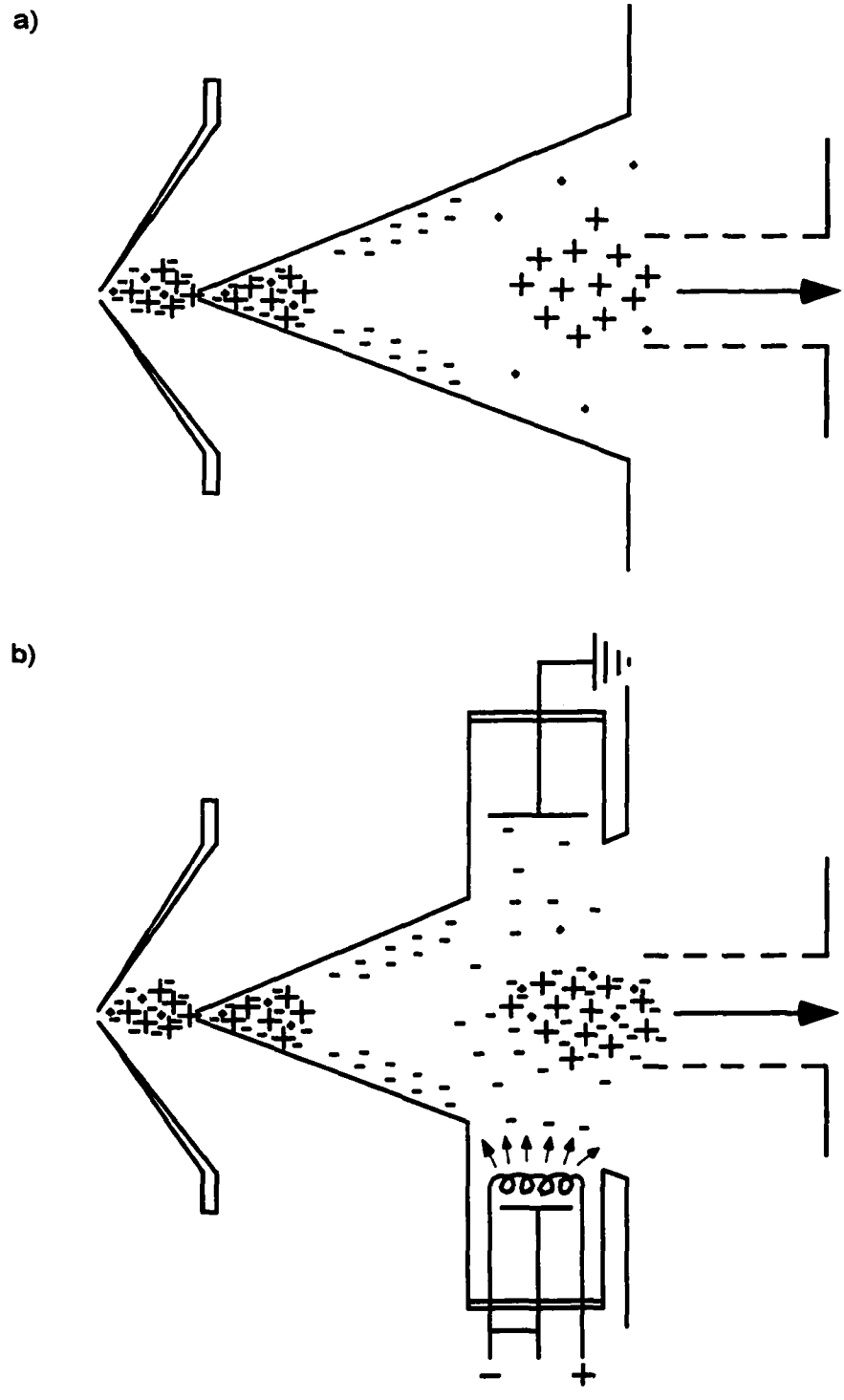

Figure 5. Proposed mechanism for the attenuation of space charge repulsion and matrix effects with the electron-enhanced skimmer. See text for explanation.
For clarity, only electrons (-), light analyte ions (•) and heavy matrix ions (+) are shown here, all other ions (e.g. Ar^+, ArH^+, O^+, H_2O^+, etc.) are left out.

CHAPTER 5. GENERAL CONCLUSION

Superior analytical capabilities, minimal interference and cost effectiveness collectively have always been the ultimate goal of ICP-MS instrumentation development. Such a goal has been made a few steps closer with the preceding studies in this dissertation.

To reduce the high operating cost of the ICP, a new externally air-cooled low-flow torch has been developed and successfully demonstrated for ICP-MS applications. Unlike the earlier designs of air-cooled torches [1-2], the current torch has pressurized air blown through a closed air jacket onto and around the exterior of the outer tube, thus providing effective and more homogeneous cooling without suffering from the air turbulence to the plasma and requiring no modifications to the load coil. Though a wide range of operating forward powers and outer gas flows can be utilized, a plasma operated at 850 W with the outer gas flow rate of approximately 4.5 L/min offers the best compromise between the analytical merits and the economical perspective. Overall, this low-flow plasma exhibits nearly identical desirable analytical capabilities of the conventional ICP while consuming significantly less argon and power.

A methodology that can alleviate space charge and matrix effects has been developed and detailed in chapters 3 and 4. The skimmer is equipped with a supplemental electron source similar to an electron impact ionizer. This source supplies moderate energy electrons, which presumably neutralize or reduce some of the excess positive charge in the ion beam downstream of the skimmer, thus reducing the space charge repulsion between ions. The overall ion transmission efficiency and consequent analyte ion sensitivities as well as the matrix effects are drastically improved while other critical analytical aspects, such as metal

oxide ion ratio, doubly charged ion ratio, and background ions remain relatively unchanged under the operation of this electron source. The source is unique in that it allows a full control of electron emission and electron energy with a simple electronic circuit. This feature is beneficial as the matrix effects can be mitigated to a greater extent when the source is operated under electron-rich (high current) mode where a charge titration technique, of which the operating conditions of the electron source are optimized to accommodate the presence of concomitant elements in a matrix-rich sample prior to the analysis, is employed. The matrix-induced suppression of analyte signal can be greatly minimized for practically all analyte and matrix elements. In addition, the results of this study can also be used as further evidence to clarify that space charge effects are indeed dominated behind the skimmer.

The prominent analytical characteristics and benefits of the new air-cooled low-flow torch and the modified skimmer suggest several possible areas for future research. Considering all the preceding works have been performed entirely on a particular homemade instrument, there is an obvious need for its performance evaluation on commercial ICP-MS systems. Evaluating the low-flow torch on a commercial ICP-MS should be straightforward as the overall physical dimension of the torch is almost identical to a conventional torch and no modification is necessary. However, due to differences in the interface and ion lens configurations of each commercial system, slight modifications of the electron source may be needed but certainly not out of reach.

Apparently the enhanced ion transmission efficiency obtained with supplemental electrons, as observed by increased analyte sensitivities, is still far less significant than the estimated loss of the overall ion transmission. This clearly suggests that the designs of the electron source, skimmer, and ion lens system can be further improved in order for the

technique to perform to its perfection. Finally, the measurements of physical properties, e.g. electron density, temperature, etc., of the air-cooled low-flow plasma would also be worthy experiments.

References

1. Ripson, P. A. M., de Galan, L., and de Ruiter, J. W., *Spectrochim. Acta, Part B*, 1982, **37**, 733.

2. van der Plas, P. S. C., de Waaij, A. C., and de Galan, L., *Spectrochim. Acta, Part B*, 1985, **40**, 1457.

ACKNOWLEDGEMENTS

First and foremost, I would like to express my deep sincere appreciation to my major professor, Dr. R. S. Houk, for his guidance, support, patience, generosity and understanding during my stay at Iowa State University. His tremendous knowledge, expertise and great visions in ICP-MS and analytical chemistry have made my research experiences extremely valuable and enjoyable. I am very grateful to have been able to work for him.

I wish to thank Dr. Dennis Johnson, Dr. Marc Porter, Dr. Patricia Thiel and Dr. David Laird for being my committee members. Graduate study at Iowa State has been a wonderful experience for me. To that, I thank all the professors, department of chemistry and the university for giving me the opportunity to join the program and providing me with such exceptional education.

I would like to thank all the former and current members of the Houk group not only for their experimental assistance and discussions but also for the great friendship they have given me. There are too many to name here, but I would like to give special thanks to some: Scott Clemons, Lloyd Allen, Shen Luan, Steve Johnson, Mike Minnich, Al Gwizdala, Jay Leach, Ma'an Amad, Sahana Mollah, Zhiyang Du, Towhid Hasan, and David Aeschliman. I wish each and every one of you the best.

I am also indebted to many people at Iowa State and Ames Laboratory for helping me in many ways. I wish to greatly acknowledge all the people who have contributed behind my projects, especially Trond Forre of the chemistry glass shop, Dick and Terry of the chemistry machine shop, Jerry, Steve and Charlie of the Ames Lab machine shop, and staffs at the

electronic services. Thanks to Ho-ming Pang and Royce Winge for helping me set up a new data acquisition system and spectrometer for emission experiments.

This work was performed at Ames Laboratory under Contract No. W-7405-Eng-82 with the U.S. Department of Energy. The United States government has assigned the DOE Report number IS-T 1893 to this thesis.

Thanks go to all the support staffs here at ISU and Ames Lab: Brenda (our secretary) and the staffs at the chemistry department office, Brian, Frank, Keith and Gary at the storeroom/warehouse, Drew, Vicki, Ricki and Deb for keeping the lab safe and clean.

There are several other people that I would specially like to thank: Linda Houk for her generosity of constantly bringing in treats and hosting parties for the whole group members, Joe Burnett for a great friendship and his assistance in my Chem 316 T.A. duty, Nawapak Eua-anant and all my friends who have made my life in graduate school bearable and enjoyable. Thanks to all the people who contributed in different ways that may not have been mentioned here, you are certainly appreciated.

Thanks to Joicy, my miniature schnauzer dog, who has always been there everyday to welcome me home and cheer me up every time I am down with her tail wagging and sloppy wet kisses.

I would like to express my profound appreciation to Nalena Lesiuk for her love, support, patience, understanding and encouragement which have been the ultimate blessing for me through these years in graduate school.

Finally, I wish to thank my family. I am extremely grateful to my parents, Porntip and Kasem, for the constant and unconditional love and support they have given me through my whole life. The patience and courage that my mom has shown while fighting through

many recent long years of kidney disease, surgeries, dialysis and kidney transplant have been such an inspiration and motivation for me throughout my education. I also would like to thank my sisters and brothers for being so supportive and taking such a good care of mom during all these years that I have been away.

Thank you all.